Karlsruhe Institute of Technology

Higher-Order Numerical Homogenization for Wave Propagation in Strongly Heterogeneous Media

Zur Erlangung des akademischen Grades eines

Doktors der Naturwissenschaften

von der KIT-Fakultät für Mathematik des
Karlsruher Instituts für Technologie (KIT)
genehmigte

Dissertation

von

Felix Krumbiegel

Tag der mündlichen Prüfung: 11. Februar 2026

1. Referent: JProf. Dr. Roland Maier
2. Referentin: Prof. Dr. Barbara Verfürth

Acknowledgments

First, and foremost I want to thank my supervisor Roland Maier who took me in as his first PhD student. And I am grateful for the support and trust that I got. I also want to thank his group who helped with discussions and advice.

Then, I would like to thank Barbara Verfürth who kindly offered to referee my thesis.

Further, I thank Marlis Hochbruck and her team for taking me in when I got to the KIT.

For the support throughout my PhD I like to thank the CRC 1173 – Project-ID 258734477 - Deutsche Forschungsgemeinschaft (DFG, German Research Foundation) who supported me to share my research and develop personal skills.

I also want to thank my co-authors Balaje Kalyanaraman and Siyang Wang.

Last but not least I thank my family and friends for their support. Especially, thank you to my parents, my sister and my partner Selina for always being there.

Abstract

This thesis is concerned with the numerical solution of the acoustic wave equation, where the wave propagates through a non-smooth, highly heterogeneous medium. This setup poses many challenges for classical methods as the heterogeneity of the medium needs to be resolved, and high regularity is required for higher-order convergence. Herein, we present a novel tailor-made numerical homogenization strategy that builds on coarse piece-wise polynomials and corrects them accordingly such that higher-order convergence can be obtained without globally refining all scales of the medium. In this thesis, the numerical homogenization strategy is first introduced and analyzed in a prototypical setting providing a basis. Further, the method is fully discretized to obtain a computable method. Finally, it is shown that the calculation of these spaces can be performed localized and fully parallelized on small subdomains without affecting the convergence.

Contents

List of Figures

List of Tables

1 Introduction

Motivation

Modeling complex phenomena in nature or the performance of a specific material in an engineering application is commonly done by partial differential equations (PDEs). Specifically, the PDE describes the underlying physics as close as possible and the solution to the governing equation is the response of a physical quantity of interest such as the density of a wave to the environment. That could, e.g., be an acoustic wave that transports noise from an engine to the surrounding environment. An interesting application is to develop a noise-cancelling material that reduces the noise pollution in the surrounding as effectively as possible subject to certain constraints as weight, size, etc.

In practise, it typically is quite expensive and/or time-intensive to first create a material that is then tested in a real-world environment or in a laboratory. These problems provoke the use of computer simulations that provide insight into whether a material is suited or not for a given application. Thus, these numerical calculations need to do the heavy lifting and demand a plethora of requirements. The simulations first and foremost should be highly accurate, and furthermore, it should be a priori known that the simulation will have a certain accuracy if a given amount of computational resources are put in. If you have proven that a method can achieve a set accuracy, then the calculations should also be as cheap as possible, both in storage and computational effort. Another important property of numerical simulations is the robustness with respect to parameters, that is, if a modelled material is sufficient for its application, then slight adjustments to said material should still be applicable to the numerical simulations without any major reworks. To lesser extent a numerical method should also be easy to implement. This in the long term may save time when setting up, enhancing and debugging implementations.

A prominent method for solving PDEs is the finite element method (FEM), e.g., the higher-order *hp*-FEM by Babuška and Dorr (1981). Typically, solutions to PDEs are elements of infinite-dimensional spaces. Thus, a first step is to find a finite-dimensional subspace in which a solution (to a slightly modified problem) can be found such that the numerical method has most of the properties mentioned above. The FEM constructs such a finite-dimensional space by first decomposing the domain into a mesh, and then seeking a solution consisting of functions that are polynomials on each element of the mesh. The process of finding a solution in these subspaces then results in a linear system of equations that can be efficiently solved with appropriate solvers. Reasons that make the FEM a widely-used method are

manifold. The first being that one can show an a priori error estimate. This means that you know, up to a certain degree (what exactly this means will be elaborated at a later stage), if you put in enough computational power, you will have a particular accuracy. Furthermore, by design lie all degrees of freedom in the simulation on corners (nodes) of elements of the mesh, and they communicate information only locally to neighbouring nodes. This leads to low connectivity and sparse matrices in the linear system. Sparse means that a high percentage of entries in the system matrix are zero and with tailor-made strategies these matrices can be stored at low costs and solving the spare system is computationally highly efficient. Lastly, the FEM is also quite simple to implement, and the implementation does not depend on a forcing term or a material coefficient. This means if a new material is considered, the change in the implementation is only switching out the input data.

However, there is not one numerical method for everything, and the FEM also has its drawbacks. Recall from above, the accuracy of the numerical solution can be verified for a set computational effort only up to a certain degree. This means that it can be shown that asymptotically the numerical solution converges to the exact solution. However, how good the approximation is for a given computational effort depends on different factors. These factors typically are the data that is given to the PDE. More precisely, the underlying domain, the material coefficient or a source may contribute to worse approximation with similar costs. For many challenges that arise when dealing with either 'bad' data, the FEM can be adapted by putting in more a priori information to tailor the FEM to the problem at hand. In the following, we briefly present one example of 'bad' data that pose difficulties for the classical FEM. These challenges are the main focus of this thesis, where a tailor-made FEM-based method is designed.

The first challenge considered are non-smooth material coefficients. An example could be a composite material, e.g., a homogeneous medium that is reinforced with potentially very small fibers that have vastly different properties. In this case the coefficient that models this material has rapid and non-smooth jumps across these fibers. This yields solutions that may in general have low regularity. In order to show that the finite element (FE) solution has a good accuracy a certain regularity of the solution to the PDE is necessary. This may potentially lead to poorer approximation with similar computational effort compared to PDEs with smooth material coefficients. An example how the classical FEM can deal with such materials is by adaptively refining the mesh. This means that in the proximity of such jumps the accuracy can be increased by locally increasing the computational effort. Overall, the so-called adaptive FEM can recover the accuracy of the classical FEM with similar computational costs, see, e.g., (Babuška and Rheinboldt, 1978; Guo and Oh, 1994; Dörfler, 1996; Verfürth, 2013). However, if these fibers are present everywhere in the material the mesh needs to be globally refined. This then has again the same problem as the classical FEM. Furthermore, if these fibers are comparably small with respect to the size of the medium, then the classical FEM also yields a low

accuracy, especially if the mesh is not sufficiently refined. This can be interpreted that the oscillations that exist in the medium also exist on the solution and if the polynomials in the finite-dimensional FEM space are chosen to be too coarse, they cannot properly map these oscillations. The insufficient approximation can be remedied by refining the mesh. However, this comes with large computational costs. It is even more noticeable if the PDE is time-dependent. Then a linear system needs to be solved at every (discrete) point in time and the costs multiply.

Another enhancement of the classical FEM to overcome difficulties when simulating heterogeneous materials is the so-called generalized FEM first introduced by Babuška and Osborn (1983). Therein the authors laid the cornerstone for most numerical homogenization strategies, especially, the method considered in this thesis. The idea of numerical homogenization is solving PDEs with highly oscillatory materials by setting up coarse FE spaces that might not resolve the oscillations and adapt them appropriately to fit to the materials. This strategy typically comes with some computational overhead as the adaption has to be set up first. However, the benefit that the resulting linear system is comparably small greatly outweighs the costs of the setup. This is even more apparent if multiple forcing functions are present or if time-dependent problems are considered.

Numerical homogenization

In the context of numerical solutions to PDEs with highly oscillatory coefficients, there exists a plethora of strategies that efficiently solve the problem. A major approach is using analytical homogenization theory. Assume that there exists a fine scale ε that is the oscillation scale of the material. The idea is to understand the limit PDE as $\varepsilon \to 0$. The homogenized PDE is then independent of the oscillations and can be efficiently solved using standard or higher-order FEM. An example for a prominent method is the *heterogeneous multiscale method* (E and Engquist, 2003). The idea is to obtain the homogenized coefficient locally on each element by solving a cell problem which is derived using, e.g., the so-called G-convergence. Analytical homogenization can be generalized using higher-order asymptotic expansions as in the foundational work (Bensoussan et al., 1978). These typically require additional assumptions on the material, e.g., (quasi)-periodicity or scale separation. In practise, this can potentially be quite limiting and in our current setting, where we consider a general non-smooth material that can be non-periodic and does not have the scale separation property we require a different approach. For more information and a historic outline of multiscale methods that do not require scale separation see (Altmann, Henning, and Peterseim, 2021).

Numerical homogenization in this context deals with multiscale problems by splitting up the solution space in a coarse space consisting for example of polynomials and a remainder space. The remainder space is typically referred to as fine-scale

or detail space. It contains information on the oscillations of the PDE coefficient. While functions in the coarse space approximate the solution to a PDE with oscillatory coefficients suboptimally, the goal of numerical homogenization is to include information from the fine-scale space into the coarse-scale space and thus yields better approximation in the coarse regime.

One of the earliest numerical homogenization strategies, the so-called *variational multiscale method* (VMM), was first proposed by Hughes (1995), and later refined in (Hughes, Feijóo, Mazzei, and Quincy, 1998). The idea of the VMM is to split the solution space into a coarse space typically consisting of polynomials and a fine-scale residual space, which contains information on the oscillations introduced by the material coefficient. The fine-scale information is obtained by a so-called fine-scale Green's function which is obtained from the residual of the coarse solution which is contained in the fine-scale space.

The method considered in this thesis is closely related to the VMM, the so-called *localized orthogonal decomposition* (LOD) method introduced by Målqvist and Peterseim (2014) splits the solution space into the classical coarse FE space and corrects the coarse functions with an appropriate orthogonal projection into the remainder space. Employing this projection it can be shown that the method yields an error estimate similar to coarse FEMs that does not depend on the oscillations of the material coefficient. However, to obtain the fine-scale corrections global problem needs to be solved which is rather expensive. Målqvist and Peterseim (2014) have shown that these corrections are quasi-local in the sense that they obey an exponential decay that makes it possible to localize the calculation of the corrections to small subdomains that are embarrassingly parallel to compute. For more details, refer to the (Målqvist and Peterseim, 2021). While the original localization strategy had resulted in a localization error with suboptimal scaling with respect to the mesh size, this was later fixed by Henning and Peterseim (2013). Further, a novel localization strategy was introduced by Hauck and Peterseim (2023), the *super-localized orthogonal decomposition* method. Therein the right-hand side of the corrector problem is chosen in an optimal way. In practise, the method shows improved localization compared to the standard LOD method, however, a rigorous proof is still open.

Closely related to the LOD method, is an approach by (Owhadi, Zhang, and Berlyand, 2014) considering rough polyharmonic splines. Here, a bi-harmonic energy is minimized to obtain localized basis functions that inherit information on the oscillatory coefficient. Furthermore, many similarities to the LOD method can be drawn to the game-theoretic approach to numerical homogenization in Owhadi (2017); Owhadi and Scovel (2019), the so-called *gamblets*. There, the energy of an elliptic PDE is minimized under a constraint.

The multiscale FEM introduced by Hou and Wu (1997), where on each coarse block a local sub-problem is calculated to incorporate information on the oscillations in coarse shape functions. The method can be computed completely local, however, relies on homogenization theory for errors analysis. Efendiev, Galvis, and Hou

(2013) extended the framework by choosing snapshots in an offline phase which are then chosen based on a global spectral decomposition.

Another method that is based on the generalized FEM is the work (Babuška and Lipton, 2011), the so-called *multiscale-spectral generalized FEM* (MS-GFEM), where the domain is decomposed into subsets, where on each subset an eigenvalue problem is considered. The solutions to the eigenvalue problems are then glued together using a partition of unity approach. This work was later improved upon by Ma, Scheichl, and Dodwell (2022), and combined with a mixed FEM to resolve the fine-scales in Ma and Scheichl (2022). An advantage of spectral approaches is the exponential error convergence with respect to the number of eigenvalues.

In this thesis we consider a higher-order extension of the LOD method as space discretization. The method has first been proposed for an elliptic model problem by Maier (2021). The idea of this work is to start with a higher-order discontinuous polynomial space and minimize the elliptic energy under the constraint that the minimizer retains the projection into the polynomial space. The localization strategy in the work by Maier (2021) is suboptimal which has been fixed in the later work (Dong, Hauck, and Maier, 2023). Furthermore, a recent work by Hauck, Lozinski, and Maier (2025) developed a generalized framework for higher-order LOD (ho-LOD) methods with a novel localization strategy.

Herein, we consider the acoustic wave equation with the main challenge, that we have a very rough and highly oscillatory PDE coefficient. This setting has been previously analyzed using the classical LOD method by Abdulle and Henning (2017), where the implicit Crank–Nicolson time discretization is applied, and by Maier and Peterseim (2019), where the explicit leapfrog scheme is used to propagate through time. Furthermore, Peterseim and Schedensack (2017) used numerical homogenization techniques to relax the CFL condition for the acoustic wave equation. Geevers and Maier (2023) developed a mass-lumping strategy to augment LOD strategies in space with fast explicit time stepping. The gamblet approach has been applied to the wave equation in Owhadi and Zhang (2017).

Furthermore, higher-order methods can effectively model PDEs. Besides the *hp*-FEM (Babuška and Dorr, 1981) mentioned earlier (see also (Schwab, 1998)), there are several other higher-order FEM methods. Such as the discontinuous FEM, where we refer to the book (Hesthaven and Warburton, 2008), where the polynomial space consists of discontinuous piece-wise polynomials. Further, there is the hybridizable discontinuous Galerkin FEM introduced by Cockburn, Gopalakrishnan, and Lazarov (2009), and applied to the wave equation in (Nguyen, Peraire, and Cockburn, 2011). Here, the idea is to use the hybrid formulation of the elliptic/hyperbolic PDE and apply discontinuous FEM. Then the degrees of freedom can be chosen on the boundary of the elements, and the resulting system has low connectivity.

In the context of hybrid higher-order multiscale methods have been introduced in (Harder, Paredes, and Valentin, 2013; Araya, Harder, Paredes, and Valentin, 2013; Cicuttin, Ern, and Lemaire, 2019). However, these methods generally require more

regularity assumptions.

Contribution

This thesis considers wave propagation in highly oscillatory media. The goal is to first illustrate the challenges that arise when a strongly heterogeneous medium is present and what can be done to remedy such issues. Further, we provide insights into how the ho-LOD method can underperform for time-dependent PDEs when a non-smooth material coefficient is present. This thesis contains contents from the contributions (Krumbiegel and Maier, 2025; Kalyanaraman, Krumbiegel, Maier, and Wang, 2025) by the author.

Chapter 2 of this thesis builds the foundation of the ho-LOD applied to an elliptic PDE. In this chapter we briefly summarize why the classical FEM yields suboptimal error convergence when dealing with highly oscillatory coefficients. Subsequently, we introduce two localization strategies for ho-LOD methods, the first work by Maier (2021), and the follow-up with an improved localization strategy (Dong, Hauck, and Maier, 2023). Therein, we provide a comprehensive review of the previous works.

Chapter 3 contains the main contributions to the field of higher-order numerical homogenization. At first, it is theoretically analyzed how the prototypical (i.e. non-localized) ho-LOD method does not yield the higher-order as in the elliptic setting. Herein we find that the ho-LOD method is tailored to an elliptic PDE and by the nature of time-dependent problems, the error of the ho-LOD method depends on the regularity of the solution such that only second-order convergence can be shown. In Chapter 3 the so-called *enriched correction operator* is introduced which is designed to deal with residual of the ho-LOD solution and provide a higher-order convergence independent of the regularity of the solution. However, in the prototypical setting presented the enriched correction operator requires knowledge of the solution to the PDE which is in practise not feasible. The next challenge is thus to develop a novel enriched correction space which can be applied for solving the wave equation. We construct an expansion of the solution in certain discrete spaces which may recover the higher-order convergence from the elliptic setting by putting in some more computational effort. With the construction of the enriched correction operator and the successful discretization, the main challenge then is in constructing a computable method. This is done through localization of the correctors. We find that the enriched corrector operator obeys an exponential decay, similar to the ho-LOD correction operator, however, the localization strategy of the ho-LOD method is suboptimal in the current setting. Applying this strategy to the enriched correction operator yields corrector problems on near global subdomains which would make the enriched ho-LOD unfeasible. In this thesis we will provide a novel localization strategy that will allow all basis functions to be localized to subdomains of equal sizes, while preserving exponential errors.

The numerical experiments are performed in Python with the code published in `https://github.com/FelixKrumbiegel/eholod.git`.

The author acknowledges support by the state of Baden-Württemberg through bwHPC.

Notation

For any finite -dimensional space V, we denote the restriction to a subdomain $S \subset \Omega$ of a domain Ω by $V(S)$ in the sense that $v \in V(S)$, if $v \in V$ and $\operatorname{supp} v \subset S$. Further, we denote with $a \lesssim b$ if there exists a constant $C > 0$ such that $a \leq Cb$, where the constant may not depend on the mesh sizes H, h, the localization parameter ℓ, the oscillation scale ε or the time step τ.

2 Higher-order numerical homogenization

The core concepts and necessary terminology that we have touched on in the Introduction are refined herein, providing the essential foundation for the main contribution in the following chapter.

The results given subsequently are standard considerations and introduce the reader to the topic at hand and serve as an introduction to the mathematical foundation. The numerical strategy analyzed in this paper is based on a higher-order localized orthogonal decomposition (ho-LOD) method. The ho-LOD method was first introduced by Maier (2021) applied to a specific linear elliptic partial differential equation (PDE).

Thus, in this chapter Section 2.1 is first concerned with the underlying PDE, an elliptic model problem, and the existence of (approximate) solutions to such PDEs. We continue presenting a higher-order finite element method (FEM), a classical numerical scheme that is concerned with the approximation of said solutions. Specifically, we briefly discuss the *hp*-FEM first proposed by Babuška and Dorr (1981). The *hp*-FEM creates a finite-dimensional subspace, consisting of piece-wise higher-order polynomials, of the solution space in which the method finds an optimal (in a certain sense) solution with highly accurate approximation. This strategy is a higher-order strategy, which means that faster convergence with respect to the mesh size can be achieved. However, in the present setting where strongly heterogeneous media are modeled, FEMs suffer from a mesh resolution condition and require great computational costs for good approximations.

Section 2.2 illustrates how numerical homogenization strategies aim at reducing the computational cost while attaining high approximation quality on the example of the ho-LOD method. The basis for the method is a higher-order discontinuous polynomial space which is suitably adapted. Thus, the strategy obeys the higher-order convergence with respect to the mesh size similar to the *hp*-FEM. The ho-LOD method builds on a higher-order polynomial space and constructs so-called *bubble functions*, that are corrected to adapt the polynomials, respective bubbles, such that the new subspace is better suited to the problem at hand.

A great benefit of the newly constructed subspace is the fact that this space can be pre-computed in an offline step, which is particularly useful for time-dependent problems. Furthermore, each computation can be localized to small regions, and is embarrassingly parallel. Section 2.3 is concerned with different localization strategies.

2.1 Space discretization and finite elements

First, Section 2.1.1 is concerned with introducing the linear elliptic PDE. We give some standard results on the existence and uniqueness of solutions. Afterwards, we lay the foundation of the ho-LOD in Section 2.1.2.

Finally, we briefly introduce the *hp*-FEM and motivate the use of numerical homogenization strategies by presenting limits of classical FEMs in Section 2.1.3.

2.1.1 Elliptic model problem

In this chapter, we introduce the *hp*-FEM and ho-LOD on the following elliptic model problem. We seek a solution $u \in H_0^1(\Omega)$ such that

$$\begin{aligned} -\operatorname{div}(A\nabla u) &= f \qquad \text{in } \Omega, \\ u &= 0 \qquad \text{on } \Gamma = \partial\Omega, \end{aligned} \tag{2.1}$$

where Ω denotes an open and bounded Lipschitz domain. Let for the right-hand side $f \in L^2(\Omega)$ hold, and for the coefficient $A \in L^\infty(\Omega, \mathbb{R}^{d\times d})$. Further, let A be symmetric and fulfill

$$\alpha|\boldsymbol{\xi}|^2 \leq A(x)\boldsymbol{\xi}\cdot\boldsymbol{\xi} \leq \beta|\boldsymbol{\xi}|^2, \tag{2.2}$$

for almost every $x \in \Omega$ and all $\boldsymbol{\xi} \in \mathbb{R}^d$. Under these assumptions, there exists a unique solution $u \in H_0^1(\Omega)$ to the variational formulation of the elliptic model problem (2.1) given by

$$a(u,v) = (f,v)_{L^2(\Omega)}, \tag{2.3}$$

for all $v \in H_0^1(\Omega)$, where

$$a(u,v) \coloneqq \int_\Omega A\nabla u \cdot \nabla v \,\mathrm{d}x, \tag{2.4}$$

for any $u, v \in H_0^1(\Omega)$. The existence and uniqueness is a direct consequence of the Lax-Milgram theorem, cf. (Babuška, 1970/71, Thm. 2.1). We can verify the assumptions of the Lax-Milgram theorem by observing that the space $H_0^1(\Omega)$ is a Hilbert space when equipped with the inner product $(\nabla\cdot, \nabla\cdot)_{L^2(\Omega)}$. This follows from the Poincaré inequality (see, e.g., (Brenner, 2003)), i.e., for any $v \in H_0^1(\Omega)$ we have that

$$\|v\|_{L^2(\Omega)} \leq C_{\mathrm{P}}\|\nabla v\|_{L^2(\Omega)}, \tag{2.5}$$

where C_{P} depends on the domain Ω. Furthermore, using (2.2) we obtain coercivity of the bilinear form $a(\cdot,\cdot)$, given for any $v \in H_0^1(\Omega)$ by the estimate

$$\alpha\|\nabla v\|_{L^2(\Omega)}^2 \leq a(v,v), \tag{2.6}$$

and boundedness of $a(\cdot,\cdot)$, which for any $u, v \in H_0^1(\Omega)$ yields

$$a(u,v) \leq \beta\|\nabla u\|_{L^2(\Omega)}\|\nabla v\|_{L^2(\Omega)}. \tag{2.7}$$

Lastly, boundedness of the linear functional $(f, \cdot)_{L^2(\Omega)}$ follows by employing the Hölder inequality. Furthermore, the Lax-Milgram theorem states that the solution u obeys the following stability estimate

$$\|\nabla u\|_{L^2(\Omega)} \leq \frac{C_{\mathrm{P}}}{\alpha} \|f\|_{L^2(\Omega)}. \tag{2.8}$$

We note that in general $f \in H^{-1}(\Omega)$ is sufficient to ensure existence and uniqueness of the solution $u \in H_0^1(\Omega)$. However, the condition $f \in L^2(\Omega)$ is typically necessary for an error estimation of the FEM, and it is reasonable to assume this additional regularity of the right-hand side.

Further, for simplicity, we assume in the remainder of this work that the coefficient is scalar-valued. This special case is still covered by the above analysis by taking a scalar coefficient $A \in L^\infty(\Omega)$ and multiplying it by an identity matrix $I^{d\times d}$.

2.1.2 Space discretization

This section is mainly used to introduce the necessary ingredients for the ho-LOD method. We begin by defining a piece-wise polynomial subspace $V_H \subset L^2(\Omega)$, that acts as the foundation of the ho-LOD method. To construct such a space, we have a given quasi-uniform decomposition of the domain Ω into a set of regular d-rectangles $\{\mathcal{T}_H\}_{H>0}$ with the (coarse) mesh size H. For further details, refer to Ciarlet (1978, Chs. 2 & 3). We note that more general meshes could be considered, e.g., d-simplices or d-parallelograms. However, for our analysis, the quasi-uniformity and regularity are crucial properties of the mesh.

From now on, we specifically demand that the coefficient is highly oscillatory and, for ease of presentation, assume that there exists the smallest scale $0 < \varepsilon \ll 1$ on which we have the variations. In the following, we denote mesh sizes H that do not resolve all the fine oscillations of the PDE coefficient A. In cases where we require a mesh that resolves all oscillations of A we denote that mesh by $\mathcal{T}_h$ for mesh size $h < \varepsilon$. Further, consider the mesh $\mathcal{T}_h$ to be a refinement of the coarse mesh $\mathcal{T}_H$.

For the construction of the discrete spaces we choose a polynomial degree $p \in \mathbb{N}_0$ and denote the space of polynomials up to partial degree p on a subdomain $S \subset \Omega$ by $\mathbb{P}_p(S)$. The discrete space V_H is then given by the space of piece-wise (with respect to the mesh) polynomials

$$V_H = \{v \in L^2(\Omega) \mid \forall K \in \mathcal{T}_H \colon v|_K \in \mathbb{P}_p(K)\}. \tag{2.9}$$

We denote the continuous counterpart (with boundary conditions applied) by

$$\bar{V}_H = \{v \in C(\Omega) \mid \forall K \in \mathcal{T}_H \colon v|_K \in \mathbb{P}_p(K)\} \cap H_0^1(\Omega). \tag{2.10}$$

Next, we define the $L^2(\Omega)$-projection $\Pi_H \colon L^2(\Omega) \to V_H$ onto the space of piece-wise polynomials that are allowed to be discontinuous across element faces. On any

element $K \in \mathcal{T}_H$, the projection is given element-wise for any $v \in L^2(\Omega)$ by

$$((\Pi_H v)|_K, v_H)_{L^2(K)} = (v|_K, v_H)_{L^2(K)}, \tag{2.11}$$

for all $v_H \in V_H(K)$. Choosing the function $v_H = (\Pi_H v)|_K$ in (2.11) yields the L^2-stability of the projection

$$\|\Pi_H v\|_{L^2(K)} \leq \|v\|_{L^2(K)}. \tag{2.12}$$

In the following we discuss the following approximation properties of the L^2-projection onto V_H, see, e.g., (Houston, Schwab, and Süli, 2002). There exists a generic constant $C_{\mathrm{pr}} > 0$ independent of H and p, such that for any $v \in H^k(\Omega)$ and $K \in \mathcal{T}_H$ holds

$$\|v - \Pi_H v\|_{L^2(K)} \leq C_{\mathrm{pr}} H^{\kappa} \Phi(p, \kappa) \|v\|_{H^{\kappa}(K)}, \tag{2.13}$$

where $\kappa = \min\{k, p+1\}$, and

$$\Phi(p, \kappa) = \sqrt{\frac{(p+1-\kappa)!}{(p+1+\kappa)!}}.$$

In particular, for $k = 1$ we have that

$$\Phi(p, 1) \lesssim (p+1)^{-1}.$$

Further, we have the inverse estimate for polynomials, see, e.g., (Süli, Houston, and Schwab, 2000), for each $K \in \mathcal{T}_H$ and $v_H \in V_H(K)$ there exists a constant $C_{\mathrm{inv}} > 0$ independent of H and p such that

$$\|\nabla v_H\|_{L^2(K)} \leq C_{\mathrm{inv}} \frac{p^2}{H} \|v_H\|_{L^2(K)}. \tag{2.14}$$

We can sum up each of the equations (2.11)–(2.13) and (2.14) over all elements $K \in \mathcal{T}_H$ to obtain equivalent global estimates on Ω. Since (2.13) is stated on a single element K and then summed up to obtain a global estimate, it is sufficient that the function v has the required regularity on each element $K \in \mathcal{T}_H$, i.e.,

$$v \in H^k(\mathcal{T}_H) \coloneqq \{v \in L^2(\Omega) \mid v \in H^k(K) \text{ for all } K \in \mathcal{T}_H\}. \tag{2.15}$$

We note that

$$H^0(\mathcal{T}_H) = L^2(\Omega).$$

2.1.3 Pre-asymptotic effects of the finite element method

The FEM is a well-established method for the numerical approximation of solutions to PDEs such as the variational form (2.3). It offers efficient computation and rich a priori error analysis. We give a short introduction to the FEM on the example of the *hp*-FEM method analyzed in Babuška and Suri (1987).

***hp*-finite element method.** Seek a solution $u_H \in \bar{V}_H$ such that

$$a(u_H, v_H) = (f, v_H)_{L^2(\Omega)}, \tag{2.16}$$

for all $v_H \in \bar{V}_H$. Analogously to above, the existence and uniqueness of the solution u_H follows directly from the Lax-Milgram theorem, since the space $\bar{V}_H$ is a closed subspace of $H_0^1(\Omega)$. To obtain an a priori error estimate, first use v_H as test function in (2.3) and subtract the discrete counterpart (2.16) to obtain the so-called *Galerkin orthogonality*

$$a(u - u_H, v_H) = 0. \tag{2.17}$$

Since the Galerkin orthogonality (2.17) holds for any $v_H \in \bar{V}_H$, it can now be used to prove the quasi-best approximation property, also known as Céa's lemma

$$\|\nabla(u - u_H)\|_{L^2(\Omega)} \leq \frac{\beta}{\alpha} \inf_{v_H \in \bar{V}_H} \|\nabla(u - v_H)\|_{L^2(\Omega)}. \tag{2.18}$$

This quasi-best approximation property can now be used to insert any function in V_H, that has provably good approximation properties. Then we may obtain the following error estimate as by Babuška and Suri (1987)

$$\|\nabla(u - u_H)\|_{L^2(\Omega)} \lesssim \frac{H^{\kappa-1}}{p^{k-1}} \|u\|_{H^\kappa(\Omega)}, \tag{2.19}$$

where $\kappa = \min\{k, p+1\}$, and the constant is independent of H and p. This estimate is crucial for the FEM, as it provably ensures that the approximated solution is close to the weak solution of the PDE up to a constant. However, the constant can be very limiting in certain scenarios. One such scenario is the presence of a highly oscillatory and non-smooth coefficient A. The results of this are two-fold. First, consider a coefficient that is only piece-wise constant, i.e., $A \in L^\infty(\Omega)$. In this setting, we have that the solution in general does not yield the regularity $u \in H^k(\Omega)$ for any $k \geq 2$. More precisely, we have that $u \in H^{1+\delta}(\Omega)$ for some $\delta < 1$. In this case the best error convergence (for $p = 1$) that can be expected is

$$\|\nabla(u - u_H)\|_{L^2(\Omega)} \lesssim H^\delta \|u\|_{H^{1+\delta}(\Omega)}.$$

Since the computational effort of the FEM scales with $\mathcal{O}(H^{-d})$ using the FEM for general L^∞-coefficients is unfeasible. Guo and Oh (1994) proposed a strategy for the *hp*-FEM, where the mesh is not uniformly refined but geometrically refined around corners where the coefficient emits jumps. Using this refinement strategy Guo and Oh (1994) have used that the solution may only have singularities at the corners, and employed weighted spaces to show that solutions have higher regularity away from the singularities. There, it was finally shown that with this adaptive refinement of the mesh size the exponential convergence with respect to the degrees of freedom, i.e., the computational effort, of the classical *hp*-FEM could be recovered.

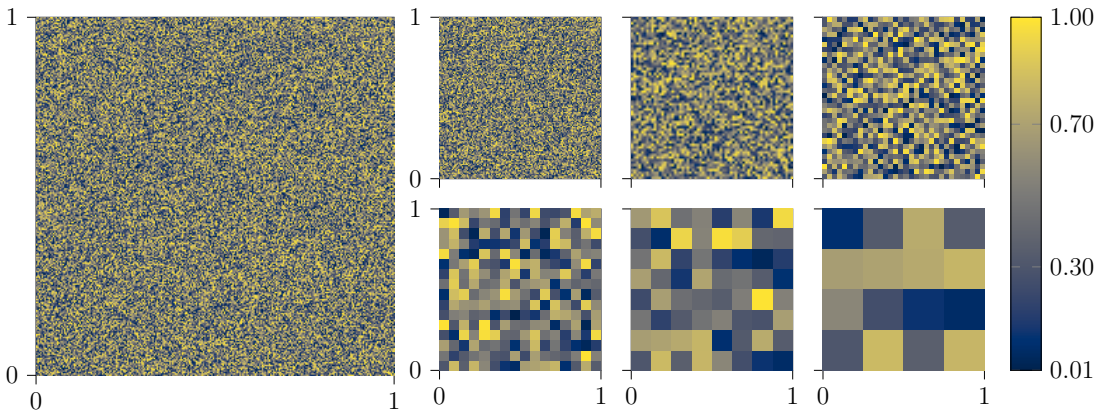

Figure 2.1: Coefficient A_ε on the left-hand side with oscillations on the scale 2^{-8}, and further coefficients A_ε oscillating on different scales (2^{-7}, 2^{-6}, 2^{-5}, 2^{-4}, 2^{-3}, 2^{-2}) used to demonstrate the pre-asymptotic effect of the FEM presented in Figure 2.2.

However, if we also consider that the jumps exist at many points in the domain and their distance $\varepsilon \ll H$ is small with respect to the mesh size, then local adaptive refinement is essentially a global refinement and the reduced computational effort of the adaptive method does not emerge. We note that the low regularity of the solution also holds similarly for the acoustic wave equation considered in Chapter 3 and this discussion remains valid there.

Second, consider now a coefficient that oscillates on a very fine scale $\varepsilon \ll H$, which has a further disadvantage in addition to the first case. Even if the coefficient is sufficiently smooth, and the solution has higher regularity $u \in H^k(\Omega)$, a reduced error convergence is observed if the fine-scale parameter is not resolved. This is also known as the *pre-asymptotic effect* of the FEM, and explained in the following. Since we have a sufficiently regular solution, the *hp*-FEM emits the error estimate (2.19). However, since the coefficient is highly oscillating, the norms of the higher derivatives of the solution scale with the inverse of the fine-scale parameter, i.e.,

$$\|u\|_{H^k(\Omega)} \lesssim \varepsilon^{-s},$$

for some positive $s \leq k-1$. That is, the error reads

$$\|\nabla(u - u_H)\|_{L^2(\Omega)} \lesssim \frac{H^{\kappa-1}}{p^{k-1}} \|u\|_{H^\kappa(\Omega)} \lesssim \frac{H^{\kappa-1}}{\varepsilon^s} \frac{1}{p^{k-1}}.$$

If the mesh is not sufficiently refined, i.e., in this case $H \gtrsim c(p)\varepsilon^{\frac{s}{\kappa+1}}$, then the a priori error estimate is larger than 1 and thus has no meaning. The pre-asymptotic effect is illustrated in the following Example 2.1.

Example 2.1 (Pre-asymptotic effect of the FEM)**.** The following example presents the pre-asymptotic effect of the FEM on the example of the $Q1$-FEM, i.e., we choose piece-wise linear functions $\bar{V}_H$ with $p = 1$. Given is a set of coefficients as shown in Figure 2.1. Here, the coefficient A_ε portrayed on the left-hand side oscillates on the fine scale $\varepsilon = 2^{-8}$. The other group of six coefficients from left to right, top to bottom oscillate on scales $\varepsilon = 2^{-7}$, $\varepsilon = 2^{-6}$, $\varepsilon = 2^{-5}$, $\varepsilon = 2^{-4}$, $\varepsilon = 2^{-3}$, and $\varepsilon = 2^{-2}$, respectively. For each coefficient we have $\alpha = 1$ and $\beta = 10$. The right-hand side is given by $f(x) \equiv 1$ on the domain $\Omega = (0, 1)^2$.

Table 2.1: Relative errors in the H_0^1-norm and the corresponding experimental order of convergence for two different values of ε.

H	**Error** $\varepsilon = 2^{-2}$	**EOC**	**Error** $\varepsilon = 2^{-7}$	**EOC**
2^{-1}	0.7578921333998212	—	0.717113735857691	—
2^{-2}	0.6266807004252238	0.27	0.5822603920573785	0.30
2^{-3}	0.3266826068230689	0.94	0.5367775359346275	0.12
2^{-4}	0.1661367476997543	0.98	0.5214845101011764	0.04
2^{-5}	0.08363309007953967	0.99	0.5086409327593817	0.04
2^{-6}	0.0418083452389872	1.00	0.46659432955366825	0.12
2^{-7}	0.02050681218667057	1.03	0.2553376156476374	0.87
2^{-8}	0.009216291041980315	1.15	0.13081604737188351	0.96

Considering that we use first-order finite element, we should expect an error convergence of order $\mathcal{O}(H)$. However, here comes into play that the coefficient have fine-scale oscillations. Let us assume for the moment that the solution has the regularity $u \in H^2(\Omega)$. Then the norm of the second-order derivative of the solution scales like $\mathcal{O}(\varepsilon^{-1})$ which would dominate the mesh size for coarse meshes. This confirms the discussion above, that we obtain the pre-asymptotic effect of the FEM for coarse mesh sizes, that is also observed as the error stagnates in Figure 2.2. Once the oscillation scale is finally resolved by the mesh size, here $H \approx \varepsilon$, we observe that the error is eventually converging. Here, the convergence appears to be almost first order. This could be explained either by the fact that the solution is almost in $H^2(\Omega)$, or by the fact that the error estimate for the hp-FEM in (2.19) only required that the solution has the necessary regularity on the mesh, i.e., $u \in H^k(\mathcal{T}_H)$.

This example outlines the difficulties that arise when dealing with non-smooth, highly oscillatory coefficients. First, we need to put in a large amount of computational power to solve the PDE numerically for mesh sizes that resolve the fine-scale. This is even more apparent when moving away from elliptic problems and considering time-dependent PDEs. In that case these resulting large system need to be solved for each discrete time step which multiplies the large costs. Furthermore, even if the oscillation scale is resolved, there is no guarantee that the solution is satisfying. Taking a look into Figure 2.2, we observe that, e.g., for $\varepsilon = 2^{-6}$ the error

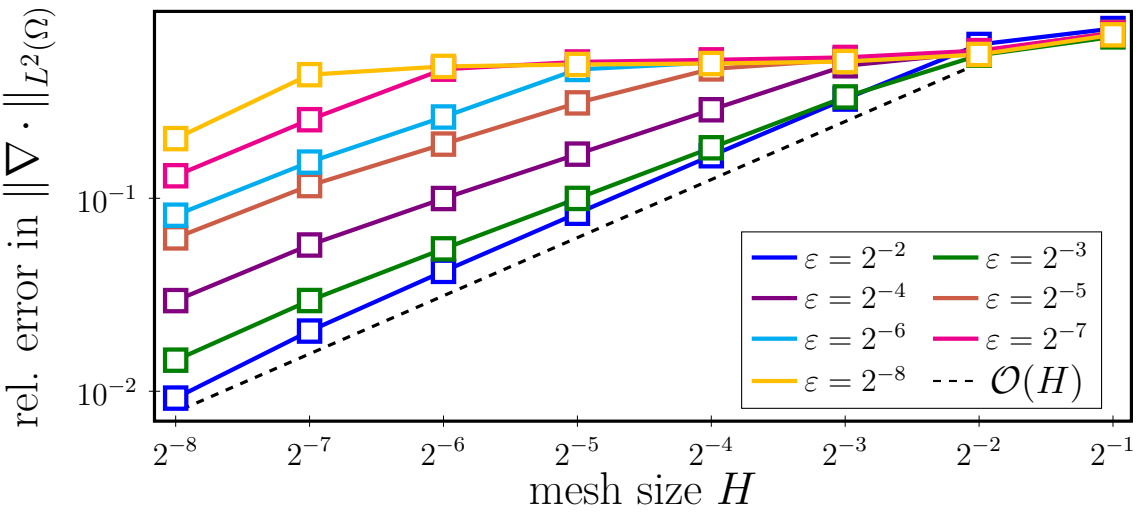

Figure 2.2: Relative errors in the H_0^1-norm $\|\nabla \cdot\|_{L^2(\Omega)}$ for the $Q1$-FEM for different mesh sizes H. Each line represents the error of the FEM-solution for a different coefficient from Figure 2.1 that oscillate on different scales.

of the FEM is barely below 10% for the mesh size $H = 2^{-8}$. Another problem with the FEM is that even once the fine-scale is resolved, the error convergence is still influenced by the regularity of the solution, and we may have very slow convergence. Lastly, if there is no a priori knowledge on the size of the oscillations in the material, there is also no indicator how to properly choose the mesh refinement. In this case, we have no guess whether the FEM solution is at all accurate.

This example motivates the use of numerical homogenization methods that are suited to the oscillatory behavior of the coefficient. In the following section we present an approach to overcome the pre-asymptotic effect of the FEM, that allows us to work with coarse meshes $\mathcal{T}_H$. We show that the error scales ε-independently, and independent of the regularity of the solution like $\mathcal{O}(H^\kappa)$ for some $\kappa \in \mathbb{N}$.

2.2 Numerical homogenization

In the previous section, we demonstrated how the classical FEM suffers from pre-asymptotic effects which leads to a stagnation of the energy error at mesh size H that do not resolve all oscillations of the PDE coefficient. Thus, there is a need for newly problem-adapted methods that effectively deal with the reduced convergence while reducing the computational overhead. The construction in this section follows the work (Krumbiegel and Maier, 2025).

2.2.1 Prototypical higher-order LOD

A prominent example for numerical homogenization is the localized orthogonal decomposition (LOD) method. The LOD method was first introduced by Målqvist and Peterseim (2014) applied to the elliptic model problem (2.1). The main idea of the LOD method is to construct a coarse scale space by adapting polynomials using so-called *corrections* that incorporate the oscillatory behavior of the coefficient.

A higher-order extension of the LOD (ho-LOD) method was introduced by Maier (2021) and uses higher-order discontinuous polynomials as basis for the construction of the coarse multiscale space, where the new space is set up using basis functions that are minimized with respect to the energy norm. The localization of this method (more details in Section 2.3) is suboptimal as the error made by the localization scales with the inverse of the mesh size. The method was refined by Dong, Hauck, and Maier (2023), where these pollution effects when localization is introduced were mitigated. This section introduces the ho-LOD method from (Maier, 2021) and follows the work by Krumbiegel and Maier (2025), while adding details from the previously mentioned works.

As demonstrated in Example 2.1, the FEM space $\bar{V}_H$, which also holds for V_H, is not well-suited for the approximation of the solution u to the variational problem (2.3). This results from the nature of coarse space $\bar{V}_H$ that is not integrating any information about the oscillatory behavior of the coefficient A. This stems from the fact that the coarse polynomials are unable to capture all fine oscillations that are present on the solution u.

The idea of the ho-LOD method is to obtain information that lie in the *fine-scale space*, sometimes also referred to as the detail space, which is defined to be the kernel

$$W \coloneqq \ker \Pi_H|_{H_0^1(\Omega)}$$

of the L^2-projection into the discontinuous space V_H. The information is obtained via the *correction operator* $\mathcal{C}\colon H_0^1(\Omega) \to W$, which is defined for any $v \in H_0^1(\Omega)$ as the orthogonal projection $\mathcal{C}v \in W$ into the kernel space with respect to the energy inner product $a(\,\cdot\,,\,\cdot\,)$, i.e.,

$$a(\mathcal{C}v, w) = a(v, w), \tag{2.20}$$

for all $w \in W$.

In the classical LOD setting the space $\bar{V}_H$ is considered for $p = 1$. Here, the polynomial space $\bar{V}_H \subset H_0^1(\Omega)$ is conforming, and the multiscale space can readily be defined by $(\mathrm{id} - \mathcal{C})\bar{V}_H$. However, for the discontinuous space V_H this construction is not possible since we require the multiscale space to be a conforming subspace, such that we need to adapt the approach. The idea is to create a conforming function space $B_H \subset H_0^1(\Omega)$ that has equal L^2-projections as the discontinuous polynomial space, i.e., $\Pi_H B_H = V_H$. The existence of such a function space can be derived from the following lemma.

Lemma 2.1 (Maier (2021, Cor. 3.6))**.** *Let $\{K_j\}_{j=1}^N \subset \mathcal{T}_H$ be a set of elements and $v_H \in V_H$ such that*

$$v_H|_{\Omega\setminus R} = 0, \quad \text{where } R = \bigcup_{j=1}^{N} K_j. \tag{2.21}$$

Then, there exists a function $b \in H_0^1(R)$ with $b|_{\Omega\setminus R} = 0$ such that $\Pi_H b = v_H$ and

$$\|\nabla b\|_{L^2(R)} \leq C_{\mathrm{b}} \frac{p^2}{H} \|v_H\|_{L^2(R)}. \tag{2.22}$$

To create the conforming space, let us first introduce a basis $\bigcup_{K\in\mathcal{T}_H} \{\Lambda_{K,j}\}_{j=1}^{(p+1)^d}$ of the space V_H, where $\Lambda_{K,j}(x) = \prod_{n=1}^d L_n(x_n)$ is the product of one-dimensional Legendre polynomials L_n of degree $p_n \leq p$ shifted to the element K. Here, we implicitly require a mapping, that maps each index $j \mapsto (p_1, \dots, p_d)$ to a multi-index of polynomial degrees. We note that this mapping can be chosen arbitrarily. From Lemma 2.1 it follows, that there exists a *bubble function* $b_{K,j} \in H_0^1(K)$ to each Legendre basis function $\Lambda_{K,j}$ such that $\Pi_H b_{K,j} = \Lambda_{K,j}$. Employing the bubble functions as basis functions, we define the *bubble space* as the conforming subspace

$$B_H \coloneqq \operatorname{span} \bigcup_{K\in\mathcal{T}_H} \{b_{K,j}\}_{j=1}^{(p+1)^d} \subset H_0^1(\Omega). \tag{2.23}$$

Next, define the *bubble operator*

$$\mathcal{B}_H \colon V_H \to B_H, \qquad \Lambda_{K,j} \mapsto \mathcal{B}_H \Lambda_{K,j} = b_{K,j}, \tag{2.24}$$

that maps each Legendre basis function to a corresponding bubble function, and is extended linearly to the whole space V_H. Furthermore, the bubble operator can be extended to $L^2(\Omega)$ by concatenation with the L^2-projection, i.e., $\mathcal{B}_H = \mathcal{B}_H \circ \Pi_H$. By Lemma 2.1 we have the following stability of the bubble operator for any $v \in L^2(K)$

$$\|\nabla \mathcal{B}_H v\|_{L^2(K)} \leq C_{\mathrm{b}} \frac{p^2}{H} \|v\|_{L^2(K)}. \tag{2.25}$$

The space B_H has by construction the same coarse dimension as the discontinuous polynomial space V_H. Furthermore, from Lemma 2.1 it follows that the bubble functions retain the local support of the underlying Legendre basis functions. This important property is crucial for the localization of the multiscale basis functions in Section 2.3. In the spirit of the (classical) LOD method, we can now apply the correction operator $\mathcal{C}$ to the bubble functions. This leads to the definition of the *prototypical multiscale space* $\widetilde{V}_H$ given by

$$\widetilde{V}_H = (\mathrm{id} - \mathcal{C}) B_H. \tag{2.26}$$

Furthermore, define the prototypical multiscale basis function canonically by

$$\tilde{\Lambda}_{K,j} = (\mathrm{id} - \mathcal{C}) b_{K,j}. \tag{2.27}$$

In this instance 'prototypical' refers to the non-localized version of ho-LOD spaces and methods. More precisely, we have that the basis functions are defined globally on the whole domain. This is indicated in Figure 2.3, where in the last row examples of prototypical multiscale functions are portrayed. There, the support of the multiscale basis functions in increased with respect to the bubbles, and in fact the support is the whole domain Ω. These global basis functions result in high computational costs which would make this method unfeasible in practice. However, in Section 2.3, we find that they decay exponentially away from the support of the bubble functions and this makes it possible to localize the multiscale basis functions to subdomains. Thus, the prototypical setting presented here is an ideal setting, that is practically unfeasible.

By construction, we have that the dimensions of the multiscale space $\widetilde{V}_H$ and the discontinuous polynomial space V_H coincide, i.e., $\dim(\widetilde{V}_H) = \dim(V_H)$. Furthermore, the multiscale space $\widetilde{V}_H$ and the fine-scale space W are orthogonal with respect to the energy inner product $a(\,\cdot\,,\,\cdot\,)$ and together span the whole space $H_0^1(\Omega)$, i.e.,

$$H_0^1(\Omega) = \widetilde{V}_H \oplus_a W. \tag{2.28}$$

This can be seen by the following. Let $v \in H_0^1(\Omega)$ be chosen arbitrarily. Then we have that

$$(\mathrm{id} - \mathcal{B}_H) v \in W,$$

and thus also

$$\begin{aligned} (\mathrm{id} - \mathcal{C}) v &= (\mathrm{id} - \mathcal{C}) \mathcal{B}_H v + (\mathrm{id} - \mathcal{C})(\mathrm{id} - \mathcal{B}_H) v \\ &= (\mathrm{id} - \mathcal{C}) \mathcal{B}_H v \in \widetilde{V}_H. \end{aligned} \tag{2.29}$$

Overall this yields

$$\begin{aligned} v &= (\mathrm{id} - \mathcal{C}) v + \mathcal{C} v \\ &= (\mathrm{id} - \mathcal{C}) \mathcal{B}_H v + \mathcal{C} v \in \widetilde{V}_H + W, \end{aligned}$$

which shows that

$$H_0^1(\Omega) \subset \widetilde{V}_H + W.$$

With this property the orthogonal decomposition (2.28) follows since both spaces $\widetilde{V}_H$ and W are conforming, and the a-orthogonality

$$a((\mathrm{id} - \mathcal{C}) v, w) = 0$$

for all $w \in W$. This important property will be used later to show the higher-order convergence rate of the ho-LOD method.

Remark 2.2 (Construction of the bubble functions). In practice, it is possible to construct a basis of the multiscale space $\widetilde{V}_H$ defined in (2.26) without constructing any bubble functions corresponding to Legendre basis functions. This is done by solving a minimization problem, see Section 2.3.1. However, once localization of the multiscale basis functions is introduced, it becomes necessary to explicitly calculate some bubble functions. This can be done in practice by solving a local $(p+1)^d \times (p+1)^d$ linear system, see (Dong, Hauck, and Maier, 2023, Rem. 7.1) for a thorough construction.

Figure 2.3 shows an example of bubble functions $b_{K,1}$, with their corresponding multiscale basis functions $\tilde{\Lambda}_{K,1}$. Here, we can observe that the bubble functions are as opposed to the constant Legendre polynomial $\Lambda_{K,1}$ in the space $H^1_0(K)$. Further, on the left column the polynomial space is constructed with $p = 0$ and on the right column with $p = 2$. Here, we see that dependent on the polynomial degree p, the bubble functions may differ.

In the last row of Figure 2.3 the multiscale basis functions $\tilde{\Lambda}_{K,j}$ are portrayed that correspond to the bubble functions in their respective column. We observe that the functions inherit a similar structure but appear to have an increased support than the element K. In fact the prototypical multiscale basis function are globally defined on the domain Ω. This comes with large computational costs. However, as indicated in the plots these multiscale basis functions have an (exponential) decay property away from the support of the corresponding bubble functions. This is a crucial attribute that allows truncation of the underlying support and yields a computationally feasible method, for more details see the following Section 2.3.

Prototypical p-LOD method. We now use the conforming higher-order multiscale space as trial and test space in the variational formulation of the elliptic model problem (2.3). This yields the following prototypical ho-LOD method, known as the *prototypical p-LOD method*. Seek a function $\tilde{u}_H \in \widetilde{V}_H$ such that

$$a(\tilde{u}_H, \tilde{v}_H) = (f, \tilde{v}_H)_{L^2(\Omega)}, \tag{2.30}$$

for all $\tilde{v}_H \in \widetilde{V}_H$. The existence and uniqueness of the solution $\tilde{u}_H$ follows directly from the Lax-Milgram theorem, and the error of the prototypical p-LOD method reads as follows.

Theorem 2.2 (Error of the prototypical p-LOD method)**.** *Let $f \in H^k(\mathcal{T}_H)$ for some $k \in \mathbb{N}_0$. Further, let $u \in H^1_0(\Omega)$ be the solution to* (2.3)*, and $\tilde{u}_H \in \widetilde{V}_H$ be the solution to* (2.30)*. Then, the following error estimate holds*

$$\|\nabla(u - \tilde{u}_H)\|_{L^2(\Omega)} \lesssim \frac{C_{\mathrm{pr}}^2}{\alpha} \frac{\Phi(p,\kappa)}{p+1} H^{\kappa+1} \|f\|_{H^\kappa(\mathcal{T}_H)}, \tag{2.31}$$

where $\kappa = \min\{k, p+1\}$, and the constant is independent of H, p, and the oscillations of the coefficient A.

Proof. The proof is similar to (Maier, 2021, Thm. 3.1). Since $\widetilde{V}_H \subset H_0^1(\Omega)$, we have a conforming method, and thus the Galerkin orthogonality holds, see (2.17),

$$a(u - \tilde{u}_H, \tilde{v}_H) = 0. \tag{2.32}$$

The Galerkin orthogonality shows that the error $u - \tilde{u}_H$ is orthogonal to $\widetilde{V}_H$ with respect to the energy inner product $a(\,\cdot\,,\,\cdot\,)$. Employing the orthogonal decomposition (2.28) we have that the error lies in the fine-scale space

$$u - \tilde{u}_H \in W. \tag{2.33}$$

Thus, we can show the convergence rates in the theorem in the next two steps. First, we use the coercivity (2.6) to bound the square of the H_0^1-error by the energy inner product, then we employ the Galerkin orthogonality (2.32) and the variational formulation (2.3) to obtain

$$\begin{aligned} \alpha \|\nabla(u - \tilde{u}_H)\|_{L^2(\Omega)}^2 &\leq a(u - \tilde{u}_H, u - \tilde{u}_H) \\ &= a(u, u - \tilde{u}_H) \\ &= (f, u - \tilde{u}_H)_{L^2(\Omega)}. \end{aligned} \tag{2.34}$$

Finally, we make use of the fact that the error lies in the fine-scale space (2.33), i.e., we have $\Pi_H(u - \tilde{u}_H) = 0$. This and Cauchy-Schwarz inequality with the approximation property (2.13) of the L^2-projection leads to

$$\begin{aligned} (f, u - \tilde{u}_H)_{L^2(\Omega)} &= ((\mathrm{id} - \Pi_H) f, (\mathrm{id} - \Pi_H)(u - \tilde{u}_H))_{L^2(\Omega)} \\ &\leq \|(\mathrm{id} - \Pi_H) f\|_{L^2(\Omega)} \|(\mathrm{id} - \Pi_H)(u - \tilde{u}_H)\|_{L^2(\Omega)} \\ &\lesssim C_{\mathrm{pr}}^2 \frac{\Phi(p, \kappa)}{p+1} H^{\kappa+1} \|f\|_{H^\kappa(\mathcal{T}_H)} \|\nabla(u - \tilde{u}_H)\|_{L^2(\Omega)}, \end{aligned} \tag{2.35}$$

The error estimate (2.31) now follows by combining the estimate (2.34) with (2.35) and dividing by $\alpha \|\nabla(u - \tilde{u}_H)\|_{L^2(\Omega)}$. □

Remark 2.3 (L^2-error estimate for the prototypical p-LOD method). It is possible to derive an L^2-error estimate for the p-LOD method employing $\Pi_H(u - \tilde{u}_H) = 0$. That is, we have

$$\begin{aligned} \|u - \tilde{u}_H\|_{L^2(\Omega)} &= \|(\mathrm{id} - \Pi_H)(u - \tilde{u}_H)\|_{L^2(\Omega)} \\ &\lesssim C_{\mathrm{pr}} \frac{1}{p+1} H \|\nabla(u - \tilde{u}_H)\|_{L^2(\Omega)}. \end{aligned}$$

Theorem 2.2 yields the L^2-error estimate

$$\|u - \tilde{u}_H\|_{L^2(\Omega)} \lesssim \frac{C_{\mathrm{pr}}^3}{\alpha} \frac{\Phi(p, \kappa)}{(p+1)^2} H^{\kappa+2} \|f\|_{H^\kappa(\mathcal{T}_H)},$$

where $\kappa = \min\{k, p+1\}$. □

In practice, the corrector problem (2.20) with the bubble functions $b_{K,j} \in H_0^1(\Omega)$ on the right-hand side needs to be discretized as well to obtain a computable method. This is typically done by simply replacing the full space $H_0^1(\Omega)$ with a discrete subspace $\bar{V}_h \subset H_0^1(\Omega)$ in similar fashion to (2.16). Note that we require $h \lesssim \varepsilon$. In this setting the bubble functions in the construction are replaced by discrete bubble function in the sense that $b_{K,j} \in \bar{V}_h(K) \subset H_0^1(K)$. For a detailed analysis of the existence of such discrete bubble functions, we refer to Maier (2021, Sec. 4.3).

The prototypical p-LOD method then approximates the fine FEM solution u_h to (2.16) which then has the same error bounds with respect to the coarse mesh size H. Furthermore, we can also apply the error estimate (2.19) to obtain an error bound of the fully-discrete prototypical p-LOD method (cf. (Maier, 2021, Thm. 4.9))

$$\begin{aligned} \|\nabla(u - \tilde{u}_H)\|_{L^2(\Omega)} &\leq \|\nabla(u - u_h)\|_{L^2(\Omega)} + \|\nabla(u_h - \tilde{u}_H)\|_{L^2(\Omega)} \\ &\lesssim \|\nabla(u - u_h)\|_{L^2(\Omega)} + H^{\kappa+1}\|f\|_{H^k(\mathcal{T}_H)}, \end{aligned} \tag{2.36}$$

where $\kappa = \min\{k, p+1\}$ as above. Note that for the numerical experiments, we construct $\bar{V}_h$ with $p = 1$, which is reasonable as we cannot expect higher regularity (≥ 2) of the solution. This error estimate can be interpreted in the way that we can get arbitrarily close to a fine FEM solution of the problem, however the error to the exact solution to the PDE is then bounded by the fine FEM error.

2.3 Localization

This section is concerned with the localization of the multiscale basis functions $\tilde{\Lambda}_{K,j}$. As mentioned in Remark 2.2, the multiscale basis functions generally infer globally defined functions, which comes with a large computational overhead if the prototypical p-LOD method (2.30) has to be solved, where the system matrix is a dense stiffness matrix. However, the plots in the last row of Figure 2.3 indicate that the multiscale basis functions have a decay away from the support of the corresponding bubble functions. This promotes the idea to truncate the domain on which the multiscale basis functions are calculated. In fact, it can be rigorously proven, that the $\tilde{\Lambda}_{K,j}$ obey an exponential decay away from the element K.

In the literature there exist different localization strategies, which we briefly mention here. The original p-LOD was introduced in (Maier, 2021). It constructs its multiscale basis functions using an energy-minimizer subject to a constraint. In the global (i.e. without localization) setting the p-LOD method is equivalent to the construction from Section 2.2.1. However, the localization strategy introduces a suboptimal localization error constant. This was improved later by Dong, Hauck, and Maier (2023). We provide a short review in Section 2.3.1.

The localization strategy used in this thesis is based on the *stabilized p-LOD* (*sp*-LOD) method, cf. (Dong, Hauck, and Maier, 2023), that builds on the construction

given in Section 2.2.1. The sp-LOD method first adjusts the bubble functions corresponding to the constant Legendre polynomials to obtain a mesh-size-independent localization error bound. More details are given in Section 2.3.2.

2.3.1 Localization strategy of a higher-order LOD

In the work by Maier (2021), the author developed a localization strategy for the p-LOD method. The author showed that the multiscale basis functions can equivalently be obtained by minimizing the elliptic energy under the constraint that the L^2-projection is preserved. That minimization problem can then be localized to small subdomains and the localized multiscale basis functions can then be used similarly to the previous section. However, a drawback of this first localization strategy is that the localization error has mesh-dependent error constant, which can be observed in numerical experiments. This pollution has been dealt with in a later work by Dong, Hauck, and Maier (2023), that is summarized in Section 2.3.2. Here we first introduce the localization strategy from (Maier, 2021), see also (Maier, 2020).

First, we define the operator

$$\mathcal{R} \coloneqq \mathrm{id} - \mathcal{C}. \tag{2.37}$$

Then, by (Maier, 2020, Rem. 2.3.4) we have that this operator can equivalently be defined for any $v_H \in V_H$ by the following constraint minimization problem

$$\mathcal{R}v_H \coloneqq \operatorname*{argmin}_{v \in H_0^1(\Omega)} a(v,v), \qquad \text{s.t.} \qquad \Pi_H v = v_H. \tag{2.38}$$

As indicated in Remark 2.2 the multiscale basis functions $\tilde{\Lambda}_{K,j}$ decay exponentially away from the support of the corresponding Legendre basis functions $\Lambda_{K,j}$. To define the localized multiscale basis functions on subdomains, we define for any $\ell \in \mathbb{N}$ the ℓ-Patch $\mathtt{N}^\ell(S)$ around a subdomain $S \subset \Omega$, recursively, by

$$\mathtt{N}^1(S) \coloneqq \operatorname{int} \bigcup \{\overline{K} \in \mathcal{T}_H \mid \overline{K} \cap \overline{S} \neq \emptyset\}, \qquad \mathtt{N}^{\ell+1}(S) = \mathtt{N}^1(\mathtt{N}^\ell(S)), \quad \ell \in \mathbb{N}. \tag{2.39}$$

In the following we also abbreviate $\mathtt{N}(S) = \mathtt{N}^1(S)$, and $\mathtt{N}^0(S) = S$.

The localized operator is now defined for any basis function $\Lambda_{K,j}$ by solving the following minimization problem

$$\mathcal{R}^{[\ell]}\Lambda_{K,j} \coloneqq \operatorname*{argmin}_{v \in H_0^1(\mathtt{N}^\ell(K))} a(v,v), \qquad \text{s.t.} \qquad \Pi_H v = \Lambda_{K,j}. \tag{2.40}$$

The corresponding localized multiscale space is then defined as the span of the basis functions

$$\widetilde{U}_H^{[\ell]} = \operatorname{span} \bigcup_{K \in \mathcal{T}_H} \{\mathcal{R}^{[\ell]}\Lambda_{K,j}\}_{j=1}^{(p+1)^d}. \tag{2.41}$$

p-LOD method. The p-LOD method seeks a function $\tilde{u}_H \in \widetilde{U}_H^{[\ell]}$ such that

$$a(\tilde{u}_H, \tilde{v}_H) = (f, \tilde{v}_H)_{L^2(\Omega)}, \tag{2.42}$$

for all $\tilde{v}_H \in \widetilde{U}_H^{[\ell]}$. The p-LOD method then has the following error estimate

Theorem 2.3 (Error of the p-LOD method (Maier, 2021, Thm 4.4))**.** *Let $\ell \in \mathbb{N}$ and $f \in H^k(\mathcal{T}_H)$. Further, let $u \in H_0^1(\Omega)$ be the weak solution to* (2.3) *and $\tilde{u}_H \in \widetilde{U}_H^{[\ell]}$ be the solution to* (2.42)*. Then*

$$\|\nabla(u - \tilde{u}_H)\|_{L^2(\Omega)} \lesssim H^{\kappa+1}\|f\|_{H^k(\mathcal{T}_H)} + H^{-1}\ell^{\frac{d-1}{2}}\exp(-C\ell)\|f\|_{L^2(\Omega)}, \tag{2.43}$$

where $\kappa = \min\{k, p+1\}$.

Here, we can observe the factor H^{-1} in front of the second term on the right-hand side of (2.43). This pollution can be seen in the convergence plots Figure 2.6. That is, if ℓ is chosen a priori, then refining the mesh might result in an overall worse error. More information is provided in Example 2.5.

2.3.2 Stabilization of the localization strategy

The localization strategy presented in the work by Dong, Hauck, and Maier (2023) is based on the correction operator $\mathcal{C}$ and splits it into its element-wise contributions. The image of each of these contributions have an exponential decay, which can be used to localize them to patches and subsequently put together for a localized correction operator. However, in order to obtain a mesh-size-independent localization bound, the bubble functions $b_{K,1}$ corresponding to the constant Legendre polynomials need to be slightly adjusted. This section follows the works by Krumbiegel and Maier (2025) and Dong, Hauck, and Maier (2023).

We start by defining the *element-wise correction operator* $\mathcal{C}_K \colon H_0^1(\Omega) \to W$ for any $v \in H_0^1(\Omega)$ as the solution $\mathcal{C}_K v \in W$ to

$$a(\mathcal{C}_K v, w) = a|_K(v, w) \tag{2.44}$$

for all $w \in W$, where the restriction of the inner product is given by

$$a|_K(v, w) = \int_K A\nabla v \cdot \nabla w \,\mathrm{d}x$$

for all $v, w \in H_0^1(\Omega)$. Then by definition we have

$$\mathcal{C} = \sum_{K \in \mathcal{T}_H} \mathcal{C}_K.$$

The element-wise correction operators $\mathcal{C}_K$ are subject to the following exponential decay away from the element $K \in \mathcal{T}_H$.

Lemma 2.4 (Dong, Hauck, and Maier (2023, Lem. 5.1))**.** *There exists a constant $C_\mathrm{d} > 0$, independent of H, ℓ, K, such that for all $K \in \mathcal{T}_H$, $v \in H_0^1(\Omega)$, and $\ell \in \mathbb{N}$ we have*

$$\|\nabla \mathcal{C}_K v\|_{L^2(\Omega \setminus \mathtt{N}^\ell(K))} \leq \exp(-C_\mathrm{d}\ell)\|\nabla \mathcal{C}_K v\|_{L^2(\Omega)}. \tag{2.45}$$

We provide this lemma without proof as the proof is similar to the one provided for Lemma 3.17. We denote with $W(\mathtt{N}^\ell(K))$ the restriction, in the sense of localized support, of functions $w \in W$ to the patch $\mathtt{N}^\ell(K)$. The exponential decay result for the element-wise correction operator motivates the following construction of the *localized element-wise correction operators* $\mathcal{C}_K^{[\ell]} \colon H_0^1(\Omega) \to W(\mathtt{N}^\ell(K))$ given for any $v \in H_0^1(\Omega)$ as the solution $\mathcal{C}_K^{[\ell]} v$ to

$$a(\mathcal{C}_K^{[\ell]} v, w) = a|_K(v, w) \tag{2.46}$$

for all $w \in W(\mathtt{N}^\ell(K))$. The *localized correction operator* $\mathcal{C}^{[\ell]}$ is then defined by the sum of the element-wise counterparts

$$\mathcal{C}^{[\ell]} \coloneqq \sum_{K \in \mathcal{T}_H} \mathcal{C}_K^{[\ell]}. \tag{2.47}$$

If we choose $\ell \geq \frac{\operatorname{diam}\Omega}{H}$, which we formally denote by $\ell = \infty$, then the right-hand side of (2.46) is stated on the whole domain, and we have $\mathcal{C}_K^{[\infty]} = \mathcal{C}_K$ and $\mathcal{C}^{[\infty]} = \mathcal{C}$. For the localized correction operator we can employ the decay result in Lemma 2.4 to obtain the following localization error estimate.

Lemma 2.5 (Dong, Hauck, and Maier (2023, Lem. 5.2))**.** *There exists a constant $C_\mathrm{loc} > 0$, independent of H, ℓ, such that for all $v \in H_0^1(\Omega)$ and $\ell \in \mathbb{N}$ we have*

$$\|\nabla(\mathcal{C} - \mathcal{C}^{[\ell]})v\|_{L^2(\Omega)} \leq C_\mathrm{loc}\ell^{\frac{d}{2}} \exp(-C_\mathrm{d}\ell)\|\nabla v\|_{L^2(\Omega)}, \tag{2.48}$$

where C_d is the constant from Lemma 2.4.

The idea of the proof is to split the localized and global correction operators into their element-wise counterparts. Then, using that the patches have a finite overlap the estimate in Lemma 2.5 follows from the auxiliary lemma stated below. Again, we omit the proof as the subsequent Theorem 3.19 employs similar techniques. For completeness, we present (without proof) the following auxiliary lemma. The proof of this lemma is similar to the proof of Lemma 3.18.

Lemma 2.6 (Dong, Hauck, and Maier (2023, Lem. A.1))**.** *There exists a constant $C_\mathrm{E} > 0$, independent of H, ℓ, K, such that for all $v \in H_0^1(\Omega)$, $K \in \mathcal{T}_H$, and $\ell \in \mathbb{N}$ it holds*

$$\|\nabla(\mathcal{C}_K - \mathcal{C}_K^{[\ell]})v\|_{L^2(\Omega)} \leq C_\mathrm{E} \exp(-C_\mathrm{d}\ell)\|\nabla \mathcal{C}_K v\|_{L^2(\Omega)}, \tag{2.49}$$

where C_d is the constant from Lemma 2.4.

The straight-forward procedure going from this point would be by simply applying the localized correction operator to the bubble functions similarly to (2.26). That is, we replace the trial and test spaces in (2.30) by the localized spaces and seek a function $\tilde{u}_H \in (\mathrm{id} - \mathcal{C}^{[\ell]})B_H$ such that

$$a(\tilde{u}_H, \tilde{v}_H) = (f, \tilde{v}_H)_{L^2(\Omega)},$$

for all $\tilde{v}_H \in (\mathrm{id} - \mathcal{C}^{[\ell]})B_H$. However, this application is equivalent to the localization strategy presented in Section 2.3.1 and results in a suboptimal localization error, which results from the scaling of the bubble functions. Specifically, the first bubble function corresponding to the constant Legendre polynomial is not well-suited. Thus, in the following we construct a new set of bubble functions that have increased support but in return yield a much better localization result.

The stabilization of the p-LOD method as used by Dong, Hauck, and Maier (2023) utilizes a quasi-interpolation operator $\mathcal{P}_H$, see also (Altmann, Henning, and Peterseim, 2021, Ex. 3.11). The operator is given for any $v \in L^2(\Omega)$ by (see (Dong, Hauck, and Maier, 2023, eq. (3.6)))

$$\mathcal{P}_H v = \mathcal{I}_H v + \mathcal{B}_H(v - \mathcal{I}_H)v, \tag{2.50}$$

where the quasi-interpolation operator $\mathcal{I}_H = \mathcal{E}_H \circ \Pi_H^0$ onto continuous piece-wise linear polynomials is given as the concatenation of the L^2-projection Π_H^0 onto V_H for $p = 0$, and an averaging operator $\mathcal{E}_H$ onto $\bar{V}_H$ for $p = 1$. More precisely, the L^2-projection Π_H^0 onto piece-wise constants is given for any $v \in L^2(\Omega)$ by

$$(\Pi_H^0 v, v_H)_{L^2(\Omega)} = (v, v_H)_{L^2(\Omega)}$$

for all $v_H \in V_H$ defined with $p = 0$, and $\mathcal{E}_H$ is defined for any piece-wise constant $v_H \in V_H$ for $p = 0$ at any inner node $z \in \mathcal{T}_H$ by

$$(\mathcal{E}_H v_H)(z) = \frac{1}{|\{K \in \mathcal{T}_H \mid z \in K\}|} \sum_{K \in \mathcal{T}_H \,:\, z \in K} v_H|_K(z),$$

and $(\mathcal{E}_H v_H)(z) = 0$ for boundary nodes $z \in \Gamma$. The quasi-interpolation has the following properties.

Lemma 2.7 (Dong, Hauck, and Maier (2023, Lem. 3.3))**.** *The operator $\mathcal{P}_H$ is a projection, i.e., it satisfies $\mathcal{P}_H = \mathcal{P}_H^2$. Moreover, its kernel coincides with the kernel of Π_H, i.e.,*

$$\ker \Pi_H = \ker \mathcal{P}_H.$$

Further, there exists a constant $C_{\mathrm{xb}} > 0$, which solely depends on the regularity of the mesh $\mathcal{T}_H$, such that for all $v \in H_0^1(\Omega)$ and $K \in \mathcal{T}_H$ holds

$$\|\nabla \mathcal{P}_H v\|_{L^2(K)} + H^{-1}\|(\mathrm{id} - \mathcal{P}_H)v\|_{L^2(K)} \leq C_{\mathrm{xb}} \|\nabla v\|_{L^2(\mathtt{N}(K))}. \tag{2.51}$$

Remark 2.4 (Effect of the extended bubble functions). By design, $\mathcal{P}_H$ only has an effect on the bubble functions $b_{K,1}$, see also (Dong, Hauck, and Maier, 2023, Lem. 6.1). In Figure 2.4 a bubble function $b_{K,1}$ on the left-hand side is portrayed. Note that this is the same function as in the previous Figure 2.3 and is the bubble function constructed from the constant Legendre polynomial. On the right-hand side we show the corresponding extended bubble function $\mathfrak{b}_{K,1} = \mathcal{P}_H b_{K,1}$. We can observe that the support of the functions is slightly increased. We refer to (Krumbiegel and Maier, 2025) for a constructive approach and a different illustration.

s*p*-LOD method. The extended bubble operator $\mathcal{P}_H$ is now used to construct the *extended bubble space* $U_H = \mathcal{P}_H V_H = \mathcal{P}_H L^2(\Omega) \subset H_0^1(\Omega)$. This conforming space can be used as the foundation to construct a localized multiscale space

$$\widetilde{V}_H^{[\ell]} = (\mathrm{id} - \mathcal{C}^{[\ell]}) U_H \tag{2.52}$$

that is able to overcome the pollution effect from the p-LOD method. This yields the following ho-LOD method, the so-called *stabilized p-LOD* (sp-LOD) method, that seeks a function $\tilde{u}_H \in \widetilde{V}_H^{[\ell]}$ such that

$$a(\tilde{u}_H, \tilde{v}_H) = (f, \tilde{v}_H)_{L^2(\Omega)} \tag{2.53}$$

for all $\tilde{v}_H \in \widetilde{V}_H^{[\ell]}$. We note that for $\ell = \infty$ this construction coincides with the construction of the prototypical p-LOD method in Section 2.2.1. The sp-LOD method now yields the following error estimate.

Theorem 2.8 (Error of the sp-LOD method (Dong, Hauck, and Maier, 2023, Thm. 6.2))**.** *Let $\ell \in \mathbb{N}$ and $f \in H^k(\mathcal{T}_H)$. Further, let $u \in H_0^1(\Omega)$ be the weak solution to* (2.3) *and $\tilde{u}_H \in \widetilde{V}_H^{[\ell]}$ be the solution to* (2.53)*, respectively. Then*

$$\|\nabla(u - \tilde{u}_H)\|_{L^2(\Omega)} \lesssim H^{\kappa+1} \|f\|_{H^k(\mathcal{T}_H)} + \ell^{\frac{d}{2}} \exp(-C_{\mathrm{d}} \ell) \|f\|_{L^2(\Omega)}, \tag{2.54}$$

where $\kappa = \min\{k, p+1\}$.

Again, we omit a proof of this theorem. However, we provide a rigorous proof with localization estimates of a ho-LOD method at a later stage in Theorem 3.24 (applied to the wave equation). The idea is to split the errors into two parts, the first part is the error of the prototypical method which can be bounded by Theorem 2.2 and a localization error, which can be bounded by inserting an ideal mapping into the discrete space $\widetilde{V}_H^{[\ell]}$ using Céas lemma, and applying Lemma 2.5.

Example 2.5. Here, we solve the elliptic model problem (2.3). We apply the localized versions of both the p-LOD and sp-LOD methods with polynomial degrees $0, \dots, 4$. The PDE coefficient A_1 is given in Figure 2.5 and has strong oscillations on the fine-scale $\varepsilon = 2^{-8}$. We prescribed zero boundary data and the source is given by

$$f(x) = 2\pi^2 \sin(\pi x_1) \sin(\pi x_2).$$

The reference solution is given as a FE solution $u_h \in V_h$ on a mesh with mesh size $h = 2^{-9}$. Herein, the right-hand side is sufficiently smooth, and we expect to observe the optimal error convergence of order $\mathcal{O}(H^{p+2})$. For every polynomial degree, if the localization parameter is chosen appropriately, we find that the optimal error convergence is observed for both the p-LOD and sp-LOD solutions. We also readily plotted the two different localization strategies together such that the effect of the stabilization can be observed comparing lines in the same color with each other. Generally, for the p-LOD method we find that once the localization parameter does not yield the optimal convergence, the error increases when refining the mesh. This pollution effect is stabilized by the sp-LOD, where it can be observed that the error reaches a plateau when decreasing the mesh size and keeping the localization parameter constant.

As this chapter was more of a review of the existing higher-order LOD methods, the upcoming chapter will feature the application to the wave equation and a completely novel method with a rigorous error analysis. In the following chapter we apply the sp-LOD method to the linear acoustic wave equation.

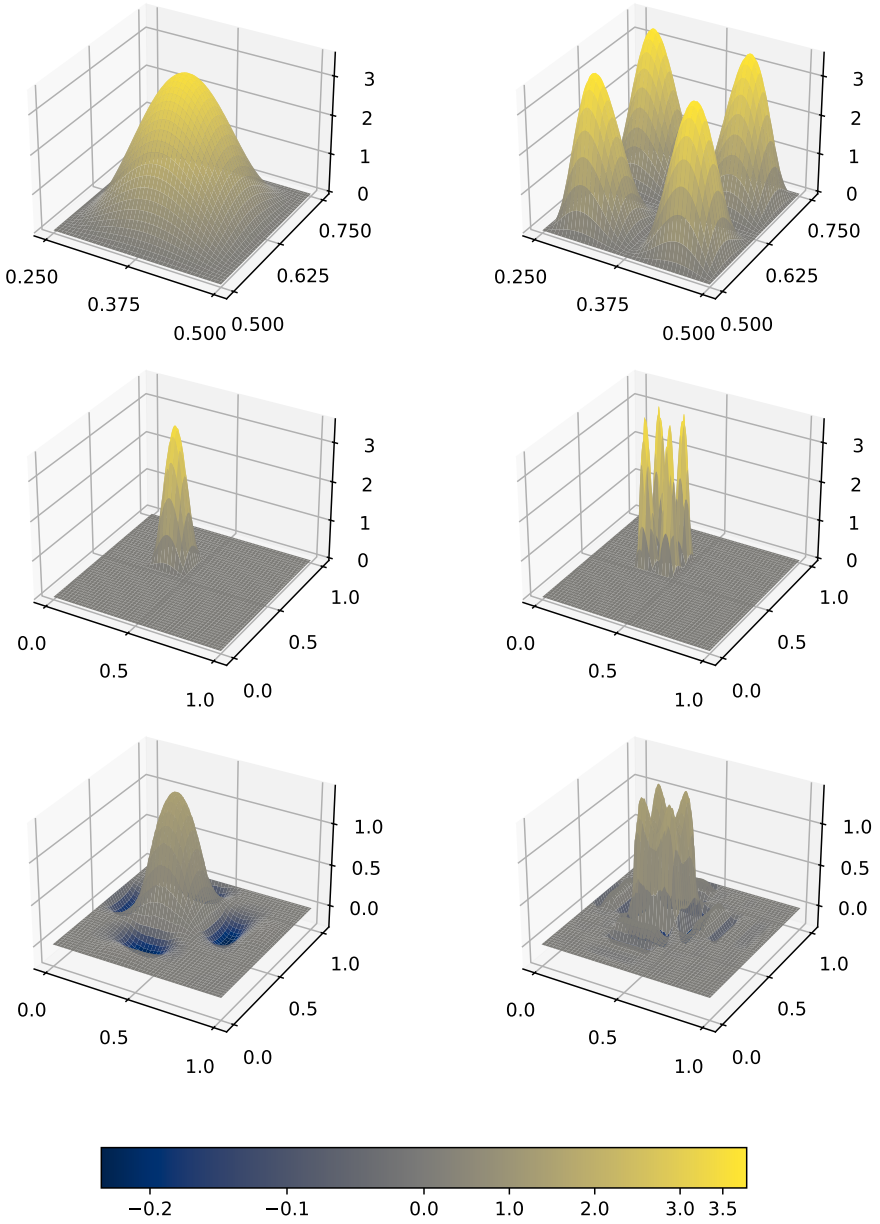

Figure 2.3: Portrayed are examples for bubble functions $b_{K,1}$ corresponding to a constant Legendre polynomial $\Lambda_{K,1}$ for the spaces V_H (with $p = 0$, left, and with $p = 2$, right). The first row shows $b_{K,1}$ locally on K, and the second row on the full domain Ω. In the third row the corrected multiscale basis functions $\tilde{\Lambda}_{K,1}$ corresponding to the bubble functions in their respective row can be observed.

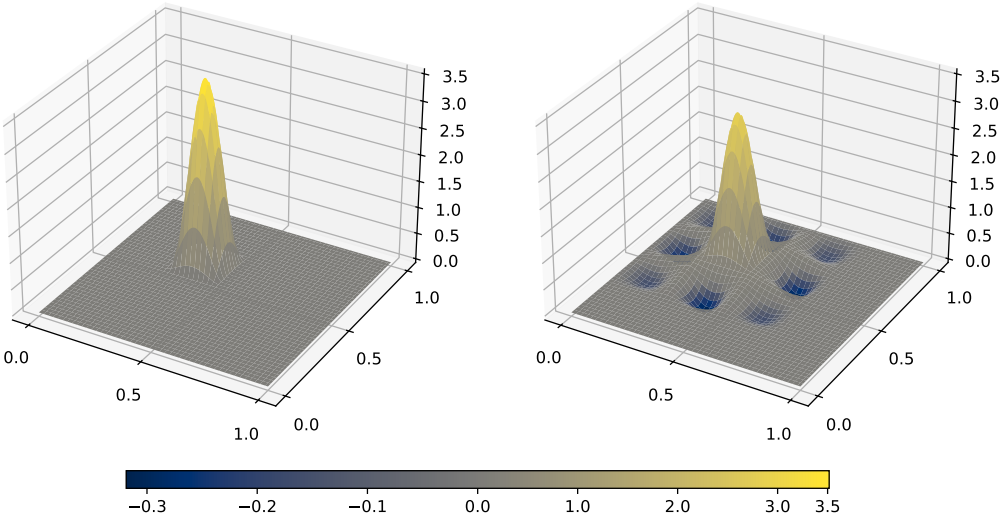

Figure 2.4: Portrayed is an example of a bubble function $b_{K,1}$ corresponding to the constant Legendre polynomial $\Lambda_{K,1}$ (left). The right-hand side shows the corresponding extended bubble function $\mathfrak{b}_{K,1}$ with increased support.

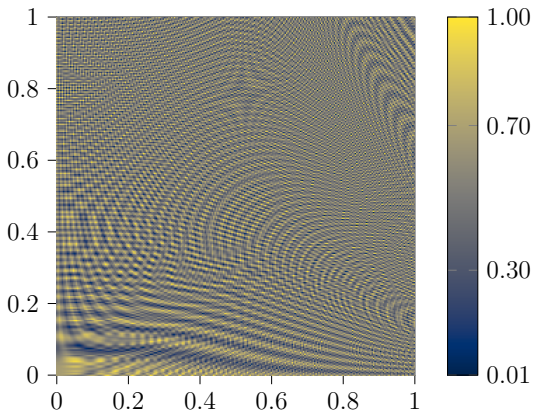

Figure 2.5: The plot above depicts a material coefficient A_1 that has some coarse structure with rapid jumps on a scale $\varepsilon = 2^{-8}$.

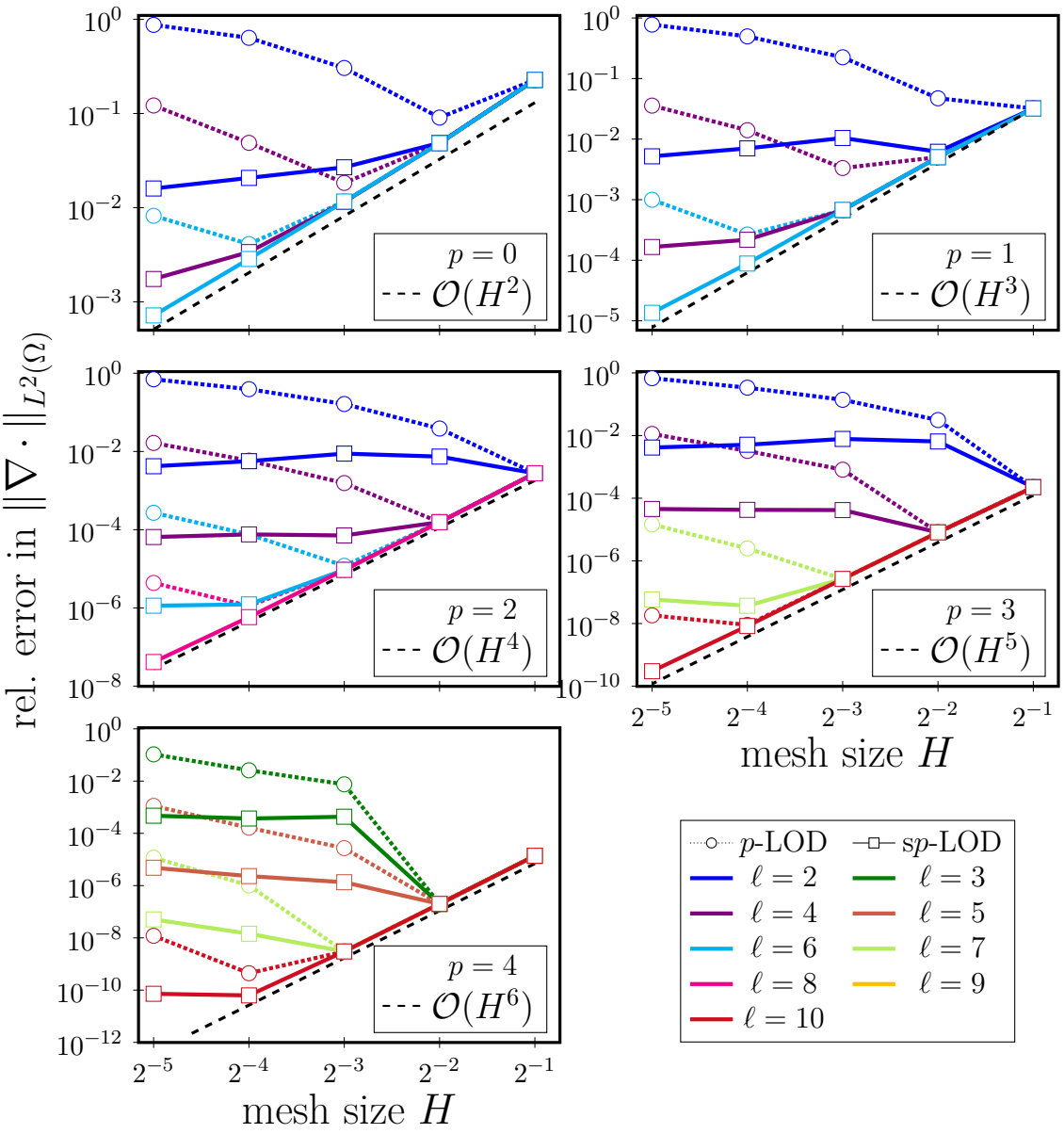

Figure 2.6: Relative errors in the norm $\|\nabla \cdot\|_{L^2(\Omega)}$ for the coefficient A_1 from figure 2.5 that oscillates on the scale $\varepsilon = 2^{-8}$. The plot shows four different polynomial degrees and compares the error for the localization strategy of the p-LOD in a dotted and the sp-LOD in a solid line.

3 Higher-order numerical homogenization for the wave equation

We transition now from foundational concepts, where we reviewed a higher-order localized orthogonal decomposition (ho-LOD) method applied to an elliptic model problem, to novel contribution, presenting the principal finding. First, we show that straight-forward application of the ho-LOD method results in a reduced error convergence. We revisit this result and present a solution that yields optimal higher-order convergence for wave equations. This chapter follows in major ways the works (Krumbiegel and Maier, 2025; Kalyanaraman, Krumbiegel, Maier, and Wang, 2025), where the method designed in the latter is herein adjusted to the acoustic wave equation.

Section 3.1 introduces the acoustic wave equation and the variational formulation that is the basis for the remainder of this thesis. Importantly, in this section we find the regularity assumptions on the data with a small discussion.

In Section 3.2, we apply the prototypical sp-LOD method from Section 2.2.1 to the acoustic wave equation. Note that in the prototypical setting, the sp-LOD and the p-LOD method coincide, and we denote the method for simplicity with sp-LOD. Here, we exclude the localization of the method to present the findings in the most modest way possible. The main discovery in this section is the suboptimal spatial error convergence of the prototypical sp-LOD method. In Chapter 2, we proved that for the elliptic model problem the convergence is $\mathcal{O}(H^{p+2})$ provided the right-hand side is sufficiently regular. However, for the wave equation, we show that error convergence of only $\mathcal{O}(H^2)$ can be expected even if the right-hand side has high spatial regularity. This section includes a complete semi-discrete error analysis.

This suboptimal convergence rate of the prototypical sp-LOD method in space invokes the need for an extension of the existing method that can recover the optimal rate of the elliptic setting for the wave equation. In the spirit of the LOD method, Section 3.3 defines a new operator that maps into the kernel space W and is thus able to obtain oscillations similar to the classical correction operator $\mathcal{C}$. This operator can then be used to enrich the existing (prototypical) multiscale space that then provably yields the optimal spatial convergence. This section analyzes an ideal (prototypical) scenario and gives a first idea how the so-called enriched correction can recover optimal convergence for the semi-discrete problem.

The principal finding is presented in Section 3.4. Here, we prove that the enriched correction operator obeys an exponential decay similar to the classical corrector. This decay can then be used to derive a localization result that eventually allows for

localization of all basis functions to patches of the same size. This very important property results in a higher-order numerical homogenization strategy that is computationally feasible. Further, we start with the localized multiscale spaces created by the sp-LOD method and enrich them with localized enriched corrections that we use as trial and test spaces and show that these spaces have the optimal convergence rate promised in the elliptic setting.

Finally, we combine the enriched higher-order LOD with a time discretization scheme in Section 3.5 and prove a fully-discrete error estimate.

3.1 Weak formulation and well-posedness

This section introduces the acoustic wave equation. We give regularity assumptions on the data that is required for the existence of a solution with a certain regularity. Similar to the elliptic setting, we cannot expect spatial regularity of the solution beyond second order. The novel method in this thesis, however, requires high temporal regularity of the solution and the right-hand side. For a more detailed analysis, refer to Remark 3.2.

3.1.1 Acoustic wave equation and variational formulation

We consider the following linear acoustic wave equation, where we seek a function u such that

$$\begin{aligned} \partial_t^2 u - \operatorname{div}(A\nabla u) &= f && \text{in } [0,T)\times\Omega,\\ u &= 0 && \text{on } [0,T)\times\Gamma,\\ u &= u_0 && \text{in } \{0\}\times\Omega,\\ \partial_t u &= v_0 && \text{in } \{0\}\times\Omega, \end{aligned} \tag{3.1}$$

where the domain Ω and boundary Γ are defined as in Section 2.1.1, with a given final time $T > 0$. Furthermore, let the coefficient A be defined as before in (2.2), specifically, it is constant in time. Recall, that the coefficient is highly oscillatory, and we assume for simplicity that there exists the smallest oscillation scale $\varepsilon > 0$. Similar to above, we assume that $f\colon [0,T] \to L^2(\Omega)$. The variational formulation seeks a function $u\colon [0,T] \to H_0^1(\Omega)$ such that

$$\langle \partial_t^2 u, v\rangle_{H^{-1}(\Omega)\times H_0^1(\Omega)} + a(u,v) = (f,v)_{L^2(\Omega)}, \tag{3.2}$$

for all $v \in H_0^1(\Omega)$ with the initial conditions given by $u(0,\cdot) = u_0$ and $\partial_t u(0,\cdot) = v_0$.

The following regularity assumptions on the right-hand side and the initial conditions ensure that a solution exists which is unique and has the appropriate regularity for the analysis in this section.

Assumption 3.1 (Compatibility and well-preparedness)**.** Let $k, m \in \mathbb{N}_0$. Consider the following well-preparedness and compatibility assumptions:

(A1) et $f \in C^m([0,T]; H^k(\mathcal{T}_H))$,
(A2) let $u(0) = u_0 \in H_0^1(\Omega)$, and $\partial_t u(0) = v_0 \in H_0^1(\Omega)$
(A3) let $\partial_t^\nu u(0) = \partial_t^{\nu-2} f(0) - \operatorname{div}(A\nabla\partial_t^{\nu-2}u(0)) \in H_0^1(\Omega)$, for $\nu = 2, \dots, m$,
(A4) let $\partial_t^{m+1} u(0) = \partial_t^{m-1} f(0) - \operatorname{div}(A\nabla\partial_t^{m-1}u(0)) \in L^2(\Omega)$,
(A5) there exists a constant C_{init} that is independent of ε, such that

$$\sum_{\nu=0}^{m} \|\partial_t^\nu u(0)\|_{H^1(\Omega)} + \|\partial_t^{m+1} u(0)\|_{L^2(\Omega)} \leq C_{\text{init}}.$$

From (Lions and Magenes, 1972; Evans, 2010) it follows employing Assumption 3.1 that a unique solution u to the variational formulation (3.2) exists, with

$$u \in C^m([0,T]; H_0^1(\Omega)) \cap C^{m+1}([0,T]; L^2(\Omega)). \tag{3.3}$$

Furthermore, the norm of the solution can be bounded by a constant independent of ε such that

$$\begin{aligned}\|u\|_{C^m([0,T];H_0^1(\Omega))} + \|u\|_{C^{m+1}([0,T];L^2(\Omega))} \\ \lesssim \|\partial_t^m u(0,\cdot)\|_{H_0^1(\Omega)} + \|\partial_t^{m+1} u(0,\cdot)\|_{L^2(\Omega)} + \|f\|_{C^m([0,T];L^2(\Omega))}.\end{aligned} \tag{3.4}$$

For readability, we denote with $C_{\text{data}} > 0$ a generic constant such that

$$\begin{aligned}&\sum_{\nu=0}^{m} \|u\|_{C^\nu([0,T];H^1(\Omega))} + \|u\|_{C^{m+1}([0,T];L^2(\Omega))} \\ &\qquad \lesssim \sum_{\nu=0}^{m} \|\partial_t^\nu u(0,\cdot)\|_{H^1(\Omega)} + \|\partial_t^{m+1} u(0,\cdot)\|_{L^2(\Omega)} + \sum_{\nu=0}^{m} \|f\|_{C^\nu([0,T];H^k(\mathcal{T}_H))} \\ &\qquad \lesssim C_{\text{data}}.\end{aligned} \tag{3.5}$$

We note that the C_{data} is defined here as a constant that is able to bound all norms of the right-hand side and initial conditions. This is merely a convenience and greatly reduces the size of equations. Furthermore, we have that since C_{init} is ε-independent the constant C_{data} is also independent of ε provided the norms of the right-hand side is independent of ε. However, this is reasonable to assume.

Remark 3.2 (Regularity). By the theory (Lions and Magenes, 1972), e.g., for the right hand-side the temporal regularity $f \in H^m(0,T; H^k(\mathcal{T}_H))$ is sufficient, however, Assumption 3.1 (A1) is made for simplicity. Furthermore, the existence of a solution with the given regularity and stability is given already for $k = 0$. Similar to the elliptic setting, however, we require higher regularity of the right-hand side on the mesh such that we can obtain higher-order convergence. This is a reasonable assumption as for classical methods higher regularity of the solution is typically assumed.

For $k = 0$, Assumption 3.1 is also referred to as the *well-preparedness and compatibility condition of order m* as introduced by Abdulle and Henning (2017). Consider the elliptic operator $\operatorname{div}(A\nabla u)$, then the condition essentially describes that by product rule, the derivative of the coefficient A is in general very rough, and the solution essentially needs to be very rough as well such that the whole term is in $L^2(\Omega)$. An interpretation of this condition is that waves that are travelling through a (highly heterogeneous) medium need to fit to the PDE at the initial time as well. This assumption can, e.g., be fulfilled if the initial data (and their temporal derivatives) is $u_0, v_0, f(0,\cdot) \equiv 0$. In Example 3.13 such an example is considered. We can interpret this case as a wave that is 0 before the initial time and then excited by an external source f at a certain point in time, and then travels through the material. Another interpretation is that if the wave is already travelling through a heterogeneous material, then the wave should have oscillatory behavior itself. Thus, if there is no source present, the wave already needs to fit the PDE and thus fulfil the equation at the initial time, which is considered by Assumption 3.1 (A3).

3.2 Numerical homogenization

In this section we apply the prototypical sp-LOD method to the acoustic wave equation. These results have been previously published in (Krumbiegel and Maier, 2025). Here, we find that for the wave equation, the prototypical sp-LOD method is not well-suited for spatial discretization as it obeys a reduced convergence rate than expected from higher-order methods. The reason is illustrated in the following. We know from Chapter 2 that classical FEMs require higher regularity of the solution to obtain higher-order convergence of the FE solution. This problem has been dealt with by the prototypical sp-LOD method that requires only regularity of the right-hand side. However, if we consider the wave equation as an elliptic problem for a single time $t \in [0,T]$,

$$a(u(t),v) = (f(t),v)_{L^2(\Omega)} - \langle \partial_t^2 u(t), v\rangle_{H^{-1}(\Omega)\times H_0^1(\Omega)}$$

then the right-hand side essentially consists of two functions, the function f and the second time derivative of the solution $\partial_t^2 u$. This is why the reduced convergence appears as we cannot expect the regularity of $\partial_t^2 u$ to exceed $H_0^1(\Omega)$. With similar arguments as for the elliptic error analysis Theorem 2.2 this only yields second-order convergence, as explained in more detail in the following.

3.2.1 Convergence order reduction for a prototypical higher-order LOD

As mentioned in the above introduction, we provide a detailed analysis for the observed reduced order convergence of the prototypical sp-LOD method.

Semi-discrete prototypical s*p*-LOD method. In a first step we use the prototypical multiscale space $\widetilde{V}_H$ defined in (2.26) as trial and test space for the variational wave equation (3.2). The *semi-discrete prototypical sp-LOD method* seeks a function $\tilde{u}_H \colon [0,T] \to \widetilde{V}_H$ such that

$$(\partial_t^2 \tilde{u}_H, \tilde{v}_H)_{L^2(\Omega)} + a(\tilde{u}_H, \tilde{v}_H) = (f, \tilde{v}_H)_{L^2(\Omega)} \tag{3.6}$$

for all $\tilde{v}_H \in \widetilde{V}_H$, and all times $t \in [0,T]$, where the initial conditions are given as the projections into the multiscale space

$$\tilde{u}_H(0) = \widetilde{\mathcal{P}} u_0, \qquad \partial_t \tilde{u}_H(0) = \widetilde{\mathcal{P}} v_0. \tag{3.7}$$

That is, the projection $\widetilde{\mathcal{P}} \colon H_0^1(\Omega) \to \widetilde{V}_H$ is defined for any $v \in H_0^1(\Omega)$ by

$$a(\widetilde{\mathcal{P}} v, \tilde{v}_H) = a(v, \tilde{v}_H) \tag{3.8}$$

for all $\tilde{v}_H \in \widetilde{V}_H$. By standard ODE theory, we have by Assumption 3.1 that for the semi-discrete s*p*-LOD solution it holds

$$\tilde{u}_H \in C^m([0,T]; H_0^1(\Omega)) \cap C^{m+1}([0,T]; L^2(\Omega)). \tag{3.9}$$

Further, we have the bound

$$\sum_{\nu=0}^{m} \|\tilde{u}_H\|_{C^\nu([0,T];H^1(\Omega))} + \|\tilde{u}_H\|_{C^{m+1}([0,T];L^2(\Omega))} \lesssim C_{\mathrm{data}}.$$

For the semi-discrete s*p*-LOD method we can show the following error estimate.

Theorem 3.9 (Error estimate of the semi-discrete prototypical s*p*-LOD)**.** *Let Assumption 3.1 hold for some $k \in \mathbb{N}$ and $m \geq 4$. Further, let u be the solution to* (3.2)*, and $\tilde{u}_H$ be the solution to* (3.6)*. Then*

$$\|\partial_t(u(t) - \tilde{u}_H(t))\|_{L^2(\Omega)} + \|\nabla(u(t) - \tilde{u}_H(t))\|_{L^2(\Omega)} \lesssim_T H^2 C_{\mathrm{data}}. \tag{3.10}$$

Remark 3.3. For ease of presentation we assume $k \geq 1$ in Theorem 3.9. If Assumption 3.1 holds for $k = 0$ (and $m \geq 4$) we obtain the first-order error estimate

$$\|\partial_t(u(t) - \tilde{u}_H(t))\|_{L^2(\Omega)} + \|\nabla(u(t) - \tilde{u}_H(t))\|_{L^2(\Omega)} \lesssim_T H C_{\mathrm{data}}. \tag{3.11}$$

In Theorem 3.9 we show that we can only expect the semi-discrete prototypical s*p*-LOD solution to be second-order accurate in space, despite having optimal convergence in the elliptic setting. We prove the theorem in two steps. The first step is a classical energy estimate that bounds the error $\varphi = \tilde{u}_H - \widetilde{\mathcal{P}} u$ between the semi-discrete prototypical s*p*-LOD solution and the projection, defined in (3.8), of the weak solution into the multiscale space. We show that this error can be

bounded by the error $\varrho = u - \widetilde{\mathcal{P}}u$ between the weak solution and its projection into the multiscale space.

The second step is the estimate of the projection error ϱ itself. Here we find that employing similar arguments as in the elliptic setting results in maximum second-order convergence independent of the regularity of the right-hand side f. This indicates that the multiscale space $\widetilde{V}_H$ is suboptimal for applications to the acoustic wave equation.

The following lemma estimates the space discretization error φ. The proof is rather standard and uses the fact that φ solves a wave equation with $\partial_t^2 \varrho$ as the right-hand side. The statement follows by well-known energy estimates.

Lemma 3.10 (Space discretization error)**.** *Let Assumption 3.1 hold for some $k \in \mathbb{N}_0$ and $m \geq 1$. Further, let u be the solution to* (3.2)*, and $\tilde{u}_H$ be the solution to* (3.6)*. With $\varphi = \tilde{u}_H - \widetilde{\mathcal{P}}u$, and $\varrho = u - \widetilde{\mathcal{P}}u$, where the projection $\widetilde{\mathcal{P}}$ is defined in* (3.8)*, the following estimate holds*

$$\|\partial_t \varphi(t)\|_{L^2(\Omega)} + \|\nabla \varphi(t)\|_{L^2(\Omega)} \lesssim \int_0^t \|\partial_t^2 \varrho(s)\|_{L^2(\Omega)} \,\mathrm{d}s. \tag{3.12}$$

Proof. The proof is similar to Krumbiegel and Maier (2025) and is based on Joly (2003). We fix any $s \in [0, T]$. Then we use the variational formulation for the prototypical sp-LOD method (3.6), and the definition of the projection into the multiscale space (3.8) to obtain

$$\begin{aligned}(\partial_t^2 \varphi(s), \tilde{v}_H)_{L^2(\Omega)} + a(\varphi(s), \tilde{v}_H) \\ &= (\partial_t^2(\tilde{u}_H(s) - \widetilde{\mathcal{P}}u(s)), \tilde{v}_H)_{L^2(\Omega)} + a((\tilde{u}_H(s) - \widetilde{\mathcal{P}}u(s)), \tilde{v}_H) \\ &= (f(s), \tilde{v}_H)_{L^2(\Omega)} - (\partial_t^2 \widetilde{\mathcal{P}}u(s), \tilde{v}_H)_{L^2(\Omega)} - a(u(s), \tilde{v}_H)\end{aligned}$$

for all $\tilde{v}_H \in \widetilde{V}_H$. Next, we use the variational formulation (3.2) for the first term on the right-hand side since $\tilde{v}_H \in H_0^1(\Omega)$ is a valid test function. Thus, the spatial discretization error φ solves the semi-discrete problem

$$\begin{aligned}(\partial_t^2 \varphi(s), \tilde{v}_H)_{L^2(\Omega)} + a(\varphi(s), \tilde{v}_H) &= (\partial_t^2 u(s) - \partial_t^2 \widetilde{\mathcal{P}}u(s), \tilde{v}_H)_{L^2(\Omega)} \\ &= (\partial_t^2 \varrho(s), \tilde{v}_H)_{L^2(\Omega)}\end{aligned} \tag{3.13}$$

for all $\tilde{v}_H \in \widetilde{V}_H$. We define the semi-discrete energy of the wave equation by

$$\mathfrak{E}(t) = \tfrac{1}{2}\Big[\|\partial_t \varphi(t)\|_{L^2(\Omega)}^2 + a(\varphi(t), \varphi(t))\Big]. \tag{3.14}$$

For any function $v \in C^1([0, T]; H_0^1(\Omega))$ we have

$$\tfrac{1}{2}\partial_t (v, v)_{L^2(\Omega)} = (\partial_t v, v)_{L^2(\Omega)}, \qquad \tfrac{1}{2}\partial_t a(v, v) = a(\partial_t v, v).$$

Using these equalities we have

$$\begin{aligned}\partial_t \mathfrak{E}(s) &= \tfrac{1}{2}\partial_t(\partial_t\varphi(s), \partial_t\varphi(s))_{L^2(\Omega)} + \tfrac{1}{2}\partial_t a(\varphi(s), \varphi(s)) \\ &= (\partial_t^2\varphi(s), \partial_t\varphi(s))_{L^2(\Omega)} + a(\varphi(s), \partial_t\varphi(s)) \\ &= (\star).\end{aligned} \tag{3.15a}$$

Since $\tilde{v}_H = \partial_t\varphi(s)$ is a valid test function in (3.13) we have employing the Cauchy-Schwarz inequality

$$\begin{aligned}(\star) &= (\partial_t^2\varrho(s), \partial_t\varphi(s))_{L^2(\Omega)} \\ &\leq \|\partial_t^2\varrho(s)\|_{L^2(\Omega)}\|\partial_t\varphi(s)\|_{L^2(\Omega)} \\ &\lesssim \|\partial_t^2\varrho(s)\|_{L^2(\Omega)}\sqrt{\mathfrak{E}(s)}.\end{aligned} \tag{3.15b}$$

Using chain rule and (3.15) after division by $\sqrt{\mathfrak{E}(s)}$ we obtain

$$\begin{aligned}\partial_t\sqrt{\mathfrak{E}(s)} &= \frac{\partial_t\mathfrak{E}(s)}{2\sqrt{\mathfrak{E}(s)}} \\ &\lesssim \|\partial_t^2\varrho(s)\|_{L^2(\Omega)}.\end{aligned} \tag{3.16}$$

Finally, integrating (3.16) in time from 0 to t yields

$$\sqrt{\mathfrak{E}(t)} \lesssim \sqrt{\mathfrak{E}(0)} + \int_0^t \|\partial_t^2\varrho(s)\|_{L^2(\Omega)}\,\mathrm{d}s. \tag{3.17}$$

We have $\mathfrak{E}(0) = 0$ by the definition of the initial conditions (cf. (3.7)). Then the estimate

$$\begin{aligned}\|\partial_t\varphi(t)\|_{L^2(\Omega)} + \|\nabla\varphi(t)\|_{L^2(\Omega)} &\lesssim \sqrt{\mathfrak{E}(t)} \\ &\lesssim \int_0^t \|\partial_t^2\varrho(s)\|_{L^2(\Omega)}\,\mathrm{d}s\end{aligned}$$

proves the assertion (3.10). □

The next lemma provides an estimate for the projection error ϱ. We use that the projection error lies in the fine-scale space W to insert the L^2-projection and use standard polynomial approximation results to obtain the convergence. This lemma provides insight into the mechanics that lead to the reduced convergence.

Lemma 3.11 (Projection error)**.** *Let Assumption 3.1 hold for some $k \in \mathbb{N}_0$ and $m \geq 4$. Further, let u be the solution to (3.2). With $\varrho = u - \widetilde{\mathcal{P}}u$, where the $\widetilde{\mathcal{P}}$ is defined in (3.8), the following estimates hold for $\nu = 0, 1, 2$*

$$\|\nabla\partial_t^\nu\varrho(t)\|_{L^2(\Omega)} \lesssim H^{\kappa+1}\|f\|_{C^\nu([0,T];H^\kappa(\mathcal{T}_H))} + H^2\|\partial_t^2 u\|_{C^\nu([0,T];H^1(\Omega))}, \tag{3.18a}$$

and for $\nu = 1, 2$

$$\|\partial_t^\nu \varrho(t)\|_{L^2(\Omega)} \lesssim H^{\kappa+2}\|f\|_{C^\nu([0,T];H^\kappa(\mathcal{T}_H))} + H^3\|\partial_t^2 u\|_{C^\nu([0,T];H^1(\Omega))}, \tag{3.18b}$$

where $\kappa = \min\{k, p+1\}$.

Proof. The proof of this lemma follows along the same lines of Theorem 2.2. Let $t \in [0,T]$. Employing the definition of the projection $\widetilde{\mathcal{P}}$ we have for any $\tilde{v}_H \in \widetilde{V}_H$ that

$$a(u(t) - \widetilde{\mathcal{P}}u(t), \tilde{v}_H) = 0, \tag{3.19}$$

and thus (2.28) yields

$$\varrho(t) \in W.$$

Since the projection error lies in the kernel space, we can subtract the L^2-projection and use the approximation estimate (2.13) to obtain for $\nu = 1, 2$

$$\begin{aligned}\|\partial_t^\nu \varrho(t)\|_{L^2(\Omega)} &= \|(\mathrm{id} - \Pi_H)\partial_t^\nu \varrho(t)\|_{L^2(\Omega)} \\ &\lesssim H\|\nabla \partial_t^\nu \varrho(t)\|_{L^2(\Omega)}.\end{aligned}$$

Thus, we already have bounded the norm on the left-hand side of (3.18b) by the norm on the left-hand side of (3.18a), and it remains to show (3.18a). First, we use the coercivity of the inner product (2.6) and that the projection $\widetilde{\mathcal{P}}$ is orthogonal to ϱ with respect to $a(\cdot,\cdot)$ which yields

$$\begin{aligned}\|\nabla \varrho(t)\|_{L^2(\Omega)}^2 &\lesssim a(\varrho(t), \varrho(t)) \\ &= a(u(t) - \widetilde{\mathcal{P}}u(t), u(t) - \widetilde{\mathcal{P}}u(t)) \\ &= a(u(t), u(t) - \widetilde{\mathcal{P}}u(t)) = (\star).\end{aligned} \tag{3.20a}$$

Further, employing the variational wave equation (3.2) we obtain

$$(\star) = (f(t), u(t) - \widetilde{\mathcal{P}}u(t))_{L^2(\Omega)} - (\partial_t^2 u(t), u(t) - \widetilde{\mathcal{P}}u(t))_{L^2(\Omega)} = (\star\star). \tag{3.20b}$$

Next, we again use that the test function $\varrho(t) \in \ker \Pi_H$ lies in the kernel of the L^2-projection such that we can insert Π_H, and finally applying the Cauchy-Schwarz inequality with the approximation result (2.13) yields

$$\begin{aligned}(\star\star) &= ((\mathrm{id} - \Pi_H)f(t), (\mathrm{id} - \Pi_H)(u(t) - \widetilde{\mathcal{P}}u(t)))_{L^2(\Omega)} \\ &\quad - ((\mathrm{id} - \Pi_H)\partial_t^2 u(t), (\mathrm{id} - \Pi_H)(u(t) - \widetilde{\mathcal{P}}u(t)))_{L^2(\Omega)} \\ &\lesssim \Big[H^\kappa \|f(t)\|_{H^\kappa(\mathcal{T}_H)} + H\|\nabla \partial_t^2 u(t)\|_{L^2(\Omega)}\Big] H\|\nabla(u(t) - \widetilde{\mathcal{P}}u(t))\|_{L^2(\Omega)}.\end{aligned} \tag{3.20c}$$

Note that (3.20) also holds for $\partial_t^\nu \varrho(t)$ for $\nu = 1, 2$. Dividing both sides of (3.20) by the norm $\|\nabla \varrho(t)\|_{L^2(\Omega)}$ and taking the supremum over $t \in [0,T]$ on the right-hand side of (3.20) yields the assertion (3.18). □

This proof exhibits why the multiscale space $\widetilde{V}_H$ created by the prototypical sp-LOD method is not well-suited for time-dependent problems. We observe that the reduced convergence rate stems form the low regularity of the weak solution u. For a more detailed discussion we refer to Remark 3.4 and Examples 3.5 and 3.6 at the end of the section. Now, we first complete the proof of the error estimate for the semi-discrete solution by combining the above two lemmas.

Proof of Theorem 3.9. Let $t \in [0,T]$. First, we split the error into the space discretization error $\varphi(t) = \tilde{u}_H(t) - \widetilde{\mathcal{P}}u(t)$ and the projection error $\varrho(t) = u(t) - \widetilde{\mathcal{P}}u(t)$ of the weak solution using the triangle inequality, i.e.,

$$\begin{aligned}\|\partial_t(\tilde{u}_H(t) - u(t))\|_{L^2(\Omega)} + \|\nabla(\tilde{u}_H(t) - u(t))\|_{L^2(\Omega)} \\ \leq \|\partial_t\varphi(t)\|_{L^2(\Omega)} + \|\nabla\varphi(t)\|_{L^2(\Omega)} + \|\partial_t\varrho(t)\|_{L^2(\Omega)} + \|\nabla\varrho(t)\|_{L^2(\Omega)}. \quad (3.21)\end{aligned}$$

The first two terms can directly be estimated using Lemma 3.10, i.e.,

$$\|\partial_t\varphi(t)\|_{L^2(\Omega)} + \|\nabla\varphi(t)\|_{L^2(\Omega)} \lesssim \int_0^t \|\partial_t^2\varrho(s)\|_{L^2(\Omega)}\,\mathrm{d}s,$$

which yields

$$\begin{aligned}\|\partial_t(\tilde{u}_H(t) - u(t))\|_{L^2(\Omega)} + \|\nabla(\tilde{u}_H(t) - u(t))\|_{L^2(\Omega)} \\ \lesssim \int_0^t \|\partial_t^2\varrho(s)\|_{L^2(\Omega)}\,\mathrm{d}s + \|\partial_t\varrho(t)\|_{L^2(\Omega)} + \|\nabla\varrho(t)\|_{L^2(\Omega)} = (\star). \quad (3.22)\end{aligned}$$

Each term on the right-hand side can now be estimated using Lemma 3.11, i.e., with (3.5) the statement reads

$$\begin{aligned}\|\nabla\varrho(t)\|_{L^2(\Omega)} &\lesssim H^2 C_{\mathrm{data}}, \\ \|\partial_t\varrho(t)\|_{L^2(\Omega)} &\lesssim H^3 C_{\mathrm{data}}, \\ \|\partial_t^2\varrho(t)\|_{L^2(\Omega)} &\lesssim H^3 C_{\mathrm{data}}.\end{aligned}$$

Thus, we have using that the term under the integral is time-independent

$$\begin{aligned}(\star) &\lesssim \int_0^t H^3 C_{\mathrm{data}}\,\mathrm{d}s + H^3 C_{\mathrm{data}} + H^2 C_{\mathrm{data}} \\ &\lesssim_T H^2 C_{\mathrm{data}}.\end{aligned}$$

Note that the constant depends on any time $t \in [0,T]$. □

Remark 3.4 (Reduced convergence rates). This proof shows that we cannot expect a convergence rate beyond second order. It follows since the spatial regularity of the

solution, or, more precisely, its second time derivative is not sufficiently large. Even if we increase the spatial regularity of the right-hand side and the initial conditions, the problem lies with the coefficient. Here we pay the result for assuming the least amount of regularity in space. In the rest of this thesis, we will provide a novel strategy that fixes this suboptimal convergence and does not require any more structural assumptions on the coefficient.

This result can be interpreted that the sp-LOD method is tailored to the elliptic setting and deals very well with the elliptic differential operator. However, it is not sufficient in dealing with time-dependent problems where the PDE operator also contains the second time derivative.

In the following we also present two examples that further highlight the reduced convergence (Example 3.5) and investigate what happens if smooth but oscillatory coefficients are present (Example 3.6).

Example 3.5 (Reduced convergence rates)**.** This experiment presents what has been analyzed theoretically above. We apply the sp-LOD method to the wave equation in highly oscillatory media, specifically, the diffusion coefficient is A_1 given above in Figure 2.5 with oscillation scale $\varepsilon = 2^{-8}$. The right-hand side is given by

$$f(x,t) = 2\pi^2 \sin(\pi x_1)\sin(\pi x_2)\sin(t)^8$$

with zero initial condition such that Assumption 3.1 holds for $m = 8$. That is, by design since the well-preparedness and compatibility conditions hold, and the right-hand side and initial conditions are sufficiently smooth, the reduced convergence really only stems from the low regularity of the solution, which in turn is a result of the general L^∞-coefficient A_1. The reference solution is computed on a mesh with mesh size $h = 2^{-9}$, and we use the Crank–Nicolson time stepping with time step size $\tau = 2^{-9}$ for both the reference and the sp-LOD solution. With this choice the error should be dominated by the spatial error.

Figure 3.1 shows the relative errors $\|\nabla \cdot\|_{L^2(\Omega)}$-norm for s$p$-LOD method. The errors are plotted for three different polynomial degrees and localization parameters. We observe that for $p = 0$ we obtain the optimal second-order convergence. Further, the error for lower localization parameters (e.g., $\ell = 2$) stagnates if the mesh is refined which is in line with the stabilization of the sp-LOD method. For the higher polynomial degrees $p = 2, 4$ the errors are not of optimal order. We observe that the errors seem to have convergence order of less than 2. This most likely stems from the fact that the size of the errors is much lower and the plot eventually saturates in the second-order rate for lower mesh refinements. Furthermore, the plot shows that increasing the polynomial degree decreases the size of the error which indicates a positive scaling with respect to the polynomial degree. In fact, this can be proven by tracing the constants in Theorem 3.9, see also (Krumbiegel and Maier, 2025).

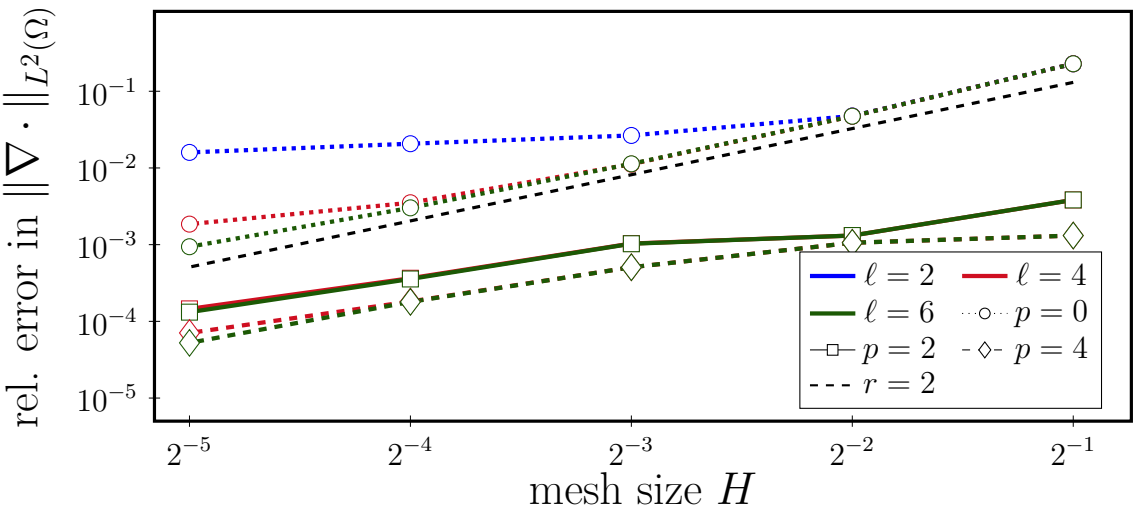

Figure 3.1: Relative errors in the norm $\|\nabla \cdot\|_{L^2(\Omega)}$ for the sp-LOD for different mesh sizes H. We can observe that independent of the polynomial degree.

Example 3.6 (Optimal convergence rates)**.** The major issue that leads to the reduced convergence rates is the low regularity of the coefficient which leads to low regularity solutions. In (Krumbiegel and Maier, 2025, Third example) an example was given, where the coefficient is smooth, and the higher-order rates can be observed. In that example the coefficient was slowly oscillating, such that in practise higher-order FEMs would also yield a similar result. Here, we solve the wave equation with the sp-LOD with a highly oscillatory but smooth coefficient $A_\varepsilon(x) = (2 + \cos(\frac{\pi x}{\varepsilon}))^{-1}$. We choose here $d = 1$ as we require a very small $\varepsilon = 2^{-15}$. In this example we choose the right-hand side $f(x,t) = 2\pi^2 \sin(\pi x)\sin(t)^8$ with zero initial conditions up to order $m = 8$ in Assumption 3.1, such that the well-preparedness and compatibility conditions hold. We use the Crank–Nicolson discretization with $\tau = 2^{-9}$ for both the fine (FEM) reference solution on a mesh with mesh size $h = 2^{-16}$ and the sp-LOD solutions with mesh sizes depicted on the x-axis in Figure 3.2.

Figure 3.2 shows the relative errors in the $\|\nabla\cdot\|_{L^2(\Omega)}$-norm. Here, we clearly observe that the higher-order rates (at least for large mesh sizes). Given the explanation in (Krumbiegel and Maier, 2025), the norms of the higher-order derivatives of the solution are expected to scale with the fine-scale ε. More precisely, we expect to have an error

$$\begin{aligned}\|\nabla(u(t) - \tilde{u}_H(t))\|_{L^2(\Omega)} &\lesssim H^{p+2}\|f(t)\|_{H^{p+1}(\mathcal{T}_H)} + H^{p+2}\|u(t)\|_{H^{p+1}(\mathcal{T}_H)} \\ &\lesssim H^{p+2}C_{\text{data}} + \frac{H^{p+2}}{\varepsilon^s}\end{aligned}$$

for some $s > 0$. This consideration would indicate a reduced error convergence or

even a plateau for coarse mesh sizes similar to the FEM in Figure 2.2. However, since this is not the case, there is a different interpretation to these results.

Here, we have an example where the coefficient is sufficiently smooth and periodic, such that we may reasonably assume that there exist a homogenized equation

$$\langle \partial_t^2 u(t), v\rangle_{H^{-1}(\Omega)\times H_0^1(\Omega)} + a_0(u(t), v) = (f(t), v)_{L^2(\Omega)},$$

where

$$a_0(u, v) = \int_\Omega A_0 \nabla u \cdot \nabla v \,\mathrm{d}x$$

with the homogenized coefficient A_0. Then, denote with u_0 the unique solution to the homogenized problem. Since the homogenized coefficient A_0 is independent of the oscillations ε, the norms of the spatial derivatives of the homogenized solution u_0 also do not depend on the fine-scale. Thus, considering the projection error we have

$$\begin{aligned}
\|\nabla(u(t) - \widetilde{\mathcal{P}}u(t))\|_{L^2(\Omega)}^2 &\lesssim a(u(t) - \widetilde{\mathcal{P}}u(t), u(t) - \widetilde{\mathcal{P}}u(t)) \\
&= (f(t), u(t) - \widetilde{\mathcal{P}}u(t))_{L^2(\Omega)} - (\partial_t^2 u(t), u(t) - \widetilde{\mathcal{P}}u(t))_{L^2(\Omega)} \\
&= (f(t), u(t) - \widetilde{\mathcal{P}}u(t))_{L^2(\Omega)} - (\partial_t^2 u_0(t), u(t) - \widetilde{\mathcal{P}}u(t))_{L^2(\Omega)} \\
&\quad - (\partial_t^2 (u(t) - u_0(t)), u(t) - \widetilde{\mathcal{P}}u(t))_{L^2(\Omega)}.
\end{aligned}$$

The first term can again be estimated with the optimal rate. The second term solves a wave equation with a smooth coefficient A_0 without oscillations. By Evans (2010) the second time derivative of u_0 has one order less than the right-hand side. Thus, under minimal assumptions, i.e., regularity of the right-hand side and the initial data, we expect one order less convergence in general. This example, however, is much smoother, and we see the optimal rate for the second term as well. Further, it is known that the left side of the third term scales like $\mathcal{O}(\varepsilon)$. Thus, this overall leads to

$$\|\nabla(u(t) - \widetilde{\mathcal{P}}u(t))\|_{L^2(\Omega)} \lesssim H^{p+2}\|f(t)\|_{H^{p+1}(\mathcal{T}_H)} + H^{p+2}\|u_0(t)\|_{H^{p+1}(\mathcal{T}_H)} + H\mathcal{O}(\varepsilon).$$

This sketch is observed by the convergence plot in Figure 3.2, where we observe the higher-order convergence rate for the sp-LOD method for coarse mesh sizes, that eventually stagnates in a plateau that is induced by the fine-scale. Here, the plateau does not decrease with H which may be explained by the fact that the p-LOD solution converges better for lower mesh sizes and the plateau appears smaller.

3.3 Enriched spaces

In the previous section we have observed that the prototypical sp-LOD method creates a suboptimal multiscale space for the discretization of the wave equation. Here,

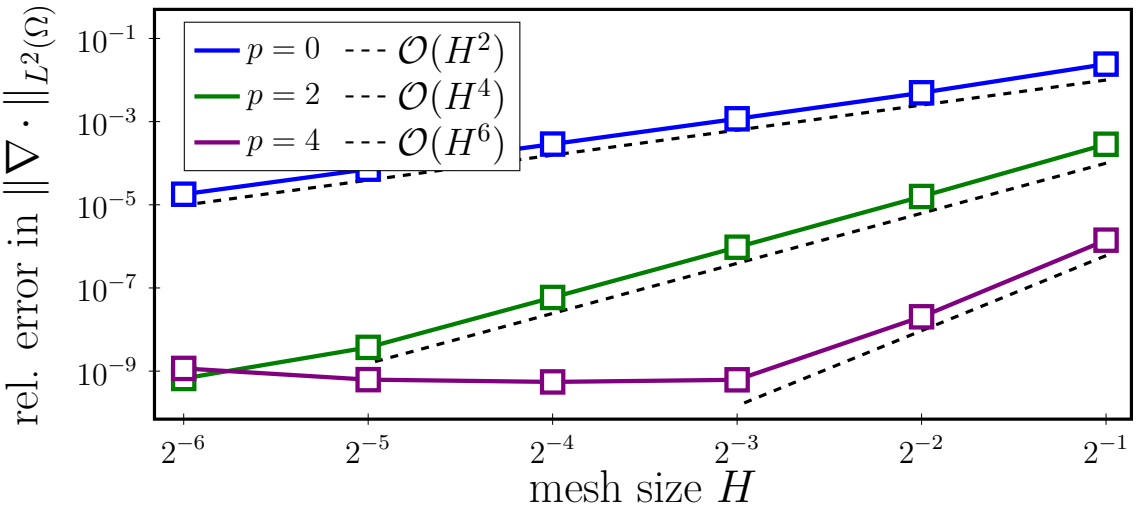

Figure 3.2: Relative errors in the norm $\|\nabla \cdot\|_{L^2(\Omega)}$ for the sp-LOD method with a smooth and highly-oscillatory ($\varepsilon = 2^{-15}$) coefficient for different mesh sizes H. Here, we observe that the method yields a higher-order convergence for coarse mesh sizes until it reaches a plateau. See Example 3.6 for a detailed discussion.

we introduce enriched spaces that will work around the reduced convergence rate. In Section 3.3.1 a novel correction operator is introduced, and we show that in an ideal setting this correction operator grants the higher-order convergence promised from the elliptic setting.

Section 3.3.2 makes the consideration in the ideal setting more concrete and introduces enriched multiscale spaces, that in a prototypical setting converge with the optimal error.

3.3.1 Enriched correction operator

We analyzed that the critical estimate is (3.20c), where the low regularity of the weak solution u results in a convergence rate of order 2 in the energy norm, regardless of the polynomial degree p. The goal of this subsection is to present the novel idea that was first introduced in Kalyanaraman, Krumbiegel, Maier, and Wang (2025) applied to a parabolic PDE. This method achieves higher-order convergence for general coefficients $A \in L^\infty(\Omega)$ in an idealized setting.

Since the problematic term is tested with functions $w \in W$, the idea is to introduce a correction operator that (in the ideal setting of this section) completely eliminates this term. Thus, let $v \in L^2(\Omega)$. Define the *enriched correction operator* $\mathcal{D}\colon L^2(\Omega) \to W$ as the solution to the variational problem

$$a(\mathcal{D}v, w) = -(v, w)_{L^2(\Omega)} \tag{3.23}$$

for all $w \in W$. The following theorem shows that the enriched correction operator potentially can be used to obtain higher-order convergence of the p-LOD method for time-dependent PDEs. The idea is, that the $\widetilde{\mathcal{P}}$ is further corrected by the image of the solution under the enriched correction operator $\mathcal{D}$. By design this enriched correction then eliminates the term with reduced convergence rate, as observed in the proof.

Theorem 3.12. *Let Assumption 3.1 hold for some $k \in \mathbb{N}_0$ and $m \geq 4$. Further, let u be the solution to the variational formulation* (3.2)*. Then*

$$\|\nabla(u(t) - (\widetilde{\mathcal{P}}u(t) + \mathcal{D}(\partial_t^2 u(t))))\|_{L^2(\Omega)} \lesssim H^{\kappa+1} C_{\mathrm{data}}, \tag{3.24}$$

where $\kappa = \min\{k, p+1\}$.

Proof. The proof is very similar to the proof of Lemma 3.11. Recall that

$$\varrho(t) = u(t) - \widetilde{\mathcal{P}}u(t) \in W.$$

Thus, by the definition of the enriched correction operator we also have

$$\psi(t) \coloneqq u(t) - (\widetilde{\mathcal{P}}u(t) + \mathcal{D}(\partial_t^2 u(t))) \in W.$$

Then the projection $\widetilde{\mathcal{P}}$ is orthogonal to $\psi(t)$, and we have, using the coercivity (2.6), that

$$\begin{aligned} \|\nabla\psi(t)\|_{L^2(\Omega)}^2 &\lesssim a(\psi(t), \psi(t)) \\ &= a(u(t) - (\widetilde{\mathcal{P}}u(t) + \mathcal{D}(\partial_t^2 u(t))), \psi(t)) \\ &= a(u(t) - \mathcal{D}(\partial_t^2 u(t)), \psi(t)) = (\star). \end{aligned} \tag{3.25a}$$

Next, we employ the variational wave equation (3.2) and the definition of the enriched correction operator to obtain

$$\begin{aligned} (\star) &= a(u(t) - \mathcal{D}(\partial_t^2 u(t)), \psi(t)) \\ &= (f(t), \psi(t))_{L^2(\Omega)} - (\partial_t^2 u(t), \psi(t))_{L^2(\Omega)} - a(\mathcal{D}(\partial_t^2 u(t)), \psi(t)) \\ &= (f(t), \psi(t))_{L^2(\Omega)} = (\star\star). \end{aligned} \tag{3.25b}$$

Here, we can again subtract the L^2-projection, since $\psi(t) \in W$, and then use the approximation result (2.13) to obtain

$$\begin{aligned} (\star\star) &= ((\mathrm{id} - \Pi_H) f(t), (\mathrm{id} - \Pi_H)\psi(t))_{L^2(\Omega)} \\ &\lesssim H^\kappa \|f(t)\|_{H^\kappa(\mathcal{T}_H)} H \|\nabla\psi(t)\|_{L^2(\Omega)}. \end{aligned} \tag{3.25c}$$

Dividing both sides of (3.25) by the norm $\|\nabla\psi\|_{L^2(\Omega)}$ and taking the supremum over all $t \in [0, T]$ on the right-hand side yields combined with (3.5) the assertion

$$\|\nabla\psi(t)\|_{L^2(\Omega)} \lesssim H^{\kappa+1} \|f(t)\|_{H^\kappa(\mathcal{T}_H)} \lesssim H^{\kappa+1} C_{\mathrm{data}}. \qquad \square$$

Remark 3.7. We note that the enriched corrections have a similar structure as the right-hand side corrections introduced by Hellman and Målqvist (2017). However, herein the enriched correction operator is used to correct the low regularity of the solution and yield a higher-order approximation of the eho-LOD method that is regularity-independent. In contrast, Hellman and Målqvist (2017) use the right-hand side corrections for an elliptic model problem for its exponential decay property to represent the LOD-error only as an exponential decay error. In practice, the right-hand side corrections need to be calculated online while the enriched corrections can be pre-computed and re-used for many right-hand sides.

3.3.2 Towards a prototypical enriched higher-order space

In the previous section we defined the enriched correction operator that may be able to recover the optimal convergence rate from the elliptic setting. Theorem 3.12 indicates that in the ideal setting, where we have access to the second time derivative of the weak solution u, the enriched correction operator is exactly what we are looking for. However, in practice it is not feasible to obtain this information. Thus, we need another design which replaces the projection $\widetilde{\mathcal{P}}u+\mathcal{D}(\partial_t^2 u)$ by an appropriate computable function. The idea is to replace the weak solution by an approximation of it in the multiscale space. Specifically, we replace

$$\partial_t^2 u \approx \partial_t^2 \widetilde{\mathcal{P}} u.$$

We note that this projection still is not computable, however, it is reasonable to consider this projection as we will later approximate this function in the discrete space. We already know from the theory above (cf. Lemma 3.11) that the projection can be bounded by the sum of two terms. One is of optimal order $H^{\kappa+1}$ that depends only on the regularity of the right-hand side, and one of suboptimal order H^2 that depends on the regularity of the weak solution itself. We now expect that the term $\mathcal{D}(\partial_t^2\widetilde{\mathcal{P}}u)$ is a good approximation to the term $\mathcal{D}(\partial_t^2 u)$ and is then (almost) able to compensate for the suboptimal term in similarly to Theorem 3.12. However, since we are only able to correct the projection of the weak solution, we expect that the enriched correction only recovers two orders of convergence which then leads to an overall error of $\mathcal{O}(H^4)$.

To be more precise, we know that

$$\|\nabla(u(t) - \widetilde{\mathcal{P}}u(t))\|_{L^2(\Omega)} \lesssim H^{\kappa+1} + H^2.$$

We now expect with arguments similar to Theorem 3.12 and Lemma 3.11 employing

the definition of the enriched correction operator that

$$\begin{aligned}
&\|\nabla(u(t) - (\widetilde{\mathcal{P}}u(t) + \mathcal{D}(\partial_t^2 \widetilde{\mathcal{P}}u(t))))\|_{L^2(\Omega)} \\
&\quad \leq \|\nabla(u(t) - (\widetilde{\mathcal{P}}u(t) + \mathcal{D}(\partial_t^2 u(t))))\|_{L^2(\Omega)} + \|\nabla(\mathcal{D}(\partial_t^2 u(t)) - \mathcal{D}(\partial_t^2 \widetilde{\mathcal{P}}u(t)))\|_{L^2(\Omega)} \\
&\quad \lesssim H^{\kappa+1} + H^2 \|\nabla \partial_t^2 (u(t) - \widetilde{\mathcal{P}}u(t))\|_{L^2(\Omega)} \\
&\quad \lesssim H^{\kappa+1} + H^2(H^{\kappa+1} + H^2).
\end{aligned}$$

Thus, we observe that this term has better convergence, i.e., we know that the term $\widetilde{\mathcal{P}}u + \mathcal{D}(\partial_t^2 \widetilde{\mathcal{P}}u)$ is a better approximation of the solution than $\widetilde{\mathcal{P}}u$. That is we may choose

$$\partial_t^2 u \approx \partial_t^2 (\widetilde{\mathcal{P}}u + \mathcal{D}(\partial_t^2 \widetilde{\mathcal{P}}u))$$

as an approximation. As we have indicated above, the enriched correction operator applied to the multiscale projection is able to correct reduced convergence rates that stem from the residual of the projection by two additional orders of convergence. However, in the end another low-regularity residual $\partial_t^2(u - \widetilde{\mathcal{P}}u)$ still remains, which makes another adjustment using the enriched correction operator necessary. Thus, we expect to have two additional orders of accuracy. We iterate this process j times. This leads to the following expansion

$$\partial_t^2 u \approx \sum_{\nu=0}^{j} \mathcal{D}^\nu (\partial_t^{2\nu} \widetilde{\mathcal{P}}u(t)), \tag{3.26}$$

where each term in the expansion is an approximation to the residual from the previous error. We thus expect the following convergence

$$\Big\|\nabla(u(t) - \sum_{\nu=0}^{j} \mathcal{D}^\nu (\partial_t^{2\nu} \widetilde{\mathcal{P}}u(t)))\Big\|_{L^2(\Omega)} \lesssim H^{\kappa+1} + H^{2(j+1)}.$$

With an optimal choice of j we can now achieve the higher-order convergence. Note that the constructed projections still are not computable as we have no access to the solution but give us an idea on how to design a discrete space. At this point this is no rigorous proof, but rather a motivation for the design of the enriched multiscale space, which now follows. We refer to Theorem 3.13 for a rigorous analysis.

Inspired by the above considerations we provide a construction of the enriched multiscale space in the following. For any $j \in \mathbb{N}$ we define the *enriched correction space* by

$$\widehat{W}_H^j = \sum_{\nu=1}^{j} \mathcal{D}^\nu \widetilde{V}_H. \tag{3.27}$$

The *prototypical enriched multiscale space* is then defined as the sum of the prototypical s*p*-LOD space and the enriched correction space, i.e.,

$$\breve{V}_H^j = \widetilde{V}_H \oplus_a \widehat{W}_H^j. \tag{3.28}$$

We note here that the sum in (3.27) is not a direct sum, however, the enriched correction space is orthogonal to the prototypical sp-LOD space with respect to the energy inner product. By construction, we have

$$\left[\widetilde{\mathcal{P}} + \sum_{\nu=1}^{j} \mathcal{D}^{\nu}\widetilde{\mathcal{P}}\right] \colon H_0^1(\Omega) \to \check{V}_H^j.$$

This observation and considering the above argumentation, this suggests that the prototypical enriched multiscale space might be an appropriate space to obtain higher-order convergence.

Prototypical enriched higher-order LOD. We state the *prototypical enriched higher-order LOD* (eho-LOD) method for the wave equation. That is, seek a function $\check{u}_H \colon [0,T] \to \check{V}_H^j$ such that

$$(\partial_t^2 \check{u}_H, \check{v}_H)_{L^2(\Omega)} + a(\check{u}_H, \check{v}_H) = (f, \check{v}_H)_{L^2(\Omega)} \tag{3.29}$$

for all $\check{v}_H \in \check{V}_H^j$, where the initial conditions are given by

$$\check{u}_H(0) = \check{\mathcal{Q}}^j u_0, \qquad \partial_t \check{u}_H(0) = \check{\mathcal{Q}}^j v_0 \tag{3.30}$$

where the maps $\check{\mathcal{Q}}^j$ into the enriched multiscale space and $\widehat{\mathcal{Q}}^j$ into the enriched correction space are given by

$$\check{\mathcal{Q}}^j \coloneqq \widetilde{\mathcal{P}} + \widehat{\mathcal{Q}}^j, \qquad \widehat{\mathcal{Q}}^j \coloneqq \sum_{\nu=1}^{j} \mathcal{D}^{\nu}(\partial_t^{2\nu}\widetilde{\mathcal{P}}). \tag{3.31}$$

For the prototypical eho-LOD method we show the following error estimate.

Theorem 3.13 (Error of the semi-discrete prototypical eho-LOD)**.** *Let Assumption 3.1 hold for some $k \in \mathbb{N}_0$ and $m \geq 2j+4$. Further, let u be the solution to* (3.2)*, and $\check{u}_H$ be the solution to* (3.29)*. Then if $j \geq \lceil \frac{p}{2} \rceil$ we have*

$$\|\partial_t(\check{u}_H(t) - u(t))\|_{L^2(\Omega)} + \|\nabla(\check{u}_H(t) - u(t))\|_{L^2(\Omega)} \lesssim H^{\kappa+1} C_{\mathrm{data}}, \tag{3.32}$$

where $\kappa = \min\{k, p+1\}$ for a.e. $t \in [0,T]$.

We prove the error estimate in three steps. The first step is similar to Lemma 3.10. It estimates the space discretization error $\varphi = \check{u}_H - \check{\mathcal{P}}^j u$ between the semi-discrete prototypical eho-LOD solution $\check{u}_H$ and the orthogonal projection of the weak solution into the enriched multiscale space $\check{\mathcal{P}}^j u$. Here the projection $\check{\mathcal{P}}^j \colon H_0^1(\Omega) \to \check{V}_H^j$ is defined by

$$\check{\mathcal{P}}^j = \widetilde{\mathcal{P}} + \widehat{\mathcal{P}}^j \tag{3.33}$$

with the orthogonal projection $\widehat{\mathcal{P}}^j\colon H_0^1(\Omega) \to \widehat{W}_H^j$ given for any $v \in H_0^1(\Omega)$ by

$$a(\widehat{\mathcal{P}}^j v, w) = a(v, w) \tag{3.34}$$

for all $w \in \widehat{W}_H^j$. Note that since the spaces $\widetilde{V}_H$ and $\widehat{W}_H^j$ are a-orthogonal the sum is also a projection. We show that the space discretization error can be bounded by the projection error $\varrho = u - \check{\mathcal{P}}^j u$ between the weak solution and the orthogonal projection into the enriched multiscale space $\check{\mathcal{P}}^j u$, and by the mapping error $\psi = u - \check{\mathcal{Q}}^j u$ at the initial time. In the second step the projection error ϱ is estimated, and we find that it can be bounded by the mapping error ψ. The last step estimates the mapping error, which is a rigorous analysis of the considerations at the start of this section.

Lemma 3.14 (Space discretization error of the prototypical eho-LOD method)**.** *Let Assumption 3.1 hold for some $k \in \mathbb{N}_0$ and $m \geq 2j+1$. Further, let u be the solution to* (3.2)*, and $\tilde{u}_H$ be the solution to* (3.29)*. With $\varphi = \tilde{u}_H - \check{\mathcal{P}}^j u$, $\varrho = u - \check{\mathcal{P}}^j u$, and $\psi = u - \check{\mathcal{Q}}^j u$, where the projection $\check{\mathcal{P}}^j$ is defined in* (3.33) *and the mapping $\check{\mathcal{Q}}^j$ in* (3.31)*, the following estimate holds*

$$\begin{aligned}&\|\partial_t \varphi(t)\|_{L^2(\Omega)} + \|\nabla \varphi(t)\|_{L^2(\Omega)} \\ &\qquad \lesssim H\|\nabla \partial_t \psi(0)\|_{L^2(\Omega)} + \|\nabla \psi(0)\|_{L^2(\Omega)} + \int_0^t \|\partial_t^2 \varrho(s)\|_{L^2(\Omega)} \,\mathrm{d}s\end{aligned} \tag{3.35}$$

Proof. The proof follows the same ideas of Lemma 3.10 with exception for the initial energy. We fix any $s \in [0,T]$. Since $\check{\mathcal{P}}^j$ is the orthogonal projection with respect to $a(\cdot,\cdot)$ onto $\check{V}_H^j$, we have

$$a(\varrho(s), \check{v}_H) = a(u(s) - \check{\mathcal{P}}^j u(s), \check{v}_H) = 0.$$

As a result, similar to Lemma 3.10 we find that the space discretization error φ solves the semi-discrete problem

$$\begin{aligned}(\partial_t^2 \varphi(s), \check{v}_H)_{L^2(\Omega)} + a(\varphi(s), \check{v}_H) &= (\partial_t^2 \varrho(s), \check{v}_H)_{L^2(\Omega)} + a(\varrho(s), \check{v}_H) \\ &= (\partial_t^2 \varrho(s), \check{v}_H)_{L^2(\Omega)}\end{aligned} \tag{3.36}$$

for all $\check{v}_H \in \check{V}_H^j$. We define the semi-discrete energy $\mathfrak{E}(t)$ as in (3.14), i.e.,

$$\mathfrak{E}(t) = \tfrac{1}{2}\Big[\|\partial_t \varphi(t)\|_{L^2(\Omega)}^2 + a(\varphi(t), \varphi(t))\Big].$$

We choose $\partial_t \varphi(s) \in \check{V}_H^j$ as a test function in (3.36) and obtain

$$\begin{aligned}\partial_t \mathfrak{E}(s) &= (\partial_t^2 \varrho(s), \partial_t \varphi(s))_{L^2(\Omega)} \\ &\lesssim \|\partial_t^2 \varrho(s)\|_{L^2(\Omega)} \sqrt{\mathfrak{E}(s)}.\end{aligned} \tag{3.37}$$

Next, we divide by $\sqrt{\mathfrak{E}(s)}$ and integrate in time from 0 to t which yields

$$\sqrt{\mathfrak{E}(t)} \lesssim \sqrt{\mathfrak{E}(0)} + \int_0^t \|\partial_t^2 \varrho(s)\|_{L^2(\Omega)} \,\mathrm{d}s. \tag{3.38}$$

Similar to above we have

$$\|\partial_t \varphi(t)\|_{L^2(\Omega)} + \|\nabla \varphi(t)\|_{L^2(\Omega)} \lesssim \sqrt{\mathfrak{E}(t)},$$

which gives the following estimate for the space discretization error

$$\|\partial_t \varphi(t)\|_{L^2(\Omega)} + \|\nabla \varphi(t)\|_{L^2(\Omega)} \lesssim \sqrt{\mathfrak{E}(0)} + \int_0^t \|\partial_t^2 \varrho(s)\|_{L^2(\Omega)} \,\mathrm{d}s. \tag{3.39}$$

Consider the initial energy $\mathfrak{E}(0)$ on the right-hand side of (3.39). It can be bounded using the boundedness (2.7) of the energy inner product by

$$\begin{aligned} \sqrt{\mathfrak{E}(0)} &\leq \|\partial_t \varphi(0)\|_{L^2(\Omega)} + \sqrt{a(\varphi(0), \varphi(0))} \\ &\lesssim \|\partial_t \varphi(0)\|_{L^2(\Omega)} + \|\nabla \varphi(0)\|_{L^2(\Omega)}. \end{aligned} \tag{3.40}$$

Further, we have by the definition of the projection (3.33) and the choice for the initial conditions (3.30) that

$$\begin{aligned} \varphi(0) &= \breve{u}_H(0) - \breve{\mathcal{P}}^j u(0) \\ &= \widetilde{\mathcal{P}} u(0) + \widehat{\mathcal{Q}}^j u(0) - \widetilde{\mathcal{P}} u(0) - \widehat{\mathcal{P}}^j u(0) \\ &= \widehat{\mathcal{Q}}^j u(0) - \widehat{\mathcal{P}}^j u(0) \in \widehat{W}_H^j \subset W, \end{aligned} \tag{3.41a}$$

and thus subtracting the L^2-projection and using the approximation (2.13) we have

$$\begin{aligned} \|\partial_t \varphi(0)\|_{L^2(\Omega)} &= \|(\mathrm{id} - \Pi_H)\partial_t \varphi(0)\|_{L^2(\Omega)} \\ &\lesssim H \|\nabla \partial_t \varphi(0)\|_{L^2(\Omega)}. \end{aligned} \tag{3.41b}$$

Finally, we show with the coercivity (2.6), the definitions of the projection (3.34), the fact that $\varphi(0) \in W$ that

$$\begin{aligned} \|\nabla \varphi(0)\|_{L^2(\Omega)}^2 &\lesssim a(\varphi(0), \varphi(0)) \\ &= a(\breve{u}_H(0) - \breve{\mathcal{P}}^j u(0), \varphi(0)) \\ &= a(\breve{\mathcal{Q}}^j u(0) - \widehat{\mathcal{P}}^j u(0), \varphi(0)) = (\star). \end{aligned} \tag{3.42a}$$

Further, since the test function is $\varphi(0) \in \widehat{W}_H^j$ we can employ the definition of ψ and the Cauchy-Schwarz inequality such that

$$\begin{aligned} (\star) &= a(\breve{\mathcal{Q}}^j u(0) - u(0), \varphi(0)) \\ &= -a(\psi(0), \varphi(0)) \\ &\lesssim \|\nabla \psi(0)\|_{L^2(\Omega)} \|\nabla \varphi(0)\|_{L^2(\Omega)}, \end{aligned} \tag{3.42b}$$

Dividing (3.42) by the norm $\|\nabla\varphi(0)\|_{L^2(\Omega)}$ yields

$$\|\nabla\varphi(0)\|_{L^2(\Omega)} \lesssim \|\nabla\psi\|_{L^2(\Omega)}, \tag{3.43a}$$

which holds similarly for

$$\|\nabla\partial_t\varphi(0)\|_{L^2(\Omega)} \lesssim \|\nabla\partial_t\psi(0)\|_{L^2(\Omega)}. \tag{3.43b}$$

Employing (3.40) and (3.43) in the error estimate (3.39) yields the assertion. □

Lemma 3.15 (Projection error of the prototypical eho-LOD method)**.** *Let Assumption 3.1 hold for some $k \in \mathbb{N}_0$ and $m \geq 2j+2$. Further, let u be the solution to* (3.2)*, and $\check{u}_H$ be the solution to* (3.29)*. With $\varrho = u - \check{\mathcal{P}}^j u$, and $\psi = u - \check{\mathcal{Q}}^j u$, where the projection $\check{\mathcal{P}}^j$ is defined in* (3.33) *and the mapping $\check{\mathcal{Q}}^j$ in* (3.31)*, the following estimate holds for $\nu = 0, 1, 2$*

$$\|\nabla\partial_t^\nu\varrho(t)\|_{L^2(\Omega)} \lesssim \|\nabla\partial_t^\nu\psi(t)\|_{L^2(\Omega)}, \tag{3.44a}$$

and for $\nu = 1, 2$

$$\|\partial_t^\nu\varrho(t)\|_{L^2(\Omega)} \lesssim H\|\nabla\partial_t^\nu\psi(t)\|_{L^2(\Omega)}. \tag{3.44b}$$

Proof. Fix any $s \in [0, T]$. We have by definition of the projections

$$\varrho(s) = \underbrace{u(s) - (\widetilde{\mathcal{P}}u(s)}_{\in W} + \underbrace{\widehat{\mathcal{P}}^j u(s))}_{\in W} \in W. \tag{3.45}$$

Thus, we can subtract the L^2-projection and use the approximation (2.13) such that for $\nu = 1, 2$ we have

$$\begin{aligned} \|\partial_t^\nu\varrho(s)\|_{L^2(\Omega)} &= \|(\mathrm{id} - \Pi_H)\partial_t^\nu\varrho(s)\|_{L^2(\Omega)} \\ &\lesssim H\|\nabla\partial_t^\nu\varrho(s)\|_{L^2(\Omega)}. \end{aligned} \tag{3.46}$$

Since $\varrho(s)$ is orthogonal to any function $\check{v}_H \in \check{V}_H^j$, we may insert the mapping $\check{\mathcal{Q}}^j$ into the energy inner product, and with the coercivity (2.6) and the Cauchy-Schwarz inequality, we have

$$\begin{aligned} \|\nabla\varrho(s)\|_{L^2(\Omega)}^2 &\lesssim a(\varrho(s), \varrho(s)) \\ &= a(u(s) - \check{\mathcal{P}}^j u(s), u(s) - \check{\mathcal{P}}^j u(s)) \\ &= a(u(s) - \check{\mathcal{P}}^j u(s), u(s)) \\ &= a(u(s) - \check{\mathcal{P}}^j u(s), u(s) - \check{\mathcal{Q}}^j u(s)) \\ &\lesssim \|\nabla\varrho(s)\|_{L^2(\Omega)}\|\nabla\psi(s)\|_{L^2(\Omega)}. \end{aligned} \tag{3.47}$$

Dividing both sides by $\|\nabla\varrho(s)\|_{L^2(\Omega)}$ yields

$$\|\nabla\varrho\|_{L^2(\Omega)} \lesssim \|\nabla\psi\|_{L^2(\Omega)},$$

which holds similar for $\nu = 1, 2$, i.e.,

$$\|\nabla\partial_t^\nu\varrho(s)\|_{L^2(\Omega)} \lesssim \|\nabla\partial_t^\nu\psi(s)\|_{L^2(\Omega)}.$$

□

Finally, we estimate the mapping error ψ, which is the principal finding in this section. The following is a rigorous analysis of the considerations at the start of this section.

Theorem 3.16 (Mapping error of the prototypical eho-LOD method)**.** *Let Assumption 3.1 hold for some $k \in \mathbb{N}_0$ and $m \geq 2j+4$. Further, let u be the solution to* (3.2)*, and $\check{u}_H$ be the solution to* (3.29)*. With $\psi = u - \check{\mathcal{Q}}^j u$, where the mapping is defined in* (3.31)*, and if $j \geq \lceil \frac{p}{2} \rceil$ the following estimate holds for $\nu = 0, 1, 2$*

$$\|\nabla \partial_t^\nu \psi(t)\|_{L^2(\Omega)} \lesssim H^{\kappa+1} C_{\mathrm{data}}, \tag{3.48}$$

where $\kappa = \min\{k, p+1\}$.

The idea for the proof is similar to the above considerations and the estimate in the ideal setting Theorem 3.12. That is, the definition of $\psi = u - \check{\mathcal{Q}}^j u$ essentially mimics the expansion (3.26). In the proof, we also use the fact that the enriched corrections have small norms by artificially inserting them into the sum. This trick yields two additional orders of convergence but does not result in a computational overhead.

Remark 3.8. (Temporal regularity) In this proof, we observe that actually no spatial regularity of the solution beyond $u \in H_0^1(\Omega)$ is required. We, however, pay by this construction with additional regularity in time. Since, we consider time-independent coefficients, the regularity in time of the solution depends on the temporal regularity of the right-hand side and the well-preparedness and compatibility conditions Assumption 3.1 only. Thus, the need for additional regularity in time solely depends on the data of the PDE and is not a severe restriction.

Proof. We fix $s \in [0, T]$. Similar to (3.45) we have that

$$\psi(s) = \underbrace{u(s) - (\widetilde{\mathcal{P}} u(s)}_{\in W} + \underbrace{\widehat{\mathcal{Q}}^j u(s))}_{\in W} \in W. \tag{3.49}$$

In the following we omit the argument $s \in [0, T]$ for ease of presentation and note that it holds for each point in time. Using the coercivity (2.6), the orthogonality (2.28) and the wave equation (3.2) yields

$$\begin{aligned} \|\nabla \psi\|_{L^2(\Omega)}^2 &\lesssim a(\psi, \psi) \\ &= a(u - (\widetilde{\mathcal{P}} u + \widehat{\mathcal{Q}}^j u), \psi) \\ &= a(u - \widehat{\mathcal{Q}}^j u, \psi) \\ &= (f, \psi)_{L^2(\Omega)} - (\partial_t^2 u, \psi)_{L^2(\Omega)} - a(\widehat{\mathcal{Q}}^j u, \psi). \end{aligned} \tag{3.50}$$

With the standard approximation estimates (2.13), since $\psi \in W$, we can bound the first term with the optimal rate

$$\begin{aligned} (f, \psi)_{L^2(\Omega)} &= ((\mathrm{id} - \Pi_H) f, (\mathrm{id} - \Pi_H)\psi)_{L^2(\Omega)} \\ &\lesssim H^{\kappa+1} \|f\|_{H^\kappa(\mathcal{T}_H)} \|\nabla \psi\|_{L^2(\Omega)}, \end{aligned} \tag{3.51}$$

where $\kappa = \min\{k, p+1\}$. Thus, we focus on the second and third term of (3.50). Employing the definitions of the mapping $\widehat{\mathcal{Q}}^j$ and the enriched correction operator $\mathcal{D}$, we have

$$\begin{aligned}
&(\partial_t^2 u, \psi)_{L^2(\Omega)} + a(\widehat{\mathcal{Q}}^j u, \psi) \\
&\quad = (\partial_t^2 u, \psi)_{L^2(\Omega)} + a\left(\sum_{\nu=1}^{j} \mathcal{D}^\nu(\partial_t^{2\nu}\widetilde{\mathcal{P}}u), \psi\right) \\
&\quad = (\partial_t^2 u, \psi)_{L^2(\Omega)} - (\partial_t^2\widetilde{\mathcal{P}}u, \psi)_{L^2(\Omega)} - \left(\partial_t^2 \sum_{\nu=2}^{j} \mathcal{D}^{\nu-1}(\partial_t^{2(\nu-1)}\widetilde{\mathcal{P}}u), \psi\right)_{L^2(\Omega)} =: (\star).
\end{aligned} \tag{3.52a}$$

Using the fact that the test function $\psi \in W$, we subtract the L^2-projection and with the approximation result (2.13) we estimate

$$(\star) \lesssim H^2 \left\| \nabla \partial_t^2 (u - \widetilde{\mathcal{P}}u - \sum_{\nu=2}^{j} \mathcal{D}^{\nu-1}(\partial_t^{2(\nu-1)}\widetilde{\mathcal{P}}u)) \right\|_{L^2(\Omega)} \|\nabla\psi\|_{L^2(\Omega)}. \tag{3.52b}$$

For the first norm on the right hand-side we leverage the fact that the enriched corrections have a much better scaling compared to functions that lie in the multiscale space. This is a result of the definition of the enriched corrections, as they map into the kernel space W. That is, we insert an artificial $(j+1)$st correction and use the triangle inequality to split the norm into two parts

$$\begin{aligned}
&\left\| \nabla \partial_t^2 (u - \widetilde{\mathcal{P}}u - \sum_{\nu=2}^{j} \mathcal{D}^{\nu-1}(\partial_t^{2(\nu-1)}\widetilde{\mathcal{P}}u)) \right\|_{L^2(\Omega)} \\
&\quad \leq \left\| \nabla \partial_t^2 (u - \widetilde{\mathcal{P}}u - \sum_{\nu=2}^{j+1} \mathcal{D}^{\nu-1}(\partial_t^{2(\nu-1)}\widetilde{\mathcal{P}}u)) \right\|_{L^2(\Omega)} + \|\nabla \partial_t^2 \mathcal{D}^j(\partial_t^{2j}\widetilde{\mathcal{P}}u)\|_{L^2(\Omega)}.
\end{aligned} \tag{3.52c}$$

We note here that this additional enriched correction is only a theoretical device and does not need to be constructed in practice. However, this estimate requires additional temporal regularity of the solution. We are now able to use (3.51) and (3.52) in (3.50), which yields

$$\begin{aligned}
\|\nabla\psi\|_{L^2(\Omega)}^2 \lesssim\ & H^{\kappa+1}\|f\|_{H^\kappa(\mathcal{T}_H)}\|\nabla\psi\|_{L^2(\Omega)} \\
&+ H^2\Big[\left\| \nabla \partial_t^2 (u - \widetilde{\mathcal{P}}u - \sum_{\nu=2}^{j+1} \mathcal{D}^{\nu-1}(\partial_t^{2(\nu-1)}\widetilde{\mathcal{P}}u)) \right\|_{L^2(\Omega)} \\
&\quad + \|\nabla \partial_t^2 \mathcal{D}^j(\partial_t^{2j}\widetilde{\mathcal{P}}u)\|_{L^2(\Omega)}\Big]\|\nabla\psi\|_{L^2(\Omega)},
\end{aligned}$$

where $\kappa = \min\{k, p+1\}$. Dividing both sides by $\|\nabla\psi\|_{L^2(\Omega)}$ yields the following error estimate for the mapping error

$$\|\nabla\psi\|_{L^2(\Omega)} \lesssim H^{\kappa+1}\|f\|_{H^\kappa(\mathcal{T}_H)} + H^2\|\nabla\xi\|_{L^2(\Omega)} + H^2\|\nabla\zeta\|_{L^2(\Omega)}, \tag{3.53}$$

where we abbreviate

$$\xi = \partial_t^2(u - \widetilde{\mathcal{P}}u - \sum_{\nu=2}^{j+1} \mathcal{D}^{\nu-1}(\partial_t^{2(\nu-1)}\widetilde{\mathcal{P}}u))$$
$$\zeta = \partial_t^2 \mathcal{D}^j(\partial_t^{2j}\widetilde{\mathcal{P}}u).$$

In the following we show that both terms ξ and ζ scale with the optimal rate. For ξ we use similar arguments as above, and for ζ we use the definition of the enriched correction operator. We note that the considerations above also hold similarly for time derivatives of ψ, i.e., we have for $\nu = 0, 1, 2$

$$\|\nabla \partial_t^\nu \psi\|_{L^2(\Omega)} \lesssim H^{\kappa+1}\|\partial_t^\nu f\|_{H^\kappa(\mathcal{T}_H)} + H^2\|\nabla\partial_t^\nu \xi\|_{L^2(\Omega)} + H^2\|\nabla\partial_t^\nu \zeta\|_{L^2(\Omega)}. \tag{3.54}$$

1 Scaling of the enriched correction operator. As mentioned above the first term in (3.53) has optimal convergence, and it is left to estimate the second and third terms. We first consider the last term $\|\nabla\zeta\|_{L^2(\Omega)}$. We have $\zeta \in W$ by the definition of the enriched correction operator, and thus we use the coercivity (2.6) the definition of the enriched correction operator and the approximation of the L^2-projection (2.13) to obtain

$$\begin{aligned}\|\nabla\zeta\|_{L^2(\Omega)}^2 &\lesssim a(\partial_t^2\mathcal{D}^j(\partial_t^{2j}\widetilde{\mathcal{P}}u), \zeta)\\ &= (\partial_t^4\mathcal{D}^{j-1}(\partial_t^{2(j-1)}\widetilde{\mathcal{P}}u), \zeta)_{L^2(\Omega)}\\ &\lesssim H^2\|\nabla\partial_t^4\mathcal{D}^{j-1}(\partial_t^{2(j-1)}\widetilde{\mathcal{P}}u)\|_{L^2(\Omega)}\|\nabla\zeta\|_{L^2(\Omega)}.\end{aligned} \tag{3.55a}$$

Using the same argumentation, we can show for any $w \in W$ and any $\nu = 0, \dots, j-1$ that

$$\begin{aligned}a(\partial_t^{2(\nu+1)}\mathcal{D}^{j-\nu}(\partial_t^{2(j-\nu)}\widetilde{\mathcal{P}}u), w) &= (\partial_t^{2(\nu+2)}\mathcal{D}^{j-\nu-1}(\partial_t^{2(j-\nu-1)}\widetilde{\mathcal{P}}u), w)_{L^2(\Omega)}\\ &\lesssim H^2\|\nabla\partial_t^{2(\nu+2)}\mathcal{D}^{j-\nu-1}(\partial_t^{2(j-\nu-1)}\widetilde{\mathcal{P}}u)\|_{L^2(\Omega)}\|\nabla w\|_{L^2(\Omega)}.\end{aligned}$$

Choosing

$$w = \partial_t^{2(\nu+1)}\mathcal{D}^{j-\nu}(\partial_t^{2(j-\nu)}\widetilde{\mathcal{P}}u)$$

as a test function yields with the coercivity (2.6) for any $\nu = 0, \dots, j-1$

$$\|\nabla\partial_t^{2(\nu+1)}\mathcal{D}^{j-\nu}(\partial_t^{2(j-\nu)}\widetilde{\mathcal{P}}u)\|_{L^2(\Omega)} \lesssim H^2\|\nabla\partial_t^{2(\nu+2)}\mathcal{D}^{j-\nu-1}(\partial_t^{2(j-\nu-1)}\widetilde{\mathcal{P}}u)\|_{L^2(\Omega)} \tag{3.55b}$$

Starting from (3.55a) and dividing both sides by $\|\nabla\zeta\|_{L^2(\Omega)}$, we can apply (3.55b) recursively to obtain

$$\begin{aligned}\|\nabla\zeta\|_{L^2(\Omega)} &= \|\nabla\partial_t^2\mathcal{D}^j(\partial_t^{2j}\widetilde{\mathcal{P}}u)\|_{L^2(\Omega)}\\ &\lesssim H^2\|\nabla\partial_t^4\mathcal{D}^{j-1}(\partial_t^{2(j-1)}\widetilde{\mathcal{P}}u)\|_{L^2(\Omega)}\\ &\lesssim H^4\|\nabla\partial_t^6\mathcal{D}^{j-2}(\partial_t^{2(j-2)}\widetilde{\mathcal{P}}u)\|_{L^2(\Omega)}\\ &\lesssim H^{2j}\|\nabla\partial_t^{2(j+1)}\widetilde{\mathcal{P}}u\|_{L^2(\Omega)}.\end{aligned} \tag{3.56}$$

For the projection $\widetilde{\mathcal{P}}$ we can show with the coercivity (2.6) and the Cauchy-Schwarz inequality that

$$\begin{aligned}\|\nabla\widetilde{\mathcal{P}}u\|^2_{L^2(\Omega)} &\lesssim a(\widetilde{\mathcal{P}}u,\widetilde{\mathcal{P}}u)\\ &= a(u,\widetilde{\mathcal{P}}u)\\ &\lesssim \|\nabla u\|_{L^2(\Omega)}\|\nabla\widetilde{\mathcal{P}}u\|_{L^2(\Omega)},\end{aligned}$$

After dividing by $\|\nabla\widetilde{\mathcal{P}}u\|_{L^2(\Omega)}$ it follows

$$\|\nabla\widetilde{\mathcal{P}}u\|_{L^2(\Omega)} \lesssim \|\nabla u\|_{L^2(\Omega)}, \tag{3.57}$$

which holds similarly for $\partial_t^\nu\widetilde{\mathcal{P}}u$ for $\nu = 1,\dots,2(j+1)$. Thus, using the stability (3.57) in (3.56) we have

$$\begin{aligned}\|\nabla\zeta\|_{L^2(\Omega)} &\lesssim H^{2j}\|\nabla\partial_t^{2(j+1)}\widetilde{\mathcal{P}}u\|_{L^2(\Omega)}\\ &\lesssim H^{2j}\|\nabla\partial_t^{2(j+1)}u\|_{L^2(\Omega)}.\end{aligned} \tag{3.58}$$

Note that the estimates for the norms of the time derivatives $\|\nabla\partial_t^\nu\zeta\|_{L^2(\Omega)}$ with $\nu = 1,2$ follow analogously, i.e.,

$$\|\nabla\partial_t^\nu\zeta\|_{L^2(\Omega)} \lesssim H^{2j}\|\nabla\partial_t^{2(j+1)+\nu}u\|_{L^2(\Omega)}. \tag{3.59}$$

2 Approximation estimate for the enriched multiscale mapping. In this part we estimate the second term of (3.53). Similar to (3.49) we have that $\xi \in W$. Then we use the coercivity (2.6), the orthogonality (2.28) and the variational wave equation similar to (3.50) to obtain

$$\begin{aligned}\|\nabla\xi\|^2_{L^2(\Omega)} &\lesssim a(\partial_t^2(u-\widetilde{\mathcal{P}}u-\sum_{\nu=2}^{j+1}\mathcal{D}^{\nu-1}(\partial_t^{2(\nu-1)}\widetilde{\mathcal{P}}u)),\xi)\\ &= a(\partial_t^2(u-\sum_{\nu=2}^{j+1}\mathcal{D}^{\nu-1}(\partial_t^{2(\nu-1)}\widetilde{\mathcal{P}}u)),\xi) \qquad (3.60a)\\ &= (\partial_t^2 f-\partial_t^4 u+\partial_t^4\widetilde{\mathcal{P}}u+\sum_{\nu=3}^{j+1}\mathcal{D}^{\nu-2}(\partial_t^{2(\nu-2)}\widetilde{\mathcal{P}}u),\xi)_{L^2(\Omega)} = (\star).\end{aligned}$$

Since the test function $\xi \in W$, we can subtract the L^2-projection Π_H and use the approximation (2.13) to obtain

$$\begin{aligned}(\star) &\lesssim H^{\kappa+1}\|\partial_t^2 f\|_{H^\kappa(\mathcal{T}_H)}\|\nabla\xi\|_{L^2(\Omega)}\\ &\quad + H^2\|\nabla\partial_t^4(u-\widetilde{\mathcal{P}}u-\sum_{\nu=3}^{j+1}\mathcal{D}^{\nu-2}(\partial_t^{2(\nu-2)}\widetilde{\mathcal{P}}u))\|_{L^2(\Omega)}\|\nabla\xi\|_{L^2(\Omega)}.\end{aligned} \tag{3.60b}$$

With similar arguments we can show for any $w \in W$ and $\mu = 0, \dots, j-1$ that

$$\begin{aligned} a(\partial_t^{2(\mu+1)}(u - \widetilde{\mathcal{P}}u - \sum_{\nu=\mu+2}^{j+1} \mathcal{D}^{\nu-(\mu+1)}(\partial_t^{2(\nu-(\mu+1))}\widetilde{\mathcal{P}}u)), w) \\ \lesssim H^{\kappa+1}\|\partial_t^{2(\mu+1)} f\|_{H^\kappa(\mathcal{T}_H)}\|\nabla w\|_{L^2(\Omega)} \\ + H^2\|\nabla\partial_t^{2(\mu+2)}(u - \widetilde{\mathcal{P}}u - \sum_{\nu=\mu+3}^{j+1} \mathcal{D}^{\nu-(\mu+2)}(\partial_t^{2(\nu-(\mu+2))}\widetilde{\mathcal{P}}u))\|_{L^2(\Omega)}\|\nabla w\|_{L^2(\Omega)}. \end{aligned} \tag{3.61}$$

The choice

$$w = \partial_t^{2(\mu+1)}(u - \widetilde{\mathcal{P}}u - \sum_{\nu=\mu+2}^{j+1} \mathcal{D}^{\nu-(\mu+1)}(\partial_t^{2(\nu-(\mu+1))}\widetilde{\mathcal{P}}u))$$

and dividing by $\|\nabla w\|_{L^2(\Omega)}$ yields with the coercivity (2.6) the following error bound for any $\mu = 0, \dots, j-1$

$$\begin{aligned} \|\nabla\partial_t^{2(\mu+1)}(u - \widetilde{\mathcal{P}}u - \sum_{\nu=\mu+2}^{j+1} \mathcal{D}^{\nu-(\mu+1)}(\partial_t^{2(\nu-(\mu+1))}\widetilde{\mathcal{P}}u))\|_{L^2(\Omega)} \\ \lesssim H^{\kappa+1}\|\partial_t^{2(\mu+1)} f\|_{H^\kappa(\mathcal{T}_H)} \\ + H^2\|\nabla\partial_t^{2(\mu+2)}(u - \widetilde{\mathcal{P}}u - \sum_{\nu=\mu+3}^{j+1} \mathcal{D}^{\nu-(\mu+2)}(\partial_t^{2(\nu-(\mu+2))}\widetilde{\mathcal{P}}u))\|_{L^2(\Omega)}. \end{aligned} \tag{3.62}$$

Dividing both sides of (3.60) by $\|\nabla\xi\|_{L^2(\Omega)}$ and using (3.62) recursively yields the following estimate

$$\begin{aligned} \|\nabla\xi\|_{L^2(\Omega)} &= \|\nabla\partial_t^2(u - \widetilde{\mathcal{P}}u - \sum_{\nu=2}^{j+1} \mathcal{D}^{\nu-1}(\partial_t^{2(\nu-1)}\widetilde{\mathcal{P}}u))\|_{L^2(\Omega)} \\ &\lesssim H^{\kappa+1}\|\partial_t^2 f\|_{H^\kappa(\mathcal{T}_H)} \\ &\quad + H^2\|\nabla\partial_t^4(u - \widetilde{\mathcal{P}}u - \sum_{\nu=3}^{j+1} \mathcal{D}^{\nu-2}(\partial_t^{2(\nu-2)}\widetilde{\mathcal{P}}u))\|_{L^2(\Omega)} \\ &\lesssim H^{\kappa+1}\sum_{\nu=2}^{j+1} H^{2(\nu-2)}\|\partial_t^{2(\nu-1)} f\|_{H^\kappa(\mathcal{T}_H)} \\ &\quad + H^{2j}\|\nabla\partial_t^{2(j+1)}(u - \widetilde{\mathcal{P}}u)\|_{L^2(\Omega)}. \end{aligned} \tag{3.63}$$

For the projection $\widetilde{\mathcal{P}}$ we can show with the coercivity (2.6) and the Cauchy-Schwarz inequality that

$$\begin{aligned} \|\nabla(u - \widetilde{\mathcal{P}}u)\|_{L^2(\Omega)}^2 &\le a(u - \widetilde{\mathcal{P}}u, u - \widetilde{\mathcal{P}}u) \\ &= a(u, u - \widetilde{\mathcal{P}}u) \\ &\le \beta\|\nabla u\|_{L^2(\Omega)}\|\nabla(u - \widetilde{\mathcal{P}}u)\|_{L^2(\Omega)}, \end{aligned}$$

After dividing by $\|\nabla(u-\widetilde{\mathcal{P}}u)\|_{L^2(\Omega)}$ it follows

$$\|\nabla(u-\widetilde{\mathcal{P}}u)\|_{L^2(\Omega)} \lesssim \|\nabla u\|_{L^2(\Omega)}. \tag{3.64}$$

Finally, applying (3.64) yields

$$\begin{aligned}\|\nabla\xi\|_{L^2(\Omega)} &\lesssim H^{\kappa+1}\sum_{\nu=2}^{j+1} H^{2(\nu-2)}\|\partial_t^{2(\nu-1)}f\|_{H^\kappa(\mathcal{T}_H)} + H^{2j}\|\nabla\partial_t^{2(j+1)}(u-\widetilde{\mathcal{P}}u)\|_{L^2(\Omega)}\\ &\lesssim H^{\kappa+1}\sum_{\nu=2}^{j+1} H^{2(\nu-2)}\|\partial_t^{2(\nu-1)}f\|_{H^\kappa(\mathcal{T}_H)} + H^{2j}\|\nabla\partial_t^{2(j+1)}u\|_{L^2(\Omega)}.\end{aligned} \tag{3.65}$$

Similarly, the above estimates can be performed for the temporal derivatives $\partial_t^\mu\xi$, i.e., for $\mu=0,1,2$ we have

$$\|\nabla\partial_t^\mu\xi\|_{L^2(\Omega)} \lesssim H^{\kappa+1}\sum_{\nu=2}^{j+1} H^{2(\nu-2)}\|\partial_t^{2(\nu-1)+\mu}f\|_{H^\kappa(\mathcal{T}_H)} + H^{2j}\|\nabla\partial_t^{2(j+1)+\mu}u\|_{L^2(\Omega)}. \tag{3.66}$$

Finally, we show the assertion. Starting from (3.54) we apply (3.59) and (3.66) we have for any $\mu=0,1,2$ that

$$\begin{aligned}\|\nabla\partial_t^\mu\psi\|_{L^2(\Omega)} &\lesssim H^{\kappa+1}\|\partial_t^\mu f\|_{H^\kappa(\mathcal{T}_H)} + H^2\|\nabla\partial_t^\mu\xi\|_{L^2(\Omega)} + H^2\|\nabla\partial_t^\mu\zeta\|_{L^2(\Omega)}\\ &\lesssim H^{\kappa+1}\|\partial_t^\mu f\|_{H^\kappa(\mathcal{T}_H)}\\ &\quad + H^{\kappa+3}\sum_{\nu=2}^{j+1} H^{2(\nu-2)}\|\partial_t^{2(\nu-1)+\mu}f\|_{H^\kappa(\mathcal{T}_H)} + H^{2j+2}\|\nabla\partial_t^{2(j+1)+\mu}u\|_{L^2(\Omega)}\\ &\quad + H^{2j+2}\|\nabla\partial_t^{2(j+1)+\mu}u\|_{L^2(\Omega)}.\end{aligned} \tag{3.67}$$

Taking the supremum over all times $s\in[0,T]$ on the right-hand side yields with the definition of the constant C_{data} in (3.5)

$$\begin{aligned}\|\nabla\partial_t^\mu\psi\|_{L^2(\Omega)} &\lesssim H^{\kappa+1}\|f\|_{C^{2j+\mu}([0,T];\mathcal{T}_H)} + H^{2j+2}\|u\|_{C^{2(j+1)+\mu}([0,T];H^1(\Omega))}\\ &\lesssim \left[H^{\kappa+1}+H^{2j+2}\right]C_{\mathrm{data}}.\end{aligned} \tag{3.68}$$

The assertion follows from the choice $j=\lceil\frac{p}{2}\rceil$. □

In the proof we observe that the considerations at the start of this section can be rigorously verified. We also observe that for every order of spatial convergence we require two additional temporal regularity of the solution. We now combine the above lemmas and the theorem to prove the error estimate for the prototypical eho-LOD method. That is, we prove

$$\|\partial_t(\check{u}_H(t)-u(t))\|_{L^2(\Omega)} + \|\nabla(\check{u}_H(t)-u(t))\|_{L^2(\Omega)} \lesssim H^{\kappa+1}C_{\mathrm{data}},$$

where $\kappa=\min\{k,p+1\}$ for a.e. $t\in[0,T]$.

Proof of Theorem 3.13. Fix any $t \in [0,T]$. Similar to above we can split the error into the space discretization error φ and the projection error ϱ and use the triangle inequality to obtain

$$\begin{aligned}\|\partial_t(\check{u}_H(t)-u(t))\|_{L^2(\Omega)} + \|\nabla(\check{u}_H(t)-u(t))\|_{L^2(\Omega)} \\ \lesssim \|\partial_t\varphi(t)\|_{L^2(\Omega)} + \|\nabla\varphi(t)\|_{L^2(\Omega)} + \|\partial_t\varrho(t)\|_{L^2(\Omega)} + \|\nabla\varrho(t)\|_{L^2(\Omega)}.\end{aligned} \tag{3.69}$$

We can apply Lemma 3.14, i.e.,

$$\|\partial_t\varphi(t)\|_{L^2(\Omega)}+\|\nabla\varphi(t)\|_{L^2(\Omega)} \lesssim H\|\nabla\partial_t\psi(0)\|_{L^2(\Omega)}+\|\nabla\psi(0)\|_{L^2(\Omega)}+\int_0^t \|\partial_t^2\varrho(s)\|_{L^2(\Omega)}\,\mathrm{d}s$$

to obtain

$$\begin{aligned}\|\partial_t(\check{u}_H(t)-u(t))\|_{L^2(\Omega)} + \|\nabla(\check{u}_H(t)-u(t))\|_{L^2(\Omega)} \\ \lesssim H\|\nabla\partial_t\psi(0)\|_{L^2(\Omega)} + \|\nabla\psi(0)\|_{L^2(\Omega)} \\ + \int_0^t \|\partial_t^2\varrho(s)\|_{L^2(\Omega)}\,\mathrm{d}s + \|\partial_t\varrho(t)\|_{L^2(\Omega)} + \|\nabla\varrho(t)\|_{L^2(\Omega)}.\end{aligned} \tag{3.70}$$

Further, we can use Lemma 3.15, recall for $\nu = 1, 2$

$$\begin{aligned}\|\nabla\varrho(t)\|_{L^2(\Omega)} &\lesssim \|\nabla\psi(t)\|_{L^2(\Omega)}, \\ \|\partial_t^\nu\varrho(t)\|_{L^2(\Omega)} &\lesssim H\|\nabla\partial_t^\nu\psi(t)\|_{L^2(\Omega)},\end{aligned}$$

which overall yields

$$\begin{aligned}\|\partial_t(\check{u}_H(t)-u(t))\|_{L^2(\Omega)} + \|\nabla(\check{u}_H(t)-u(t))\|_{L^2(\Omega)} \\ \lesssim H\|\nabla\partial_t\psi(0)\|_{L^2(\Omega)} + \|\nabla\psi(0)\|_{L^2(\Omega)} \\ + H\int_0^t \|\nabla\partial_t^2\psi(s)\|_{L^2(\Omega)}\,\mathrm{d}s + H\|\nabla\partial_t\psi(t)\|_{L^2(\Omega)} + \|\nabla\psi(t)\|_{L^2(\Omega)}.\end{aligned} \tag{3.71}$$

Finally, by Theorem 3.16, i.e., for $\nu = 0, 1, 2$ with $\kappa = \min\{k, p+1\}$, we have

$$\|\nabla\partial_t^\nu\psi(t)\|_{L^2(\Omega)} \lesssim H^{\kappa+1}C_{\mathrm{data}},$$

which proves the assertion for the semi-discrete prototypical eho-LOD

$$\|\partial_t(\check{u}_H(t)-u(t))\|_{L^2(\Omega)} + \|\nabla(\check{u}_H(t)-u(t))\|_{L^2(\Omega)} \lesssim H^{\kappa+1}C_{\mathrm{data}}. \qquad \square$$

This completes the section considering the prototypical eho-LOD. The goal now is similar to the elliptic setting to create a computationally feasible method.

3.4 Localization

In the previous section we have constructed a novel enriched correction operator, that in the prototypical setting presented there, is able to recover the optimal convergence rate $\mathcal{O}(H^{p+2})$ provided the right-hand side is sufficiently regular, and the initial conditions fit to the problem. However, the enriched correction operator yields a global problem. This makes the prototypical method unfeasible, and thus a localization of the enriched corrector problem is necessary.

In Section 3.4.1 we define an element-wise enriched correction operator and show that it obeys a similar decay and localization error as the classical corrector. However, choosing the localization parameter for the element-wise enriched corrections is a deciding task. If the element-wise enriched correction operators are defined on subdomains that are chosen with the same localization parameter as the localized corrections we quickly result in oversampling domains for the basis function that span the whole domain. Naturally this is too expensive. If the localization parameter is chosen appropriately, then it can be proven that the enriched correction operators can be computed locally on patches with same size. This is a main contribution of this thesis and given in Theorem 3.19.

Section 3.4.2 then provides a semi-discrete error analysis for the eho-LOD method employing localized enriched corrections.

3.4.1 Decay and localization of the enriched correction operator

The previous section showcased first, why the prototypical sp-LOD method is not suitable for the discretization of time-dependent problems with very rough coefficients. Afterwards, we provided a strategy that in an ideal setting is able to work around low regularity in space. However, similar to the classical prototypical sp-LOD method, the prototypical eho-LOD method defines global basis functions which yields a high computational effort when solving the PDE.

This requires a novel localization strategy that ensures that the enriched corrections can be computed on subdomains with the same size as the localized correction. We derive a localization strategy for the enriched correction operator in this section. We note that this section follows the ideas from Kalyanaraman, Krumbiegel, Maier, and Wang (2025) transferred to the wave equation.

Let $G \in \mathcal{T}_H$ be an arbitrary element. We define the localized element-wise enriched correction operator $\mathcal{D}_G^{[\lambda]} \colon L^2(\Omega) \to W(\mathtt{N}^\lambda(G))$ for any $v \in L^2(\Omega)$ as the solution of

$$a|_{\mathtt{N}^\lambda(G)}(\mathcal{D}_G^{[\lambda]} v, w) = -(v, w)_{L^2(G)} \tag{3.72}$$

for all $w \in W(\mathtt{N}^\lambda(G))$. For the localized enriched correction operator we now choose for each element $G \in \mathcal{T}_H$ a different localization parameter $\lambda_G \in \mathbb{N}$, and the *localized*

enriched correction operator $\mathcal{D}^{\mathrm{loc}}\colon L^2(\Omega) \to W$ is defined by

$$\mathcal{D}^{\mathrm{loc}} = \sum_{G \in \mathcal{T}_H} \mathcal{D}_G^{[\lambda_G]}. \tag{3.73}$$

Analogously to above, if we (formally) set $\lambda_G = \infty$ we denote the *element-wise enriched correction operator* by $\mathcal{D}_G = \mathcal{D}_G^{[\infty]}$. The enriched correction operator is then given by

$$\mathcal{D} = \sum_{G \in \mathcal{T}_H} \mathcal{D}_G. \tag{3.74}$$

How the localization parameter λ_G is chosen exactly, will be determined at a later stage in Assumption 3.10. For now for readability we omit the subscript and denote the localization parameter with just λ. The element-wise enriched correction operator obeys a decay estimate similar to the one for the element-wise correction operator $\mathcal{C}_K$. The results are given in the following. The proofs are provided for completeness and follow the ideas of Dong, Hauck, and Maier (2023) rather closely.

The following lemma estimates in the H_0^1-norm where most mass of the element-wise enriched corrections $\mathcal{D}_G v$ lie. We prove an exponential decay away from the element G. This means that truncation of the support of the element-wise enriched corrections results in exponentially small errors when increasing the patch size λ.

Lemma 3.17. *Let $G \in \mathcal{T}_H$ and $\lambda \in \mathbb{N}$. Then for any $v \in L^2(\Omega)$ we have*

$$\|\nabla \mathcal{D}_G v\|_{L^2(\Omega \setminus \mathtt{N}^\lambda(G))} \lesssim \exp(-C\lambda) \|\nabla \mathcal{D}_G v\|_{L^2(\Omega)}. \tag{3.75}$$

In the proof we define a so-called cutoff function that restricts the element-wise enriched corrections to the outside of the patch (white and light grey area in Figure 3.3). Here, we crucially employ the localization of the bubble operator $\mathcal{B}_H$, see Lemma 2.1.

Proof of Lemma 3.17. We define a cutoff function $\eta \in W^{1,\infty}(\Omega)$ with

$$\begin{aligned}
&\eta \equiv 0, && \text{in } \mathtt{N}^{\lambda-1}(G), && \text{(3.76a)}\\
&\eta \equiv 1, && \text{in } \Omega \setminus \mathtt{N}^{\lambda}(G), && \text{(3.76b)}\\
&0 \le \eta \le 1, \quad \|\nabla \eta\|_{L^\infty(R)} \lesssim H^{-1}, && \text{in } R \coloneqq \mathtt{N}^{\lambda}(G) \setminus \mathtt{N}^{\lambda-1}(G). && \text{(3.76c)}
\end{aligned}$$

Consider the norm of the element-wise enriched correction operator outside the $\mathtt{N}^\lambda(G)$-patch. We have by the coercivity (2.6) and product rule that the norm is bounded by

$$\begin{aligned}
\|\nabla \mathcal{D}_G v\|^2_{L^2(\Omega \setminus \mathtt{N}^\lambda(G))} &\lesssim (A \nabla \mathcal{D}_G v, \eta \nabla \mathcal{D}_G v)_{L^2(\Omega)} \\
&= a(\mathcal{D}_G v, \eta \mathcal{D}_G v) - (A \nabla \mathcal{D}_G v, \mathcal{D}_G v \nabla \eta)_{L^2(\Omega)} = (\star).
\end{aligned} \tag{3.77a}$$

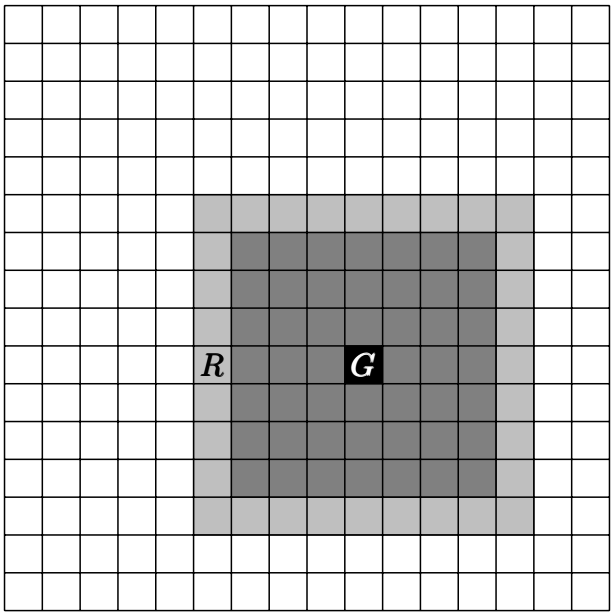

Figure 3.3: Illustration of an element G with patch $\mathtt{N}^4(G)$ depicted as the union of light and dark grey, and black. The cutoff function η defined in (3.76) is 0 in the dark grey and black, 1 in the white, and decaying in between in the light grey area.

Inserting the bubble operator yields

$$\begin{aligned}(\star) = a(\mathcal{D}_G v, (\mathrm{id} - \mathcal{B}_H)(\eta \mathcal{D}_G v)) &=: (I) \\ + a(\mathcal{D}_G v, \mathcal{B}_H(\eta \mathcal{D}_G v)) &=: (II) \\ - (A \nabla \mathcal{D}_G v, \mathcal{D}_G v \nabla \eta)_{L^2(\Omega)} &=: (III).\end{aligned} \tag{3.77b}$$

We have by the definition of the bubble operator (2.24) that

$$(\mathrm{id} - \mathcal{B}_H)(\eta \mathcal{D}_G v) \in W.$$

And by the definition of the cutoff function (3.76a), the term

$$(\mathrm{id} - \mathcal{B}_H)(\eta \mathcal{D}_G v)|_G = 0$$

vanishes in G for $\lambda \geq 1$. Thus, we can employ the definition of the element-wise enriched correction operator (3.72) to obtain

$$(I) = -(v, (\mathrm{id} - \mathcal{B}_H)(\eta \mathcal{D}_G v))_{L^2(G)} = 0. \tag{3.78}$$

Next, consider the second term (II). Since the enriched correction operator maps into the kernel space W, and by the definition of the cutoff function (3.76b) we have

$$(\eta \mathcal{D}_G v)|_{\Omega \setminus \mathtt{N}^\lambda(G)} \in W,$$

and thus since the bubble operator $\mathcal{B}_H$ maps locally to functions to the same element (Lemma 2.1)

$$\mathcal{B}_H(\eta \mathcal{D}_G v)|_{\Omega \setminus \mathbb{N}^\lambda(G)} = 0,$$

and further from the definition of the cutoff function (3.76a) follows

$$\mathcal{B}_H(\eta \mathcal{D}_G v)|_{\mathbb{N}^{\lambda-1}(G)} = 0.$$

Thus, the second term has only contributions inside the ring R, and we can bound the term using Cauchy-Schwarz inequality and the stability of the bubble operator (2.25) by

$$\begin{aligned} (II) &\lesssim \|\nabla \mathcal{D}_G v\|_{L^2(R)} \|\nabla \mathcal{B}_H(\eta \mathcal{D}_G v)\|_{L^2(R)} \\ &\lesssim H^{-1} \|\nabla \mathcal{D}_G v\|_{L^2(R)} \|\eta \mathcal{D}_G v\|_{L^2(R)} = (\star\star). \end{aligned} \tag{3.79a}$$

Further, we use that the cutoff function is bounded by 1 (cf. (3.76c)), the fact that the element-wise enriched correction operator maps into the kernel space, i.e., $\mathcal{D}_G v \in W$, and the approximation of the L^2-projection (2.13) to obtain

$$\begin{aligned} (\star\star) &\lesssim H^{-1} \|\nabla \mathcal{D}_G v\|_{L^2(R)} \|\mathcal{D}_G v\|_{L^2(R)} \\ &= H^{-1} \|\nabla \mathcal{D}_G v\|_{L^2(R)} \|(\mathrm{id} - \Pi_H)(\mathcal{D}_G v)\|_{L^2(R)} \\ &\lesssim \|\nabla \mathcal{D}_G v\|^2_{L^2(R)}. \end{aligned} \tag{3.79b}$$

Finally, we estimate the third term (III). By the definition of the cutoff function we have

$$\begin{aligned} \nabla \eta|_{\mathbb{N}^{\lambda-1}(G)} &= 0, \\ \nabla \eta|_{\Omega \setminus \mathbb{N}^\lambda(G)} &= 0, \end{aligned}$$

and thus the third term (III) has only contributions inside the ring R. Using the boundedness (2.7), the Hölder and Cauchy-Schwarz inequalities, and the boundedness (3.76c) yields

$$\begin{aligned} (III) &\lesssim \|\nabla \eta\|_{L^2(R)} (\nabla \mathcal{D}_G v, \mathcal{D}_G v)_{L^2(R)} \\ &\lesssim H^{-1} \|\nabla \mathcal{D}_G v\|_{L^2(R)} \|\mathcal{D}_G v\|_{L^2(R)} = (\star\star\star). \end{aligned} \tag{3.80a}$$

As above, we use that $\mathcal{D}_G v \in W$, and the approximation (2.13) to estimate

$$\begin{aligned} (\star\star\star) &= H^{-1} \|\nabla \mathcal{D}_G v\|_{L^2(R)} \|(\mathrm{id} - \Pi_H)(\mathcal{D}_G v)\|_{L^2(R)} \\ &\lesssim \|\nabla \mathcal{D}_G v\|^2_{L^2(R)}. \end{aligned} \tag{3.80b}$$

Employing equations (3.78) to (3.80) in (3.77), we have

$$\begin{aligned} \|\nabla \mathcal{D}_G v\|^2_{L^2(\Omega \setminus \mathbb{N}^\lambda(G))} &\lesssim \|\nabla \mathcal{D}_G v\|^2_{L^2(R)}, \\ &= \|\nabla \mathcal{D}_G v\|^2_{L^2(\Omega \setminus \mathbb{N}^{\lambda-1}(G))} - \|\nabla \mathcal{D}_G v\|^2_{L^2(\Omega \setminus \mathbb{N}^\lambda(G))}. \end{aligned} \tag{3.81}$$

Adding the last term on the right-hand side of (3.81) to both sides yields with a generic constant $C > 0$

$$(1 + C)\|\nabla \mathcal{D}_G v\|^2_{L^2(\Omega \setminus \mathtt{N}^\lambda(G))} \leq C.$$

Dividing both sides by $(1 + C)$ we obtain

$$\begin{aligned} \|\nabla \mathcal{D}_G v\|^2_{L^2(\Omega \setminus \mathtt{N}^\lambda(G))} &\leq \frac{C}{1+C} \|\nabla \mathcal{D}_G v\|^2_{L^2(\Omega \setminus \mathtt{N}^{\lambda-1}(G))} \\ \|\nabla \mathcal{D}_G v\|_{L^2(\Omega \setminus \mathtt{N}^\lambda(G))} &\leq \vartheta \|\nabla \mathcal{D}_G v\|_{L^2(\Omega \setminus \mathtt{N}^{\lambda-1}(G))}, \end{aligned} \tag{3.82}$$

where $\vartheta = \sqrt{\frac{C}{1+C}} < 1$. The last estimate corresponds to the norm in the white area of Figure 3.3 on the left-hand side and the norm in the white plus the light grey areas on the right-hand side. Thus, we have an estimate between norms after adding the norms on the ring. Since the number ϑ is independent of λ, the last inequality can be iterated such that we obtain with $C = \frac{1}{2}|\log \vartheta|$ the assertion

$$\|\nabla \mathcal{D}_G v\|_{L^2(\Omega \setminus \mathtt{N}^\lambda(G))} \leq \exp(-C\lambda) \|\nabla \mathcal{D}_G v\|_{L^2(\Omega)}. \qquad \square$$

This lemma can now directly be used to show that the localized enriched correction operator $\mathcal{D}^{\mathrm{loc}}$ introduces only en exponentially small error compared to the prototypical enriched corrector $\mathcal{D}$.

Lemma 3.18. *Let $G \in \mathcal{T}_H$ and $\lambda \in \mathbb{N}$. Then for any $v \in L^2(\Omega)$ we have*

$$\|\nabla(\mathcal{D}_G^{[\lambda]} v - \mathcal{D}_G v)\|_{L^2(\Omega)} \lesssim \exp(-C\lambda) \|\nabla \mathcal{D}_G v\|_{L^2(\Omega)}. \tag{3.83}$$

In the proof of Lemma 3.18 we find that the error fulfills a quasi-optimality property, i.e., the localized element-wise correction $\mathcal{D}_G^{[\lambda]} v$ of a function $v \in L^2(\Omega)$ is the best approximation (up to a constant) in the space $W(\mathtt{N}^\lambda(G))$. Employing a cutoff function that is zero outside the patch, we can find an approximation $w \in W(\mathtt{N}^\lambda(G))$ that only has an error on the outside of the patch and the ring R. This error can then be bounded by Lemma 3.17.

Proof of Lemma 3.18. We define a cutoff function $\eta \in W^{1,\infty}(\Omega)$ with

$$\begin{aligned} &\eta \equiv 1, && \text{in } \mathtt{N}^{\lambda-1}(G), && \text{(3.84a)} \\ &\eta \equiv 0, && \text{in } \Omega \setminus \mathtt{N}^\lambda(G), && \text{(3.84b)} \\ &0 \leq \eta \leq 1, \quad \|\nabla \eta\|_{L^\infty(R)} \lesssim H^{-1}, && \text{in } R \coloneqq \mathtt{N}^\lambda(G) \setminus \mathtt{N}^{\lambda-1}(G). && \text{(3.84c)} \end{aligned}$$

Here, the cutoff function is nonzero inside the patch and zero on the outside with the decay inside the ring R. Since the localized element-wise enriched correction operator maps into the kernel space $\mathcal{D}_G^{[\lambda]} v \in W(\mathtt{N}^\lambda(G))$ for any $v \in L^2(\Omega)$, it is a

valid test function for (3.72) with $\lambda = \infty$ as well. Thus, with the coercivity (2.6) and the Cauchy-Schwarz inequality it holds

$$\begin{aligned}\|\nabla(\mathcal{D}_G^{[\lambda]}v - \mathcal{D}_G v)\|_{L^2(\Omega)}^2 &\lesssim a((\mathcal{D}_G^{[\lambda]}v - \mathcal{D}_G v), (\mathcal{D}_G^{[\lambda]}v - \mathcal{D}_G v)) \\ &= a(\mathcal{D}_G^{[\lambda]}v - \mathcal{D}_G v, w - \mathcal{D}_G v) \\ &\lesssim \|\nabla(\mathcal{D}_G^{[\lambda]}v - \mathcal{D}_G v)\|_{L^2(\Omega)}\|\nabla(w - \mathcal{D}_G v)\|_{L^2(\Omega)}\end{aligned} \tag{3.85}$$

for any $w \in W(\mathbb{N}^\lambda(G))$. By the definition of the cutoff function (3.84b) and the locality of the bubble operator (2.24), we may choose

$$w = (\mathrm{id} - \mathcal{B}_H)(\eta \mathcal{D}_G v) \in W(\mathbb{N}^\lambda(G)).$$

This choice in (3.85) considering the support of $(\mathrm{id} - \eta)$ yields

$$\begin{aligned}\|\nabla(\mathcal{D}_G^{[\lambda]}v - \mathcal{D}_G v)\|_{L^2(\Omega)} &\lesssim \|\nabla(w - \mathcal{D}_G v)\|_{L^2(\Omega)} \\ &= \|\nabla((\mathrm{id} - \mathcal{B}_H)(\mathrm{id} - \eta)\mathcal{D}_G v)\|_{L^2(\Omega)} \\ &= \|\nabla((\mathrm{id} - \mathcal{B}_H)(\mathrm{id} - \eta)\mathcal{D}_G v)\|_{L^2(\Omega\setminus\mathbb{N}^{\lambda-1}(G))} = (\star).\end{aligned} \tag{3.86a}$$

We now use the triangle inequality to split the sums up and use the stability of the bubble operator (2.25) to obtain

$$\begin{aligned}(\star) &\leq \|\nabla((\mathrm{id} - \eta)\mathcal{D}_G v)\|_{L^2(\Omega\setminus\mathbb{N}^{\lambda-1}(G))} + \|\nabla\mathcal{B}_H(\mathrm{id} - \eta)\mathcal{D}_G v\|_{L^2(\Omega\setminus\mathbb{N}^{\lambda-1}(G))} \\ &\lesssim \|\nabla\mathcal{D}_G v\|_{L^2(\Omega\setminus\mathbb{N}^{\lambda-1}(G))} + \|\nabla(\eta\mathcal{D}_G v)\|_{L^2(\Omega\setminus\mathbb{N}^{\lambda-1}(G))} \\ &\quad + H^{-1}\|(\mathrm{id} - \eta)\mathcal{D}_G v\|_{L^2(\Omega\setminus\mathbb{N}^{\lambda-1}(G))} \\ &=: (\star\star).\end{aligned} \tag{3.86b}$$

We use the boundedness of the cutoff function (3.84), and the product rule with the triangle inequality for the second term on the right-hand side yields

$$\begin{aligned}(\star\star) &\leq \|\nabla\mathcal{D}_G v\|_{L^2(\Omega\setminus\mathbb{N}^{\lambda-1}(G))} + \|\mathcal{D}_G v\nabla\eta\|_{L^2(\Omega\setminus\mathbb{N}^{\lambda-1}(G))} + \|\eta\nabla\mathcal{D}_G v\|_{L^2(\Omega\setminus\mathbb{N}^{\lambda-1}(G))} \\ &\quad + H^{-1}\|\mathcal{D}_G v\|_{L^2(\Omega\setminus\mathbb{N}^{\lambda-1}(G))} \\ &\lesssim \left.\begin{aligned}&\|\nabla\mathcal{D}_G v\|_{L^2(\Omega\setminus\mathbb{N}^{\lambda-1}(G))} + \|\mathcal{D}_G v\nabla\eta\|_{L^2(\Omega\setminus\mathbb{N}^{\lambda-1}(G))} \\ &+H^{-1}\|\mathcal{D}_G v\|_{L^2(\Omega\setminus\mathbb{N}^{\lambda-1}(G))}\end{aligned}\right\} =: (\star\star\star).\end{aligned} \tag{3.86c}$$

Finally, we can use the Hölder inequality and the decay of the cutoff function (3.84c) for the second term on the right-hand side, and then the approximation of the L^2-projection (2.13) yields

$$\begin{aligned}(\star\star\star) &\lesssim \|\nabla\mathcal{D}_G v\|_{L^2(\Omega\setminus\mathbb{N}^{\lambda-1}(G))} + H^{-1}\|\mathcal{D}_G v\|_{L^2(\Omega\setminus\mathbb{N}^{\lambda-1}(G))} + H^{-1}\|\mathcal{D}_G v\|_{L^2(\Omega\setminus\mathbb{N}^{\lambda-1}(G))} \\ &= \|\nabla\mathcal{D}_G v\|_{L^2(\Omega\setminus\mathbb{N}^{\lambda-1}(G))} + H^{-1}\|(\mathrm{id} - \Pi_H)(\mathcal{D}_G v)\|_{L^2(\Omega\setminus\mathbb{N}^{\lambda-1}(G))} \\ &\lesssim \|\nabla\mathcal{D}_G v\|_{L^2(\Omega\setminus\mathbb{N}^{\lambda-1}(G))}.\end{aligned} \tag{3.86d}$$

Now we apply the decay result Lemma 3.17 to the right-hand side of (3.86) to obtain the assertion

$$\|\nabla(\mathcal{D}_G^{[\lambda]}v - \mathcal{D}_G v)\|_{L^2(\Omega)} \lesssim \|\nabla \mathcal{D}_G v\|_{L^2(\Omega\setminus \mathtt{N}^{\lambda-1}(G))} \lesssim \exp(-C\lambda)\|\nabla \mathcal{D}_G v\|_{L^2(\Omega)}. \qquad \square$$

With this localization result we can now prove a localization error similar to Lemma 2.5. However, as we will see in Remark 3.9 an analogue result is unfeasible. Thus, we first create the localized spaces, explain why we need a different localization strategy and then provide a novel localization error estimate.

The localized spaces are given analogously to the global spaces (3.27) and (3.28). For any $j \in \mathbb{N}$ we define the *localized enriched correction space* by

$$\widehat{W}_H^{j,\mathrm{loc}} = \sum_{\nu=1}^{j} (\mathcal{D}^{\mathrm{loc}})^{\nu} \widetilde{V}_H^{[\ell]}. \tag{3.87}$$

The *enriched multiscale space* is then defined as the sum of the s*p*-LOD space and the enriched correction space, i.e.,

$$\breve{V}_H^{j,\mathrm{loc}} = \widetilde{V}_H^{[\ell]} + \widehat{W}_H^{j,\mathrm{loc}}. \tag{3.88}$$

The goal now is to use the space $\breve{V}_H^{j,\mathrm{loc}}$ as trial and test space for the wave equation (3.2). However, beforehand we need another localization results that is used similar to Lemma 2.5 for a localization proof. In fact, it is possible to show a result that has a similar localization error as in Lemma 2.5, by replacing the corrector $\mathcal{C}^{[\ell]}$ with the enriched corrector $\mathcal{D}^{\mathrm{loc}}$. This strategy is, however, suboptimal as the following remark indicates.

Remark 3.9. Consider first the localized correction operator $\mathcal{C}^{[\ell]}$ defined in (2.47) and an arbitrary function $v \in H_0^1(\Omega)$. Then, the idea is to apply the element-wise correction operator to the function on each element separately and sum up the contributions, i.e.,

$$\mathcal{C}^{[\ell]}v = \sum_{K\in\mathcal{T}_H} \mathcal{C}_K^{[\ell]} v|_K.$$

In this case the error $(\mathcal{C} - \mathcal{C}^{[\ell]})v$ can be traced back to the error of the element-wise correction operators, see Lemma 2.5. The localization in this case works especially well, since the function $v|_K$ on the right-hand side of the corrector problem is defined locally on one element and the element-wise correction operator is defined on the patch $\mathtt{N}^{\ell}(K)$.

In contrast, this straight-forward localization does not work for the enriched correction operator, see also Figure 3.4 as a supplement to the following explanation. Based on the fact that the Lemmas 3.17 and 3.18 have the same decay and localization result, it would be possible to prove a localization estimate similar to Lemma 2.5. And for the moment, assume that this holds, i.e., that we need to choose $\lambda = \ell$ for the same localization error estimate as in Lemma 2.5. Then, consider the term

$$\xi = \mathcal{D}^{\mathrm{loc}}(\mathrm{id} - \mathcal{C}^{[\ell]})v.$$

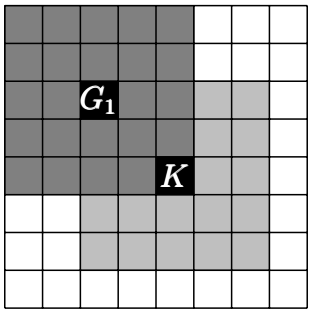

Figure 3.4: Illustration of an element K with patch $\mathtt{N}^2(K)$ for $\ell = 2$ depicted in light gray. Then, we define for the element $G_1 \in \mathtt{N}^2(K)$ the patch $\mathtt{N}^2(G_1)$ depicted in dark gray. The union of both patches is a subset of the 2ℓ-patch $\mathtt{N}^4(K)$.

We would compute this term in the following way. First, we split the classical corrector into its element-wise contributions

$$\mathcal{D}^{\mathrm{loc}}(\mathrm{id} - \mathcal{C}^{[\ell]})v = \sum_{K \in \mathcal{T}_H} \mathcal{D}^{\mathrm{loc}}(\mathrm{id} - \mathcal{C}^{[\ell]}_K)v|_K =: \sum_{K \in \mathcal{T}_H} \mathcal{D}^{\mathrm{loc}}\xi_K.$$

Crucially, we have $\operatorname{supp} \xi_K \subset \mathtt{N}^\ell(K)$, i.e., the functions is defined on the light gray region. We fix $K \in \mathcal{T}_H$, and have

$$\mathcal{D}^{\mathrm{loc}}\xi_K = \sum_{G_1 \in \mathtt{N}^\ell(K)} \mathcal{D}^{[\ell]}_{G_1}\xi_K,$$

which leads to

$$\xi = \sum_{K \in \mathcal{T}_H} \mathcal{D}^{\mathrm{loc}}\xi_K = \sum_{K \in \mathcal{T}_H} \sum_{G_1 \in \mathtt{N}^\ell(K)} \mathcal{D}^{[\ell]}_{G_1}\xi_K.$$

This is now the full representation of the function ξ, and we know by the choices of λ that the localization error is of order $\exp(-C\ell)$. However, the problem lies with the function

$$\sum_{G_1 \in \mathtt{N}^\ell(K)} \mathcal{D}^{[\ell]}_{G_1}\xi_K,$$

which is actually supported on a patch with potentially double the patch size

$$\operatorname{supp}\left(\sum_{G_1 \in \mathtt{N}^\ell(K)} \mathcal{D}^{[\ell]}_{G_1}\xi_K\right) \subset \bigcup\{\mathtt{N}^\ell(G_1) \mid G_1 \in \mathtt{N}^\ell(K)\} = \mathtt{N}^\ell(\mathtt{N}^\ell(K)) = \mathtt{N}^{2\ell}(K).$$

This problem can be observed in Figure 3.4, where each function $\mathcal{D}^{[\ell]}_{G_1}\xi_K$ is supported on the dark gray patch $\mathtt{N}^\ell(G_1)$. The union of all these patches is then included in the 2ℓ-patch. Note that this is the patch size for the first enriched correction operator only, and would increase with each subsequent enriched correction operator, i.e., for j enriched correction, the patch we would compute the basis on the patch $\mathtt{N}^{j\ell}(K)$. This would make the method unfeasible to compute, and thus a better localization strategy is required.

The remark shows that the problem is the fact that we apply the enriched correction operator $\mathcal{D}^{\mathrm{loc}}$ to basis functions that are not localized on one element, but rather on a patch $\mathtt{N}^\ell(K)$. The following localization strategy will make use of the definition of the enriched correction operator, specifically, that we allowed different localization parameters λ_G to be chosen dependent on the definition of the element enriched correction operator $\mathcal{D}_G^{[\lambda_G]}$. That is we intend to localize the element-wise correction operator $\mathcal{D}_{G_1}^{[\lambda_{G_1}]}$ applied to a basis function $\tilde{\Lambda}_{K,i} \in \widetilde{V}_H^{[\ell]}$ based on where the element $G_1 \in \mathtt{N}^\ell(K)$ lies. For the following consideration cf. also Figure 3.5. Let an arbitrary element $K \in \mathcal{T}_H$ be given. Then, for a bubble function $b_{K,i}$ the basis function

$$\operatorname{supp}\left((\mathrm{id} - \mathcal{C}_K^{[\ell]}) b_{K,i}\right) \subset \mathtt{N}^\ell(K)$$

lives on the ℓ-patch. We now construct to each element $G_1 \in \mathtt{N}^\ell(K)$ a patch with size $\lambda_{G_1}(K)$ such that the enriched correction has support only in the patch $\mathtt{N}^\ell(K)$. More precisely, we choose the localization parameter such that

$$\operatorname{supp}\left(\mathcal{D}_{G_1}^{[\lambda_{G_1}(K)]}(\mathrm{id} - \mathcal{C}_K^{[\ell]}) b_{K,i}\right) \subset \mathtt{N}^{\lambda_{G_1}(K)}(G_1) \subset \mathtt{N}^\ell(K).$$

This idea is recursively applied, i.e., for any $G_2 \subset \mathtt{N}^{\lambda_{G_1}(K)}(G_1)$ we define a localization parameter $\lambda_{G_2}(G_1)$ such that

$$\operatorname{supp}\left(\mathcal{D}_{G_2}^{[\lambda_{G_2}(G_1)]}\mathcal{D}_{G_1}^{[\lambda_{G_1}(K)]}(\mathrm{id} - \mathcal{C}_K^{[\ell]}) b_{K,i}\right) \subset \mathtt{N}^{\lambda_{G_2}(G_1)}(G_2) \subset \mathtt{N}^{\lambda_{G_1}(K)}(G_1) \subset \mathtt{N}^\ell(K).$$

Figure 3.5 shows an example of three elements, where each patch around them is defined such that the patch always is a subset of the original patch $\mathtt{N}^\ell(K)$. In order to optimally choose the localization parameters $\lambda_{G_i}(G_{i-1})$, we define the distance of a subset $S \subset \Omega$ to an element $K \in \mathcal{T}_H$ by

$$\operatorname{dist}(S, K) = \mu, \qquad \text{if } S \cap \mathtt{N}^\mu(K) \neq \emptyset \quad \text{and} \quad S \cap \mathtt{N}^{\mu-1}(K) = \emptyset. \tag{3.89}$$

Employing this definition in the above considerations we choose

$$\lambda_{G_1}(K) = \ell - \operatorname{dist}(G_1, K),$$

which ensures that the new $\lambda_{G_1}(K)$-patch is a subset of the original patch $\mathtt{N}^\ell(K)$. This idea can be transferred to any number of enriched corrections where the patch size depends on the patch of the previous enriched correction and the distance between the current and previous elements. Since the definition of the element-wise enriched correction operators becomes quite involved, we will define abbreviations for the proof of the localization result below. The following assumption summarizes and rigorously defines the patches with its patch sizes.

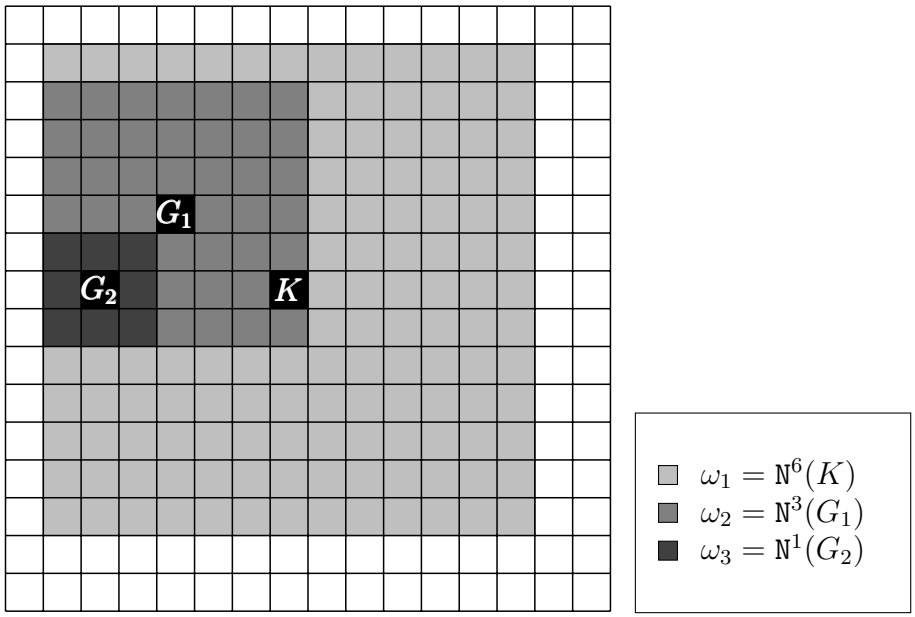

Figure 3.5: Illustration of an element K with patch $\omega_1 = \mathtt{N}^6(K)$ depicted as the union of all grays and black. Then, we define for the element $G_1 \in \mathtt{N}^6(K)$ the patch $\omega_2 = \mathtt{N}^3(G_1)$, since $3 = 6 - \mathrm{dist}(K, G_1) = 6 - 3$. Then, with similar arguments we have for $G_2 \in \mathtt{N}^3(G_1)$ the patch $\omega_3 = \mathtt{N}^1(G_2)$ with $1 = 3 - \mathrm{dist}(G_1, G_2) = 3 - 2$.

Assumption 3.10. Let any $\ell \in \mathbb{N}$ be given. Further, let $j \in \mathbb{N}$ be the numbers of enriched corrections. Then we define sequences of elements G_i, localization parameters λ_i, and patches ω_i by the following recursion. Fix an arbitrary element $K \in \mathcal{T}_H$, and let the initial term of the sequences for the elements, the localization parameters, and patches be given by

$$\begin{aligned} G_0 &\coloneqq K, \\ \lambda_0 &\coloneqq \ell, \\ \omega_1 &\coloneqq \mathtt{N}^{\lambda_0}(G_0). \end{aligned}$$

Then, recursively for $i = 1, \dots, j$, choose as the subsequent term any element with

$$G_i \subset \omega_i,$$

and define the following terms for the localization parameter for $i = 1, \dots, j$

$$\lambda_i \coloneqq \lambda_{G_i}(G_{i-1}) = \lambda_{i-1} - \operatorname{dist}(G_i, G_{i-1})$$

and patch for $i = 1, \dots, j$ by

$$\omega_{i+1} \coloneqq \mathtt{N}^{\lambda_i}(G_i).$$

This uniquely defines for any chosen sequence of elements G_i for $i = 0, \dots, j$ the sequences of localization parameters λ_i for $i = 0, \dots, j$ and patches ω_i for $i = 1, \dots, j$. Note that $\lambda_i = 0$ is allowed. Further, we also denote the sequence of increased patches for $i = 1, \dots, j$ by

$$\omega_i^{+1} \coloneqq \mathtt{N}(\omega_i) = \mathtt{N}^{\lambda_{i-1}+1}(G_{i-1}).$$

The enriched multiscale spaces are constructed by recursive application of the localized enriched correction operator. Thus, in order show that functions in this space only make an exponentially decaying error with respect to the prototypical space, we need to compare functions for each j separately. This motivates the following theorem, where we compare functions that lie in the spaces $\widehat{W}_H^\nu$ and $\widehat{W}_H^{\nu,\mathrm{loc}}$ for $\nu = 1, \dots, j$.

This theorem is the main contribution in this thesis. Here, everything we have defined and constructed above comes together. Specifically, we circumvent the problem with large patch sizes, see Remark 3.9, by choosing appropriate localization parameters.

Theorem 3.19 (Localization of the enriched correction operator)**.** *Consider Assumption 3.10 for some $\ell, j \in \mathbb{N}$. Further, let $H\ell^{d+1} \lesssim 1$. Then, for any function $v \in H_0^1(\Omega)$ and $\nu = 1, \dots, j$ we have*

$$\|\nabla((\mathcal{D}^{\mathrm{loc}})^\nu - \mathcal{D}^\nu)(\mathrm{id} - \mathcal{C}^{[\ell]})v\|_{L^2(\Omega)} \lesssim \ell^{\frac{d}{2}} \exp(-C\ell)\|\nabla v\|_{L^2(\Omega)}. \tag{3.90}$$

Remark 3.11. In Theorem 3.19 we assume that $H\ell^{d+1} \lesssim 1$. This assumption is only a technical one. This term is typically small as we have $\ell \approx |\log H|$, but for large dimensions this term can blow up for some choices of H. However, this bound is always true asymptotically for $H \to 0$.

The proof of Theorem 3.19, up to some technical details, splits the difference of enriched localization operators up such that we can apply the following lemma, which is an extension of Lemma 3.18. Further, we use the definition of the patches in Assumption 3.10 in an optimal way to show that the localization on the original ℓ-patch can be recovered.

First, we give an auxiliary lemma that employs Lemma 3.18 to bound the error of the localized enriched correction operator by the right-hand side of the corrector problem (3.72).

Lemma 3.20. *Let $G \in \mathcal{T}_H$ and $\lambda \in \mathbb{N}$. Then for any $v \in H_0^1(\Omega)$ and $w \in W$ we have*

$$a(\mathcal{D}_G^{[\lambda]} v - \mathcal{D}_G v, w) \lesssim H^2 \exp(-C\lambda) \|\nabla v\|_{L^2(G)} \|\nabla w\|_{L^2(\mathtt{N}^{\lambda+1}(G))}. \tag{3.91}$$

Proof. We define a cutoff function $\eta \in W^{1,\infty}(\Omega)$ with

$$\eta \equiv 0, \qquad \text{in } \mathtt{N}^{\lambda}(G), \tag{3.92a}$$
$$\eta \equiv 1, \qquad \text{in } \Omega \setminus \mathtt{N}^{\lambda+1}(G), \tag{3.92b}$$
$$0 \leq \eta \leq 1, \quad \|\nabla \eta\|_{L^\infty(R)} \lesssim H^{-1}, \qquad \text{in } R \coloneqq \mathtt{N}^{\lambda+1}(G) \setminus \mathtt{N}^{\lambda}(G). \tag{3.92c}$$

Employing the fact that the cutoff function vanishes on the patch (3.92a), and the fact that the bubble operator preserves the support we have that

$$\operatorname{supp}(\mathrm{id} - \mathcal{B}_H)(\eta w) \cap \operatorname{supp} \mathcal{D}_G^{[\lambda]} v = \emptyset$$

have no overlapping support. Thus, by the definition of the bubble operator, $(\mathrm{id} - \mathcal{B}_H)v \in W$ and the definition of the element-wise enriched correction operator (3.72) we have

$$\begin{aligned} a(\mathcal{D}_G^{[\lambda]} v - \mathcal{D}_G v, (\mathrm{id} - \mathcal{B}_H)(\eta w)) &= -a(\mathcal{D}_G v, (\mathrm{id} - \mathcal{B}_H)(\eta w)) \\ &= (v, (\mathrm{id} - \mathcal{B}_H)(\eta w))_{L^2(G)} \\ &= 0. \end{aligned} \tag{3.93}$$

Since $\mathcal{B}_H w = 0$ we can subtract this term from the test function, and adding (3.93) we can estimate the left-hand side of (3.91) using Cauchy-Schwarz inequality by

$$\begin{aligned} a(\mathcal{D}_G^{[\lambda]} v - \mathcal{D}_G v, w) &= a(\mathcal{D}_G^{[\lambda]} v - \mathcal{D}_G v, (\mathrm{id} - \mathcal{B}_H)(\mathrm{id} - \eta) w) \\ &\leq \|\nabla(\mathcal{D}_G^{[\lambda]} v - \mathcal{D}_G v)\|_{L^2(\Omega)} \|\nabla(\mathrm{id} - \mathcal{B}_H)(\mathrm{id} - \eta) w\|_{L^2(\Omega)} \end{aligned} \tag{3.94}$$

For the first term on the right-hand side of (3.94) we can use Lemma 3.18 to obtain

$$\|\nabla(\mathcal{D}_G^{[\lambda]}v - \mathcal{D}_G v)\|_{L^2(\Omega)} \lesssim \exp(-C\lambda)\|\nabla\mathcal{D}_G v\|_{L^2(\Omega)}. \tag{3.95}$$

Furthermore, we have that $\mathcal{D}_G v \in W$ and by the definition (3.72) and the approximation (2.13) we can estimate using the coercivity (2.6) and the Cauchy-Schwarz inequality

$$\begin{aligned}\|\nabla\mathcal{D}_G v\|_{L^2(\Omega)}^2 &\lesssim a(\mathcal{D}_G v, \mathcal{D}_G v)\\ &= -(v, \mathcal{D}_G v)_{L^2(G)}\\ &= -((\mathrm{id}-\Pi_H)v, (\mathrm{id}-\Pi_H)\mathcal{D}_G v)_{L^2(G)}\\ &\lesssim H^2\|\nabla v\|_{L^2(G)}\|\nabla\mathcal{D}_G v\|_{L^2(\Omega)}.\end{aligned} \tag{3.96}$$

For the second term on the right-hand side of (3.94) we can use similar arguments as in Lemmas 3.17 and 3.18. By the definition of the cutoff function (3.92b) we have $\mathrm{id}-\eta = 0$ outside the $(\lambda+1)$-patch. Then with the triangle inequality and the inverse estimate of the bubble operator (2.25) we have

$$\begin{aligned}\|\nabla(\mathrm{id}-\mathcal{B}_H)(\mathrm{id}-\eta)w\|_{L^2(\mathtt{N}^{\lambda+1}(G))} &\leq \|\nabla(\mathrm{id}-\eta)w\|_{L^2(\mathtt{N}^{\lambda+1}(G))}\\ &\quad + \|\nabla\mathcal{B}_H(\mathrm{id}-\eta)w\|_{L^2(\mathtt{N}^{\lambda+1}(G))}\\ &\lesssim \left.\begin{aligned}&\|\nabla w\|_{L^2(\mathtt{N}^{\lambda+1}(G))} + \|\nabla(\eta w)\|_{L^2(\mathtt{N}^{\lambda+1}(G))}\\ &+H^{-1}\|(\mathrm{id}-\eta)w\|_{L^2(\mathtt{N}^{\lambda+1}(G))}\end{aligned}\right\} =: (\star).\end{aligned} \tag{3.97a}$$

By the product rule, the boundedness of the cutoff function (3.92), the Hölder inequality and (3.92c) we have

$$\begin{aligned}(\star) &\leq \|\nabla w\|_{L^2(\mathtt{N}^{\lambda+1}(G))} + \|\eta\nabla w\|_{L^2(\mathtt{N}^{\lambda+1}(G))}\\ &\quad + \|w\nabla\eta\|_{L^2(\mathtt{N}^{\lambda+1}(G))} + H^{-1}\|w\|_{L^2(\mathtt{N}^{\lambda+1}(G))}\\ &\lesssim \|\nabla w\|_{L^2(\mathtt{N}^{\lambda+1}(G))} + \|\nabla w\|_{L^2(\mathtt{N}^{\lambda+1}(G))}\\ &\quad + H^{-1}\|w\|_{L^2(\mathtt{N}^{\lambda+1}(G))} + H^{-1}\|w\|_{L^2(\mathtt{N}^{\lambda+1}(G))} = (\star\star).\end{aligned} \tag{3.97b}$$

Since $w \in W$ we can subtract the L^2-projection and use the approximation (2.13) to obtain

$$\begin{aligned}(\star\star) &\lesssim \|\nabla w\|_{L^2(\mathtt{N}^{\lambda+1}(G))} + H^{-1}\|(\mathrm{id}-\Pi_H)w\|_{L^2(\mathtt{N}^{\lambda+1}(G))}\\ &\lesssim \|\nabla w\|_{L^2(\mathtt{N}^{\lambda+1}(G))}.\end{aligned} \tag{3.97c}$$

Dividing both sides of (3.96) by $\|\nabla\mathcal{D}_G v\|_{L^2(\Omega)}$, using it in (3.95), and combining it with (3.97) in (3.94) yields the assertion. □

Proof of Theorem 3.19. In order to be able to employ the decay and localization results Lemmas 3.17, 3.18 and 3.20 we need to split up the left-hand side of (3.90), i.e.,

$$\|\nabla((\mathcal{D}^{\mathrm{loc}})^\nu - \mathcal{D}^\nu)(\mathrm{id}-\mathcal{C}^{[\ell]})v\|_{L^2(\Omega)}$$

appropriately. By adding and subtracting the term

$$\mathcal{D}(\mathcal{D}^{\mathrm{loc}})^{\nu-1}(\mathrm{id}-\mathcal{C}^{[\ell]})v$$

we obtain the following split by the triangle inequality

$$\begin{aligned}\|\nabla((\mathcal{D}^{\mathrm{loc}})^{\nu}-\mathcal{D}^{\nu})(\mathrm{id}-\mathcal{C}^{[\ell]})v\|_{L^2(\Omega)}&\\ \lesssim \|\nabla(\mathcal{D}^{\mathrm{loc}}-\mathcal{D})(\mathcal{D}^{\mathrm{loc}})^{\nu-1}(\mathrm{id}-\mathcal{C}^{[\ell]})v\|_{L^2(\Omega)}&\\ +\|\nabla\mathcal{D}((\mathcal{D}^{\mathrm{loc}})^{\nu-1}-\mathcal{D}^{\nu-1})(\mathrm{id}-\mathcal{C}^{[\ell]})v\|_{L^2(\Omega)}.&\end{aligned} \tag{3.98}$$

The first term can readily be estimated using Lemma 3.18. To estimate the second term we use a recursive argument. Thus, consider the second term on the right-hand side of (3.98). Employing the coercivity (2.6) and the definition of the enriched correction operator (3.23) we have

$$\begin{aligned}&\|\nabla\mathcal{D}((\mathcal{D}^{\mathrm{loc}})^{\nu-1}-\mathcal{D}^{\nu-1})(\mathrm{id}-\mathcal{C}^{[\ell]})v\|^2_{L^2(\Omega)}\\ &\lesssim a(\mathcal{D}((\mathcal{D}^{\mathrm{loc}})^{\nu-1}-\mathcal{D}^{\nu-1})(\mathrm{id}-\mathcal{C}^{[\ell]})v,\mathcal{D}((\mathcal{D}^{\mathrm{loc}})^{\nu-1}-\mathcal{D}^{\nu-1})(\mathrm{id}-\mathcal{C}^{[\ell]})v)\\ &=-(((\mathcal{D}^{\mathrm{loc}})^{\nu-1}-\mathcal{D}^{\nu-1})(\mathrm{id}-\mathcal{C}^{[\ell]})v,\mathcal{D}((\mathcal{D}^{\mathrm{loc}})^{\nu-1}-\mathcal{D}^{\nu-1})(\mathrm{id}-\mathcal{C}^{[\ell]})v)_{L^2(\Omega)}\\ &=(\star).\end{aligned} \tag{3.99a}$$

Next, we apply Cauchy-Schwarz inequality, and subtract the L^2-projection Π_H, then employing the approximation (2.13) yields

$$\begin{aligned}(\star)&\lesssim \|(\mathrm{id}-\Pi_H)((\mathcal{D}^{\mathrm{loc}})^{\nu-1}-\mathcal{D}^{\nu-1})(\mathrm{id}-\mathcal{C}^{[\ell]})v\|_{L^2(\Omega)}\\ &\quad\cdot\|(\mathrm{id}-\Pi_H)\mathcal{D}((\mathcal{D}^{\mathrm{loc}})^{\nu-1}-\mathcal{D}^{\nu-1})(\mathrm{id}-\mathcal{C}^{[\ell]})v\|_{L^2(\Omega)}\\ &\lesssim H^2\|\nabla((\mathcal{D}^{\mathrm{loc}})^{\nu-1}-\mathcal{D}^{\nu-1})(\mathrm{id}-\mathcal{C}^{[\ell]})v\|_{L^2(\Omega)}\\ &\quad\cdot\|\nabla\mathcal{D}((\mathcal{D}^{\mathrm{loc}})^{\nu-1}-\mathcal{D}^{\nu-1})(\mathrm{id}-\mathcal{C}^{[\ell]})v\|_{L^2(\Omega)}.\end{aligned} \tag{3.99b}$$

Finally, we divide by

$$\|\nabla\mathcal{D}((\mathcal{D}^{\mathrm{loc}})^{\nu-1}-\mathcal{D}^{\nu-1})(\mathrm{id}-\mathcal{C}^{[\ell]})v\|_{L^2(\Omega)}$$

to obtain

$$\begin{aligned}\|\nabla\mathcal{D}((\mathcal{D}^{\mathrm{loc}})^{\nu-1}-\mathcal{D}^{\nu-1})(\mathrm{id}-\mathcal{C}^{[\ell]})v\|_{L^2(\Omega)}&\\ \lesssim H^2\|\nabla((\mathcal{D}^{\mathrm{loc}})^{\nu-1}-\mathcal{D}^{\nu-1})(\mathrm{id}-\mathcal{C}^{[\ell]})v\|_{L^2(\Omega)}&\end{aligned} \tag{3.99c}$$

We observe that the right-hand side of (3.99) is of the same form as the left-hand side of (3.98). Thus, the idea is to use (3.99) in (3.98) and apply an analogue split, i.e., we insert

$$\mathcal{D}(\mathcal{D}^{\mathrm{loc}})^{\nu-2}(\mathrm{id}-\mathcal{C}^{[\ell]})v$$

to obtain

$$\begin{aligned}
&\|\nabla((\mathcal{D}^{\mathrm{loc}})^\nu - \mathcal{D}^\nu)(\mathrm{id} - \mathcal{C}^{[\ell]})v\|_{L^2(\Omega)} \\
&\qquad \lesssim \|\nabla(\mathcal{D}^{\mathrm{loc}} - \mathcal{D})(\mathcal{D}^{\mathrm{loc}})^{\nu-1}(\mathrm{id} - \mathcal{C}^{[\ell]})v\|_{L^2(\Omega)} \\
&\qquad\quad + H^2\|\nabla((\mathcal{D}^{\mathrm{loc}})^{\nu-1} - \mathcal{D}^{\nu-1})(\mathrm{id} - \mathcal{C}^{[\ell]})v\|_{L^2(\Omega)} \\
&\qquad \lesssim \|\nabla(\mathcal{D}^{\mathrm{loc}} - \mathcal{D})(\mathcal{D}^{\mathrm{loc}})^{\nu-1}(\mathrm{id} - \mathcal{C}^{[\ell]})v\|_{L^2(\Omega)} \\
&\qquad\quad + H^2\|\nabla(\mathcal{D}^{\mathrm{loc}} - \mathcal{D})(\mathcal{D}^{\mathrm{loc}})^{\nu-2}(\mathrm{id} - \mathcal{C}^{[\ell]})v\|_{L^2(\Omega)} \\
&\qquad\quad + H^2\|\nabla\mathcal{D}((\mathcal{D}^{\mathrm{loc}})^{\nu-2} - \mathcal{D}^{\nu-2})(\mathrm{id} - \mathcal{C}^{[\ell]})v\|_{L^2(\Omega)}.
\end{aligned} \tag{3.100a}$$

For the last term on the right-hand side we can apply an analogue estimate to (3.99) which overall yields

$$\begin{aligned}
&\|\nabla((\mathcal{D}^{\mathrm{loc}})^\nu - \mathcal{D}^\nu)(\mathrm{id} - \mathcal{C}^{[\ell]})v\|_{L^2(\Omega)} \\
&\qquad \lesssim \|\nabla(\mathcal{D}^{\mathrm{loc}} - \mathcal{D})(\mathcal{D}^{\mathrm{loc}})^{\nu-1}(\mathrm{id} - \mathcal{C}^{[\ell]})v\|_{L^2(\Omega)} \\
&\qquad\quad + H^2\|\nabla(\mathcal{D}^{\mathrm{loc}} - \mathcal{D})(\mathcal{D}^{\mathrm{loc}})^{\nu-2}(\mathrm{id} - \mathcal{C}^{[\ell]})v\|_{L^2(\Omega)} \\
&\qquad\quad + H^4\|\nabla((\mathcal{D}^{\mathrm{loc}})^{\nu-2} - \mathcal{D}^{\nu-2})(\mathrm{id} - \mathcal{C}^{[\ell]})v\|_{L^2(\Omega)}.
\end{aligned} \tag{3.100b}$$

We can iteratively apply analogue estimates to (3.98) and (3.99) which yields

$$\begin{aligned}
&\|\nabla((\mathcal{D}^{\mathrm{loc}})^\nu - \mathcal{D}^\nu)(\mathrm{id} - \mathcal{C}^{[\ell]})v\|_{L^2(\Omega)} \\
&\qquad \lesssim \sum_{i=1}^{\nu} H^{2(i-1)}\|\nabla(\mathcal{D}^{\mathrm{loc}} - \mathcal{D})(\mathcal{D}^{\mathrm{loc}})^{\nu-i}(\mathrm{id} - \mathcal{C}^{[\ell]})v\|_{L^2(\Omega)}
\end{aligned} \tag{3.101}$$

Thus, the next step is the estimate of terms of the form

$$\|\nabla(\mathcal{D}^{\mathrm{loc}} - \mathcal{D})(\mathcal{D}^{\mathrm{loc}})^i(\mathrm{id} - \mathcal{C}^{[\ell]})v\|_{L^2(\Omega)}$$

for $i = 0, \dots, \nu - 1$. Here, we use the decay and localization results stated in Lemmas 3.17, 3.18 and 3.20. Thus, we need to split each correction operator into its element-wise counterparts. We make use of the definition of the patch sizes λ_i depending on the context (see Assumption 3.10). In the following we abbreviate

$$w = (\mathcal{D}^{\mathrm{loc}} - \mathcal{D})(\mathcal{D}^{\mathrm{loc}})^i(\mathrm{id} - \mathcal{C}^{[\ell]})v.$$

Then we have by coercivity (2.6) and splitting the (enriched) correction operators into its element-wise counterparts we have

$$\begin{aligned}
&\|\nabla(\mathcal{D}^{\mathrm{loc}} - \mathcal{D})(\mathcal{D}^{\mathrm{loc}})^i(\mathrm{id} - \mathcal{C}^{[\ell]})v\|^2_{L^2(\Omega)} \\
&\lesssim a((\mathcal{D}^{\mathrm{loc}} - \mathcal{D})(\mathcal{D}^{\mathrm{loc}})^i(\mathrm{id} - \mathcal{C}^{[\ell]})v, w) \\
&\lesssim \sum_{K\in\mathcal{T}_H}\sum_{G_1\in\omega_1}\cdots\sum_{G_{i+1}\in\omega_{i+1}} a((\mathcal{D}^{[\lambda_{i+1}]}_{G_{i+1}} - \mathcal{D}_{G_{i+1}})\mathcal{D}^{[\lambda_i]}_{G_i}\cdots\mathcal{D}^{[\lambda_1]}_{G_1}(v|_K - \mathcal{C}^{[\ell]}_K v), w).
\end{aligned} \tag{3.102}$$

In the following, fix $G_i \in \omega_i$. Then, the localization parameter $\lambda_{i+1} = \lambda_{G_{i+1}}(G_i)$ is properly defined for any $G_{i+1} \in \omega_{i+1} = \mathtt{N}^{\lambda_i}(G_i)$, and we consider solely the innermost sum. We first employ Lemma 3.20

$$\begin{aligned}
&\sum_{G_{i+1}\in\omega_{i+1}} a((\mathcal{D}_{G_{i+1}}^{[\lambda_{i+1}]} - \mathcal{D}_{G_{i+1}})\mathcal{D}_{G_i}^{[\lambda_i]} \cdots \mathcal{D}_{G_1}^{[\lambda_1]}(v|_K - \mathcal{C}_K^{[\ell]}v), w) \\
&\lesssim \sum_{G_{i+1}\in\omega_{i+1}} H^2 \exp(-C\lambda_{i+1}) \|\nabla \mathcal{D}_{G_i}^{[\lambda_i]} \cdots \mathcal{D}_{G_1}^{[\lambda_1]}(v|_K - \mathcal{C}_K^{[\ell]}v)\|_{L^2(G_{i+1})} \|\nabla w\|_{L^2(\omega_{i+2}^{+1})} \\
&= (\star),
\end{aligned} \tag{3.103a}$$

and then use the discrete Cauchy-Schwarz inequality to obtain

$$\begin{aligned}
(\star) \lesssim &\left(\sum_{G_{i+1}\in\omega_{i+1}} H^4 \exp(-2C\lambda_{i+1}) \|\nabla \mathcal{D}_{G_i}^{[\lambda_i]} \cdots \mathcal{D}_{G_1}^{[\lambda_1]}(v|_K - \mathcal{C}_K^{[\ell]}v)\|_{L^2(G_{i+1})}^2 \right)^{\frac{1}{2}} \\
&\cdot \left(\sum_{G_{i+1}\in\omega_{i+1}} \|\nabla w\|_{L^2(\omega_{i+2}^{+1})}^2 \right)^{\frac{1}{2}}.
\end{aligned} \tag{3.103b}$$

Next, we employ the crucial step in the analysis of our localization strategy. That is, we make use of the definition of the localization parameters, and show that the localization error of the patch ω_{i+1} can be bounded by the localization error of the patch ω_i. For this estimate define the rings R^μ around the element G_i by

$$R^\mu \coloneqq \{G \in \mathcal{T}_H \mid \operatorname{dist}(G, G_i) = \mu\}. \tag{3.104}$$

Consider the sum under the first square root on the right-hand side of (3.103). In a first step, we rewrite the sum over the patch as the sum over all rings around the element G_i, and then employ the definition of the localization parameter $\lambda_{i+1} = \lambda_i - \operatorname{dist}(G_{i+1}, G_i)$. Here, we use that $\operatorname{dist}(G_{i+1}, G_i) = \mu$ for any $G_{i+1} \in R^\mu$. Altogether, this yields

$$\begin{aligned}
&\sum_{G_{i+1}\in\omega_{i+1}} H^4 \exp(-2C\lambda_{i+1}) \|\nabla \mathcal{D}_{G_i}^{[\lambda_i]} \cdots \mathcal{D}_{G_1}^{[\lambda_1]}(v|_K - \mathcal{C}_K^{[\ell]}v)\|_{L^2(G_{i+1})}^2 \\
&= H^4 \sum_{\mu=0}^{\lambda_i} \exp(-2C\lambda_{i+1}) \|\nabla \mathcal{D}_{G_i}^{[\lambda_i]} \cdots \mathcal{D}_{G_1}^{[\lambda_1]}(v|_K - \mathcal{C}_K^{[\ell]}v)\|_{L^2(R^\mu)}^2 \\
&= H^4 \sum_{\mu=0}^{\lambda_i} \exp(-2C(\lambda_i - \mu)) \|\nabla \mathcal{D}_{G_i}^{[\lambda_i]} \cdots \mathcal{D}_{G_1}^{[\lambda_1]}(v|_K - \mathcal{C}_K^{[\ell]}v)\|_{L^2(R^\mu)}^2 =: L_1.
\end{aligned} \tag{3.105a}$$

In the next step we insert the term

$$\mathcal{D}_{G_i}\mathcal{D}_{G_{i-1}}^{[\lambda_{i-1}]} \cdots \mathcal{D}_{G_1}^{[\lambda_1]}(v|_K - \mathcal{C}_K^{[\ell]}v)$$

into the norm and employ the triangle and Young's inequalities to obtain

$$\begin{aligned} L_1 &\lesssim H^4 \sum_{\mu=0}^{\lambda_i} \exp(-2C(\lambda_i-\mu)) \\ &\qquad \Big[\|\nabla \mathcal{D}_{G_i} \mathcal{D}_{G_{i-1}}^{[\lambda_{i-1}]} \cdots \mathcal{D}_{G_1}^{[\lambda_1]} (v|_K - \mathcal{C}_K^{[\ell]} v)\|_{L^2(R^\mu)}^2 \\ &\qquad\quad + \|\nabla (\mathcal{D}_{G_i}^{[\lambda_i]} - \mathcal{D}_{G_i}) \mathcal{D}_{G_{i-1}}^{[\lambda_{i-1}]} \cdots \mathcal{D}_{G_1}^{[\lambda_1]} (v|_K - \mathcal{C}_K^{[\ell]} v)\|_{L^2(R^\mu)}^2 \Big] \\ &\lesssim H^4 \sum_{\mu=0}^{\lambda_i} \exp(-2C(\lambda_i-\mu)) \\ &\qquad \Big[\|\nabla \mathcal{D}_{G_i} \mathcal{D}_{G_{i-1}}^{[\lambda_{i-1}]} \cdots \mathcal{D}_{G_1}^{[\lambda_1]} (v|_K - \mathcal{C}_K^{[\ell]} v)\|_{L^2(\Omega \setminus \mathbb{N}^{\mu-1}(G_i))}^2 \\ &\qquad\quad + \|\nabla (\mathcal{D}_{G_i}^{[\lambda_i]} - \mathcal{D}_{G_i}) \mathcal{D}_{G_{i-1}}^{[\lambda_{i-1}]} \cdots \mathcal{D}_{G_1}^{[\lambda_1]} (v|_K - \mathcal{C}_K^{[\ell]} v)\|_{L^2(R^\mu)}^2 \Big]. \end{aligned} \tag{3.105b}$$

Summing up the last term on the right-hand side using for $\mu = 0, \dots, \lambda_i$ the estimate

$$\exp(-2C(\lambda_i - \mu)) \leq 1$$

yields

$$\begin{aligned} H^4 \sum_{\mu=0}^{\lambda_i} \exp(-2C(\lambda_i-\mu)) \|\nabla (\mathcal{D}_{G_i}^{[\lambda_i]} - \mathcal{D}_{G_i}) \mathcal{D}_{G_{i-1}}^{[\lambda_{i-1}]} \cdots \mathcal{D}_{G_1}^{[\lambda_1]} (v|_K - \mathcal{C}_K^{[\ell]} v)\|_{L^2(R^\mu)}^2 & \\ \lesssim H^4 \|\nabla (\mathcal{D}_{G_i}^{[\lambda_i]} - \mathcal{D}_{G_i}) \mathcal{D}_{G_{i-1}}^{[\lambda_{i-1}]} \cdots \mathcal{D}_{G_1}^{[\lambda_1]} (v|_K - \mathcal{C}_K^{[\ell]} v)\|_{L^2(\omega_{i+1})}^2 & \\ \lesssim H^4 \|\nabla (\mathcal{D}_{G_i}^{[\lambda_i]} - \mathcal{D}_{G_i}) \mathcal{D}_{G_{i-1}}^{[\lambda_{i-1}]} \cdots \mathcal{D}_{G_1}^{[\lambda_1]} (v|_K - \mathcal{C}_K^{[\ell]} v)\|_{L^2(\Omega)}^2 & \\ =: (\star\star). & \end{aligned} \tag{3.106a}$$

This can be further estimated using Lemma 3.18 to obtain

$$(\star\star) \lesssim H^4 \exp(-2C\lambda_i) \|\nabla \mathcal{D}_{G_i} \mathcal{D}_{G_{i-1}}^{[\lambda_{i-1}]} \cdots \mathcal{D}_{G_1}^{[\lambda_1]} (v|_K - \mathcal{C}_K^{[\ell]} v)\|_{L^2(\Omega)}^2 \tag{3.106b}$$

We now turn to the first term on the right-hand side of (3.105b). Applying Lemma 3.17 and resolving the sum yields

$$\begin{aligned} H^4 \sum_{\mu=0}^{\lambda_i} \exp(-2C(\lambda_i-\mu)) \|\nabla \mathcal{D}_{G_i} \mathcal{D}_{G_{i-1}}^{[\lambda_{i-1}]} \cdots \mathcal{D}_{G_1}^{[\lambda_1]} (v|_K - \mathcal{C}_K^{[\ell]} v)\|_{L^2(\Omega \setminus \mathbb{N}^{\mu-1}(G_i))}^2 & \\ \lesssim H^4 \sum_{\mu=0}^{\lambda_i} \exp(-2C(\lambda_i-\mu)) & \\ \qquad \exp(-2C\mu) \|\nabla \mathcal{D}_{G_i} \mathcal{D}_{G_{i-1}}^{[\lambda_{i-1}]} \cdots \mathcal{D}_{G_1}^{[\lambda_1]} (v|_K - \mathcal{C}_K^{[\ell]} v)\|_{L^2(\Omega)}^2 & \\ \lesssim H^4 \lambda_i \exp(-2C\lambda_i) \|\nabla \mathcal{D}_{G_i} \mathcal{D}_{G_{i-1}}^{[\lambda_{i-1}]} \cdots \mathcal{D}_{G_1}^{[\lambda_1]} (v|_K - \mathcal{C}_K^{[\ell]} v)\|_{L^2(\Omega)}^2. & \end{aligned} \tag{3.107}$$

Employing both (3.106) and (3.107) in (3.105) yields

$$\begin{aligned}&\sum_{G_{i+1}\in\omega_{i+1}} H^4\exp(-2C\lambda_{i+1})\|\nabla\mathcal{D}_{G_i}^{[\lambda_i]}\cdots\mathcal{D}_{G_1}^{[\lambda_1]}(v|_K-\mathcal{C}_K^{[\ell]}v)\|_{L^2(G_{i+1})}^2\\&\quad\lesssim H^4\lambda_i\exp(-2C\lambda_i)\|\nabla\mathcal{D}_{G_i}\mathcal{D}_{G_{i-1}}^{[\lambda_{i-1}]}\cdots\mathcal{D}_{G_1}^{[\lambda_1]}(v|_K-\mathcal{C}_K^{[\ell]}v)\|_{L^2(\Omega)}^2=:L_2.\end{aligned}\tag{3.108a}$$

We further use an argument as in (3.96), that is

$$\|\nabla\mathcal{D}_G v\|_{L^2(\Omega)}\lesssim H^2\|\nabla v\|_{L^2(G)}.$$

This yields

$$L_2\lesssim H^4\lambda_i\exp(-2C\lambda_i)H^4\|\nabla\mathcal{D}_{G_{i-1}}^{[\lambda_{i-1}]}\cdots\mathcal{D}_{G_1}^{[\lambda_1]}(v|_K-\mathcal{C}_K^{[\ell]}v)\|_{L^2(G_i)}^2.\tag{3.108b}$$

Plugging (3.108) into (3.103) yields

$$\begin{aligned}&\sum_{G_{i+1}\in\omega_{i+1}} a((\mathcal{D}_{G_{i+1}}^{[\lambda_{i+1}]}-\mathcal{D}_{G_{i+1}})\mathcal{D}_{G_i}^{[\lambda_i]}\cdots\mathcal{D}_{G_1}^{[\lambda_1]}(v|_K-\mathcal{C}_K^{[\ell]}v),w)\\&\quad\lesssim\left(H^4\lambda_i\exp(-2C\lambda_i)H^4\|\nabla\mathcal{D}_{G_{i-1}}^{[\lambda_{i-1}]}\cdots\mathcal{D}_{G_1}^{[\lambda_1]}(v|_K-\mathcal{C}_K^{[\ell]}v)\|_{L^2(G_i)}^2\right)^{\frac12}\\&\qquad\cdot\left(\sum_{G_{i+1}\in\omega_{i+1}}\|\nabla w\|_{L^2(\omega_{i+2}^{+1})}^2\right)^{\frac12}.\end{aligned}\tag{3.109}$$

By definition of the localization parameters, we have $\omega_{i+2}^{+1}\subset\omega_{i+1}^{+1}$, and only a finite number of patches ω_{i+2}^{+1} overlap each other (λ_i^d-times). This stems from the fact that each $\lambda_{i+1}\leq\lambda_i$ can be bounded by the patch size of the previous patch. Thus, we have for the sum in the second square root of (3.109)

$$\sum_{G_{i+1}\in\omega_{i+1}}\|\nabla w\|_{L^2(\omega_{i+2}^{+1})}^2\lesssim\lambda_i^d\|\nabla w\|_{L^2(\omega_{i+1}^{+1})}^2.\tag{3.110}$$

We can insert this back into (3.109) which yields

$$\begin{aligned}&\sum_{G_{i+1}\in\omega_{i+1}} a((\mathcal{D}_{G_{i+1}}^{[\lambda_{i+1}]}-\mathcal{D}_{G_{i+1}})\mathcal{D}_{G_i}^{[\lambda_i]}\cdots\mathcal{D}_{G_1}^{[\lambda_1]}(v|_K-\mathcal{C}_K^{[\ell]}v),w)\\&\quad\lesssim\left(H^4\lambda_i\exp(-2C\lambda_i)H^4\|\nabla\mathcal{D}_{G_{i-1}}^{[\lambda_{i-1}]}\cdots\mathcal{D}_{G_1}^{[\lambda_1]}(v|_K-\mathcal{C}_K^{[\ell]}v)\|_{L^2(G_i)}^2\right)^{\frac12}\\&\qquad\cdot\left(\lambda_i^d\|\nabla w\|_{L^2(\omega_{i+1}^{+1})}^2\right)^{\frac12}\\&\quad\lesssim H^2\lambda_i^{\frac12}\exp(-C\lambda_i)H^2\lambda_i^{\frac d2}\|\nabla\mathcal{D}_{G_{i-1}}^{[\lambda_{i-1}]}\cdots\mathcal{D}_{G_1}^{[\lambda_1]}(v|_K-\mathcal{C}_K^{[\ell]}v)\|_{L^2(G_i)}\|\nabla w\|_{L^2(\omega_{i+1}^{+1})}\\&\quad\lesssim H^2\ell^{\frac{d+1}{2}}H^2\exp(-C\lambda_i)\|\nabla\mathcal{D}_{G_{i-1}}^{[\lambda_{i-1}]}\cdots\mathcal{D}_{G_1}^{[\lambda_1]}(v|_K-\mathcal{C}_K^{[\ell]}v)\|_{L^2(G_i)}\|\nabla w\|_{L^2(\omega_{i+1}^{+1})}\end{aligned}\tag{3.111}$$

Here we can use the assumption $H^2\ell^{\frac{d+1}{2}} \lesssim 1$, and insert (3.111) into (3.102) which yields

$$\begin{aligned}
&\|\nabla(\mathcal{D}^{\mathrm{loc}} - \mathcal{D})(\mathcal{D}^{\mathrm{loc}})^i(\mathrm{id} - \mathcal{C}^{[\ell]})v\|^2_{L^2(\Omega)} \\
&\lesssim \sum_{K\in\mathcal{T}_H} \sum_{G_1\in\omega_1} \cdots \sum_{G_i\in\omega_i} H^2 \exp(-C\lambda_i)\|\nabla \mathcal{D}^{[\lambda_{i-1}]}_{G_{i-1}} \cdots \mathcal{D}^{[\lambda_1]}_{G_1}(v|_K - \mathcal{C}^{[\ell]}_K v)\|_{L^2(G_i)} \\
&\qquad\qquad \cdot \|\nabla w\|_{L^2(\omega^{+1}_{i+1})}.
\end{aligned} \tag{3.112}$$

If we, analogously to above, fix $G_{i-1} \in \omega_{i-1}$, and consider the innermost sum

$$\sum_{G_i\in\omega_i} H^2 \exp(-C\lambda_i)\|\nabla \mathcal{D}^{[\lambda_{i-1}]}_{G_{i-1}} \cdots \mathcal{D}^{[\lambda_1]}_{G_1}(v|_K - \mathcal{C}^{[\ell]}_K v)\|_{L^2(G_i)}\|\nabla w\|_{L^2(\omega^{+1}_{i+1})}.$$

Then, we find that this term is of the same structure as the term on the right-hand side of (3.103a) with the index reduced by 1, and we can use similar arguments to (3.103) to (3.112) and apply them recursively to obtain

$$\begin{aligned}
&\|\nabla(\mathcal{D}^{\mathrm{loc}} - \mathcal{D})(\mathcal{D}^{\mathrm{loc}})^i(\mathrm{id} - \mathcal{C}^{[\ell]})v\|^2_{L^2(\Omega)} \\
&\lesssim \sum_{K\in\mathcal{T}_H} \sum_{G_1\in\omega_1} \cdots \sum_{G_i\in\omega_i} H^2 \exp(-C\lambda_i)\|\nabla \mathcal{D}^{[\lambda_{i-1}]}_{G_{i-1}} \cdots \mathcal{D}^{[\lambda_1]}_{G_1}(v|_K - \mathcal{C}^{[\ell]}_K v)\|_{L^2(G_i)} \\
&\qquad\qquad \cdot \|\nabla w\|_{L^2(\omega^{+1}_{i+1})} \\
&\lesssim \sum_{K\in\mathcal{T}_H} \sum_{G_1\in\omega_1} \cdots \sum_{G_{i-1}\in\omega_{i-1}} H^2 \exp(-C\lambda_{i-1})\|\nabla \mathcal{D}^{[\lambda_{i-2}]}_{G_{i-2}} \cdots \mathcal{D}^{[\lambda_1]}_{G_1}(v|_K - \mathcal{C}^{[\ell]}_K v)\|_{L^2(G_{i-1})} \\
&\qquad\qquad \cdot \|\nabla w\|_{L^2(\omega^{+1}_{i})} \\
&\lesssim \sum_{K\in\mathcal{T}_H} \sum_{G_1\in\omega_1} H^2 \exp(-C\lambda_1)\|\nabla(v|_K - \mathcal{C}^{[\ell]}_K v)\|_{L^2(G_1)}\|\nabla w\|_{L^2(\omega^{+1}_{2})}.
\end{aligned} \tag{3.113}$$

In the final step we use similar arguments as above. That is, first we employ the discrete Cauchy-Schwarz inequality to obtain

$$\begin{aligned}
&\|\nabla(\mathcal{D}^{\mathrm{loc}} - \mathcal{D})(\mathcal{D}^{\mathrm{loc}})^i(\mathrm{id} - \mathcal{C}^{[\ell]})v\|^2_{L^2(\Omega)} \\
&\qquad \lesssim \sum_{K\in\mathcal{T}_H} \left(\sum_{G_1\in\omega_1} H^4 \exp(-2C\lambda_1)\|\nabla(v|_K - \mathcal{C}^{[\ell]}_K v)\|^2_{L^2(G_1)} \right)^{\frac{1}{2}} \\
&\qquad\qquad \cdot \left(\sum_{G_1\in\omega_1} \|\nabla w\|^2_{L^2(\omega^{+1}_2)} \right)^{\frac{1}{2}}
\end{aligned} \tag{3.114}$$

We fix $K \in \mathcal{T}_H$ and consider the sum inside the first square root first. Then we define analogously to (3.104) the rings R^μ around the element K. By the definition

of the rings and localization parameter λ_1, we can again reduce the sum to a sum of rings to obtain with the triangle and Young inequalities

$$\begin{aligned}
&\sum_{G_1\in\omega_1} H^4\exp(-2C\lambda_1)\|\nabla(v|_K-\mathcal{C}_K^{[\ell]}v)\|_{L^2(G_1)}^2\\
&\qquad\lesssim \sum_{\mu=0}^{\ell} H^4\exp(-2C\lambda_1)\|\nabla(v|_K-\mathcal{C}_K^{[\ell]}v)\|_{L^2(R^\mu)}^2\\
&\qquad\lesssim \sum_{\mu=0}^{\ell} H^4\exp(-2C(\ell-\mu))\|\nabla(v|_K-\mathcal{C}_K^{[\ell]}v)\|_{L^2(R^\mu)}^2 \qquad (3.115a)\\
&\qquad\lesssim \sum_{\mu=0}^{\ell} H^4\exp(-2C(\ell-\mu))\Big(\|\nabla v|_K\|_{L^2(R^\mu)}^2+\|\nabla\mathcal{C}_K^{[\ell]}v\|_{L^2(R^\mu)}^2\Big)=:\Xi_1
\end{aligned}$$

For the first norm on the right-hand side, the sum consist only of a single term, as $v|_K$ only has support on R^0, and in the second sum we insert $\mathcal{C}_K v$ to obtain with the triangle and Cauchy-Schwarz inequality

$$\begin{aligned}
\Xi_1 &= H^4\exp(-2C\ell)\|\nabla v\|_{L^2(K)}^2+\sum_{\mu=0}^{\ell} H^4\exp(-2C(\ell-\mu))\|\nabla\mathcal{C}_K^{[\ell]}v\|_{L^2(R^\mu)}^2\\
&\lesssim H^4\exp(-2C\ell)\|\nabla v\|_{L^2(K)}^2\\
&\quad+\sum_{\mu=0}^{\ell} H^4\exp(-2C(\ell-\mu))\Big[\|\nabla\mathcal{C}_K v\|_{L^2(R^\mu)}^2 \qquad (3.115b)\\
&\qquad\qquad+\|\nabla(\mathcal{C}_K-\mathcal{C}_K^{[\ell]})v\|_{L^2(R^\mu)}^2\Big].
\end{aligned}$$

Next, we employ Lemma 2.4 to estimate the second term

$$\begin{aligned}
&\sum_{\mu=0}^{\ell} H^4\exp(-2C(\ell-\mu))\|\nabla\mathcal{C}_K v\|_{L^2(R^\mu)}^2\\
&\qquad\qquad\le \sum_{\mu=0}^{\ell} H^4\exp(-2C(\ell-\mu))\|\nabla\mathcal{C}_K v\|_{L^2(\Omega\setminus\mathbb{N}^{\mu-1}(K))}^2\\
&\qquad\qquad\lesssim \sum_{\mu=0}^{\ell} H^4\exp(-2C(\ell-\mu))\exp(-2C\mu)\|\nabla\mathcal{C}_K v\|_{L^2(\Omega)}^2 \qquad (3.116)\\
&\qquad\qquad\lesssim \ell H^4\exp(-2C\ell)\|\nabla\mathcal{C}_K v\|_{L^2(\Omega)}^2.
\end{aligned}$$

Further, we have

$$\exp(-C(\ell-\mu))\le 1,$$

and with Lemma 2.6 we can estimate the last sum in (3.115) by

$$\begin{aligned}\sum_{\mu=0}^{\ell} H^4 \exp(-2C(\ell-\mu))\|\nabla(\mathcal{C}_K - \mathcal{C}_K^{[\ell]})v\|^2_{L^2(R^\mu)} &\leq H^4\|\nabla(\mathcal{C}_K - \mathcal{C}_K^{[\ell]})v\|^2_{L^2(\mathtt{N}^\ell(K))}\\ &\leq H^4\|\nabla(\mathcal{C}_K - \mathcal{C}_K^{[\ell]})v\|^2_{L^2(\Omega)}\\ &\lesssim H^4\exp(-2C\ell)\|\nabla\mathcal{C}_K v\|^2_{L^2(\Omega)}.\end{aligned} \tag{3.117}$$

We can now use

$$\begin{aligned}\|\nabla\mathcal{C}_K v\|^2_{L^2(\Omega)} &\lesssim a(\mathcal{C}_K v, \mathcal{C}_K v)\\ &\lesssim a|_K(v, \mathcal{C}_K v)\\ &\lesssim \|\nabla v\|_{L^2(K)}\|\nabla\mathcal{C}_K v\|_{L^2(\Omega)}.\end{aligned} \tag{3.118}$$

after dividing both sides by $\|\nabla\mathcal{C}_K v\|_{L^2(\Omega)}$. Then, insert (3.116) and (3.117) into (3.115) to obtain

$$\sum_{G_1\in\omega_1} H^4\exp(-2C\lambda_1)\|\nabla(v|_K - \mathcal{C}_K^{[\ell]}v)\|^2_{L^2(G_1)} \lesssim H^4\ell\exp(-2C\ell)\|\nabla v\|_{L^2(K)}. \tag{3.119}$$

Employing (3.119) into (3.114) yields

$$\begin{aligned}&\|\nabla(\mathcal{D}^{\mathrm{loc}} - \mathcal{D})(\mathcal{D}^{\mathrm{loc}})^i(\mathrm{id} - \mathcal{C}^{[\ell]})v\|^2_{L^2(\Omega)}\\ &\qquad\lesssim \sum_{K\in\mathcal{T}_H}\left(H^4\ell\exp(-2C\ell)\|\nabla v\|^2_{L^2(K)}\right)^{\frac{1}{2}}\left(\sum_{G_1\in\omega_1}\|\nabla w\|^2_{L^2(\omega_2^{+1})}\right)^{\frac{1}{2}}\end{aligned} \tag{3.120}$$

Using again that $\omega_2^{+1}\subset\omega_1^{+1} = \mathtt{N}^{\ell+1}(K)$ we have with the finite overlap of patches

$$\sum_{G_1\in\omega_1}\|\nabla w\|^2_{L^2(\omega_2^{+1})} \lesssim \ell^d\|\nabla w\|^2_{L^2(\mathtt{N}^{\ell+1}(K))}. \tag{3.121}$$

We use (3.121) in (3.120) which yields

$$\begin{aligned}&\|\nabla(\mathcal{D}^{\mathrm{loc}} - \mathcal{D})(\mathcal{D}^{\mathrm{loc}})^i(\mathrm{id} - \mathcal{C}^{[\ell]})v\|^2_{L^2(\Omega)}\\ &\qquad\lesssim \sum_{K\in\mathcal{T}_H}\left(H^4\ell\exp(-2C\ell)\|\nabla v\|^2_{L^2(K)}\right)^{\frac{1}{2}}\left(\ell^d\|\nabla w\|^2_{L^2(\mathtt{N}^{\ell+1}(K))}\right)^{\frac{1}{2}}\\ &\qquad= H^2\ell^{\frac{d+1}{2}}\sum_{K\in\mathcal{T}_H}\exp(-C\ell)\|\nabla v\|_{L^2(K)}\|\nabla w\|_{L^2(\mathtt{N}^{\ell+1}(K))} = \Xi_2.\end{aligned} \tag{3.122}$$

We use the assumption $H^2\ell^{\frac{d+1}{2}} \lesssim 1$ and the discrete Cauchy-Schwarz inequality to obtain

$$\Xi_2 = \left(\sum_{K\in\mathcal{T}_H}\exp(-2C\ell)\|\nabla v\|^2_{L^2(K)}\right)^{\frac{1}{2}}\left(\sum_{K\in\mathcal{T}_H}\|\nabla w\|^2_{L^2(\mathtt{N}^{\ell+1}(K))}\right)^{\frac{1}{2}}. \tag{3.123}$$

Finally, we use the finite overlap of patches

$$\sum_{K\in\mathcal{T}_H} \|\nabla w\|^2_{L^2(\mathtt{N}^{\ell+1}(K))} \lesssim \ell^d \|\nabla w\|^2_{L^2(\Omega)}$$

for the term under the second square root such that we finally obtain

$$\begin{aligned}
&\|\nabla(\mathcal{D}^{\mathrm{loc}}-\mathcal{D})(\mathcal{D}^{\mathrm{loc}})^i(\mathrm{id}-\mathcal{C}^{[\ell]})v\|^2_{L^2(\Omega)} \\
&\qquad\lesssim \left(\sum_{K\in\mathcal{T}_H} \exp(-2C\ell)\|\nabla v\|^2_{L^2(K)}\right)^{\frac{1}{2}} \left(\ell^d\|\nabla w\|^2_{L^2(\Omega)}\right)^{\frac{1}{2}} \\
&\qquad\lesssim \left(\exp(-2C\ell)\|\nabla v\|^2_{L^2(\Omega)}\right)^{\frac{1}{2}} \left(\ell^d\|\nabla w\|^2_{L^2(\Omega)}\right)^{\frac{1}{2}} \\
&\qquad\lesssim \exp(-C\ell)\|\nabla v\|_{L^2(\Omega)}\ell^{\frac{d}{2}}\|\nabla w\|_{L^2(\Omega)}.
\end{aligned} \tag{3.124}$$

With the choice made beforehand

$$w = (\mathcal{D}^{\mathrm{loc}}-\mathcal{D})(\mathcal{D}^{\mathrm{loc}})^i(\mathrm{id}-\mathcal{C}^{[\ell]})v$$

and dividing by $\|\nabla w\|_{L^2(\Omega)}$ yields the estimate

$$\|\nabla(\mathcal{D}^{\mathrm{loc}}-\mathcal{D})(\mathcal{D}^{\mathrm{loc}})^i(\mathrm{id}-\mathcal{C}^{[\ell]})v\|_{L^2(\Omega)} \lesssim \ell^{\frac{d}{2}}\exp(-C\ell)\|\nabla v\|_{L^2(\Omega)}. \tag{3.125}$$

Using this estimate in (3.101) gives

$$\begin{aligned}
&\|\nabla((\mathcal{D}^{\mathrm{loc}})^\nu-\mathcal{D}^\nu)(\mathrm{id}-\mathcal{C}^{[\ell]})v\|_{L^2(\Omega)} \\
&\qquad\lesssim \sum_{i=1}^{\nu} H^{2(i-1)}\|\nabla(\mathcal{D}^{\mathrm{loc}}-\mathcal{D})(\mathcal{D}^{\mathrm{loc}})^{\nu-i}(\mathrm{id}-\mathcal{C}^{[\ell]})v\|_{L^2(\Omega)} \\
&\qquad\lesssim \sum_{i=1}^{\nu} H^{2(i-1)}\ell^{\frac{d}{2}}\exp(-C\ell)\|\nabla v\|_{L^2(\Omega)} \\
&\qquad\lesssim \ell^{\frac{d}{2}}\exp(-C\ell)\|\nabla v\|_{L^2(\Omega)}.
\end{aligned} \tag{3.126}$$

This is the assertion (3.90). □

Remark 3.12 (Practical implementation). In practise, Theorem 3.19 allows us to compute all basis functions on the same patch $\mathtt{N}^\ell(K)$. This can be seen as follows. Assume we have a fixed patch $\mathtt{N}^\ell(K)$ and consider the first enriched correction operator $\mathcal{D}^{\mathrm{loc}}$. That is, we would split the enriched corrector into its element-wise contributions and calculate the element-wise enriched correction operators $\mathcal{D}_G^{[\lambda_G]}$ of the basis function $\Lambda_{K,i}$ with support on the patch for each element $G \in \mathtt{N}^\ell(K)$ of the patch. Assumption 3.10 now tells us that each of the element-wise contribution has support inside the whole patch $\mathtt{N}^\ell(K)$, and Theorem 3.19 yields the optimal error.

Further, we may now increase the domain on which the element-wise enriched corrector $\mathcal{D}_G^{[\lambda_G]}$ is defined to be the whole patch. Since we only increase the underlying domain, the error stays exponentially small. However, then we can simply sum up the element-wise enriched corrections on the patch $\mathtt{N}^\ell(K)$ which yields a global (on the patch) enriched corrector problem for $\mathcal{D}$.

This procedure makes the pre-computations quite efficient, as we compute first all basis functions in the multiscale space, then all for the first enriched correction space, and so on. Thus, we have to sequentially compute $(j+1)$-times a set of $H^{-d}(p+1)^d$ basis functions, that can be done in parallel.

3.4.2 Error analysis for the enriched higher-order LOD

Enriched higher-order LOD. With the localization result from the previous section we are able to efficiently compute the enriched multiscale spaces and use the localized enriched multiscale space as trial and test space in the variational form (3.2). The *enriched higher-order LOD* (eho-LOD) method seeks a function $\check{u}_H\colon [0,T] \to \check{V}_H^{j,\mathrm{loc}}$ such that

$$(\partial_t^2 \check{u}_H, \check{v}_H)_{L^2(\Omega)} + a(\check{u}_H, \check{v}_H) = (f, \check{v}_H)_{L^2(\Omega)} \tag{3.127}$$

for all $\check{v}_H \in \check{V}_H^{j,\mathrm{loc}}$, where the initial conditions are given by

$$\check{u}_H(0) = \check{\mathcal{Q}}^{j,\mathrm{loc}} u_0, \qquad \partial_t \check{u}_H(0) = \check{\mathcal{Q}}^{j,\mathrm{loc}} v_0 \tag{3.128}$$

where the maps $\check{\mathcal{Q}}^{j,\mathrm{loc}}$ into the enriched multiscale space and $\widehat{\mathcal{Q}}^{j,\mathrm{loc}}$ into the enriched correction space are given by

$$\check{\mathcal{Q}}^{j,\mathrm{loc}} \coloneqq (\mathrm{id} - \mathcal{C}^{[\ell]}) + \widehat{\mathcal{Q}}^{j,\mathrm{loc}}, \qquad \widehat{\mathcal{Q}}^{j,\mathrm{loc}} \coloneqq \sum_{\nu=1}^{j} (\mathcal{D}^{\mathrm{loc}})^\nu (\partial_t^{2\nu} (\mathrm{id} - \mathcal{C}^{[\ell]})). \tag{3.129}$$

For the eho-LOD method the following error estimate holds.

Theorem 3.21 (Error of the semi-discrete enriched higher-order LOD)**.** *Let Assumption 3.1 hold for some $k \in \mathbb{N}_0$ and $m \geq 2j+4$, and Assumption 3.10 hold for some $\ell, j \in \mathbb{N}$. Further, let u be the solution to* (3.2)*, and $\check{u}_H$ be the solution to* (3.127)*. Then if $j \geq \lceil \frac{p}{2} \rceil$ and $\ell \gtrsim |\log H|$, the following estimate holds*

$$\|\partial_t(\check{u}_H(t) - u(t))\|_{L^2(\Omega)} + \|\nabla(\check{u}_H(t) - u(t))\|_{L^2(\Omega)} \lesssim H^{\kappa+1} C_{\mathrm{data}}, \tag{3.130}$$

where $\kappa = \min\{k, p+1\}$.

We prove the error estimate in four steps. The first two steps are analogous to Lemmas 3.14 and 3.15. First, we estimate the space discretization error $\varphi = \check{u}_H - \check{\mathcal{P}}^{\mathrm{j,loc}} u$ between the semi-discrete eho-LOD solution $\check{u}_H$ and the orthogonal

projection of the weak solution into the enriched multiscale space $\breve{\mathcal{P}}^{\mathrm{j,loc}}u$, where the projection $\breve{\mathcal{P}}^{\mathrm{j,loc}}\colon H_0^1(\Omega) \to \breve{V}_H^{j,\mathrm{loc}}$ is defined by

$$\breve{\mathcal{P}}^{\mathrm{j,loc}} = \widetilde{\mathcal{P}}^{[\ell]} + \widehat{\mathcal{P}}^{\mathrm{j,loc}} \tag{3.131}$$

with the orthogonal projection $\widehat{\mathcal{P}}^{\mathrm{j,loc}}\colon H_0^1(\Omega) \to \widehat{W}_H^j$ given for any $v \in H_0^1(\Omega)$ by

$$a(\widehat{\mathcal{P}}^{\mathrm{j,loc}}v, w) = a(v, w) \tag{3.132}$$

for all $w \in \widehat{W}_H^j$. We show that the space discretization error can be bounded by the projection error $\varrho = u - \breve{\mathcal{P}}^{\mathrm{j,loc}}u$ between the weak solution and the orthogonal projection into the enriched multiscale space $\breve{\mathcal{P}}^{\mathrm{j,loc}}u$, and by the mapping error $\psi = u - \breve{\mathcal{Q}}^{j,\mathrm{loc}}u$ at the initial time. In the second step the projection error ϱ is estimated, and we find that it is bounded by the mapping error ψ. The third step now differs from the previous steps, here we need to estimate the mapping error between the localized mapping and the weak solution. We find that it can be bounded by the prototypical mapping error and a localization error. The fourth step then uses the prototypical mapping error in Theorem 3.16.

We will give the first two lemmas without proof, as the argumentation therein would be repeats of the previous results Lemmas 3.14 and 3.15.

Lemma 3.22 (Space discretization error of the eho-LOD method)**.** *Let Assumption 3.1 hold for some $k \in \mathbb{N}_0$ and $m \geq 2j+1$, and Assumption 3.10 hold for some $\ell, j \in \mathbb{N}$. Further, let u be the solution to* (3.2)*, and $\tilde{u}_H$ be the solution to* (3.127)*. With $\varphi = \tilde{u}_H - \breve{\mathcal{P}}^{\mathrm{j,loc}}u$, $\varrho = u - \breve{\mathcal{P}}^{\mathrm{j,loc}}u$, and $\psi = u - \breve{\mathcal{Q}}^{j,\mathrm{loc}}u$, where the projection $\breve{\mathcal{P}}^{\mathrm{j,loc}}$ is defined in* (3.131) *and the mapping $\breve{\mathcal{Q}}^{j,\mathrm{loc}}$ in* (3.129)*, we have*

$$\begin{aligned}&\|\partial_t\varphi(t)\|_{L^2(\Omega)} + \|\nabla\varphi(t)\|_{L^2(\Omega)} \\ &\qquad\lesssim H\|\nabla\partial_t\psi(0)\|_{L^2(\Omega)} + \|\nabla\psi(0)\|_{L^2(\Omega)} + \int_0^t \|\partial_t^2\varrho(s)\|_{L^2(\Omega)}\,\mathrm{d}s.\end{aligned} \tag{3.133}$$

Lemma 3.23 (Projection error of the eho-LOD method)**.** *Let Assumption 3.1 hold for some $k \in \mathbb{N}_0$ and $m \geq 2j+2$, and Assumption 3.10 hold for some $\ell, j \in \mathbb{N}$. Further, let u be the solution to* (3.2)*. With $\varrho = u - \breve{\mathcal{P}}^{\mathrm{j,loc}}u$, and $\psi = u - \breve{\mathcal{Q}}^{j,\mathrm{loc}}u$, where the projection $\breve{\mathcal{P}}^{\mathrm{j,loc}}$ is defined in* (3.131) *and the mapping $\breve{\mathcal{Q}}^{j,\mathrm{loc}}$ in* (3.129)*, the following estimate holds for $\nu = 0, 1, 2$*

$$\|\nabla\partial_t^\nu\varrho(t)\|_{L^2(\Omega)} \lesssim \|\nabla\partial_t^\nu\psi(t)\|_{L^2(\Omega)}, \tag{3.134a}$$

and for $\nu = 1, 2$

$$\|\partial_t^\nu\varrho(t)\|_{L^2(\Omega)} \lesssim H\|\nabla\partial_t^\nu\psi(t)\|_{L^2(\Omega)}. \tag{3.134b}$$

Theorem 3.24 (Mapping error of the enriched higher-order LOD)**.** *Let Assumption 3.1 hold for some $k \in \mathbb{N}_0$ and $m \geq 2j+4$, and Assumption 3.10 hold for some $\ell, j \in \mathbb{N}$. Further, let u be the solution to (3.2). With $\psi = u - \breve{\mathcal{Q}}^{j,\mathrm{loc}} u$, where the mapping $\breve{\mathcal{Q}}^{j,\mathrm{loc}}$ is defined in (3.31), and if $j \geq \lceil \frac{p}{2} \rceil$ the following estimate holds for $\nu = 0, 1, 2$*

$$\|\nabla \partial_t^\nu \psi(t)\|_{L^2(\Omega)} \lesssim (H^{\kappa+1} + \ell^{\frac{d}{2}} \exp(-C\ell)) C_{\mathrm{data}}, \tag{3.135}$$

where $\kappa = \min\{k, p+1\}$.

Proof. The goal in this proof is to split the estimate into a localization error that can be estimated with Theorem 3.19 and the mapping error of the prototypical eho-LOD method. That is by inserting the mapping into the global enriched multiscale space $\breve{\mathcal{Q}}^j u$ and the triangle inequality we have

$$\|\nabla(u - \breve{\mathcal{Q}}^{j,\mathrm{loc}} u)\|_{L^2(\Omega)} \lesssim \|\nabla(u - \breve{\mathcal{Q}}^j u)\|_{L^2(\Omega)} + \|\nabla(\breve{\mathcal{Q}}^j u - \breve{\mathcal{Q}}^{j,\mathrm{loc}} u)\|_{L^2(\Omega)}. \tag{3.136}$$

By Theorem 3.24 we have that the first term on the right-hand side is suitably bounded by

$$\|\nabla(u - \breve{\mathcal{Q}}^j u)\|_{L^2(\Omega)} \lesssim H^{\kappa+1} C_{\mathrm{data}}.$$

That is, we have

$$\|\nabla(u - \breve{\mathcal{Q}}^{j,\mathrm{loc}} u)\|_{L^2(\Omega)} \lesssim H^{\kappa+1} C_{\mathrm{data}} + \|\nabla(\breve{\mathcal{Q}}^j u - \breve{\mathcal{Q}}^{j,\mathrm{loc}} u)\|_{L^2(\Omega)}. \tag{3.137}$$

Thus, it is left to show that the second term on the right-hand side is reasonably bounded. We have by the definitions of the mappings using the triangle inequality that

$$\begin{aligned}
&\|\nabla(\breve{\mathcal{Q}}^j u - \breve{\mathcal{Q}}^{j,\mathrm{loc}} u)\|_{L^2(\Omega)} \\
&\quad = \|\nabla(\widetilde{\mathcal{P}} u + \sum_{\nu=1}^{j} \mathcal{D}^\nu(\partial_t^{2\nu} \widetilde{\mathcal{P}} u) - (\mathrm{id} - \mathcal{C}^{[\ell]}) u - \sum_{\nu=1}^{j} (\mathcal{D}^{\mathrm{loc}})^\nu (\partial_t^{2\nu} (\mathrm{id} - \mathcal{C}^{[\ell]}) u))\|_{L^2(\Omega)} \\
&\quad \leq \|\nabla(\widetilde{\mathcal{P}} u - (\mathrm{id} - \mathcal{C}^{[\ell]}) u)\|_{L^2(\Omega)} \qquad =: N_1 \\
&\qquad + \|\nabla(\sum_{\nu=1}^{j} \mathcal{D}^\nu(\partial_t^{2\nu} \widetilde{\mathcal{P}} u) - \sum_{\nu=1}^{j} (\mathcal{D}^{\mathrm{loc}})^\nu (\partial_t^{2\nu} (\mathrm{id} - \mathcal{C}^{[\ell]}) u))\|_{L^2(\Omega)} \qquad =: N_2
\end{aligned} \tag{3.138}$$

Employing similar arguments as in (2.29), we have for any $v \in H_0^1(\Omega)$

$$\begin{aligned}
a(\widetilde{\mathcal{P}} u, v) &= a(\widetilde{\mathcal{P}} u, (\mathrm{id} - \mathcal{C}) v) + a(\widetilde{\mathcal{P}} u, \mathcal{C} v) \\
&= a(u, (\mathrm{id} - \mathcal{C}) \mathcal{B}_H v) \\
&= a((\mathrm{id} - \mathcal{C}) u, (\mathrm{id} - \mathcal{C}) \mathcal{B}_H v) + a((\mathrm{id} - \mathcal{C}) u, \mathcal{C} v) \\
&= a((\mathrm{id} - \mathcal{C}) u, v),
\end{aligned}$$

which yields

$$\widetilde{\mathcal{P}} = \mathrm{id} - \mathcal{C}.$$

Thus, the first term can be estimated using Lemma 2.5

$$\begin{aligned} N_1 &= \|\nabla(\mathcal{C}^{[\ell]} - \mathcal{C})u\|_{L^2(\Omega)} \\ &\lesssim \ell^{\frac{d}{2}} \exp(-C\ell)\|\nabla u\|_{L^2(\Omega)}. \end{aligned} \tag{3.139}$$

Employing both (3.139) and (3.138) in (3.137) with the definition of the constant (3.5) yields

$$\begin{aligned} \|\nabla(u - \breve{\mathcal{Q}}^{j,\mathrm{loc}}u)\|_{L^2(\Omega)} &\lesssim H^{\kappa+1}C_{\mathrm{data}} + N_1 + N_2 \\ &\lesssim H^{\kappa+1}C_{\mathrm{data}} + \ell^{\frac{d}{2}} \exp(-C\ell)C_{\mathrm{data}} + N_2. \end{aligned} \tag{3.140}$$

For the second term we add and subtract

$$\sum_{\nu=1}^{j} \mathcal{D}^{\nu}(\partial_t^{2\nu}(\mathrm{id} - \mathcal{C}^{[\ell]})u),$$

which yields by triangle inequality

$$\begin{aligned} N_2 &\lesssim \|\nabla(\sum_{\nu=1}^{j}((\mathcal{D}^{\mathrm{loc}})^{\nu} - \mathcal{D}^{\nu})(\partial_t^{2\nu}(\mathrm{id} - \mathcal{C}^{[\ell]})u))\|_{L^2(\Omega)} \\ &\quad + \|\nabla(\sum_{\nu=1}^{j} \mathcal{D}^{\nu}(\partial_t^{2\nu}\widetilde{\mathcal{P}}u) - \sum_{\nu=1}^{j} \mathcal{D}^{\nu}(\partial_t^{2\nu}(\mathrm{id} - \mathcal{C}^{[\ell]})u))\|_{L^2(\Omega)} \\ &= \underbrace{\|\nabla(\sum_{\nu=1}^{j}((\mathcal{D}^{\mathrm{loc}})^{\nu} - \mathcal{D}^{\nu})(\partial_t^{2\nu}(\mathrm{id} - \mathcal{C}^{[\ell]})u))\|_{L^2(\Omega)}}_{=:\xi_1} \\ &\quad + \underbrace{\|\nabla(\sum_{\nu=1}^{j} \mathcal{D}^{\nu}(\partial_t^{2\nu}(\mathcal{C}^{[\ell]} - \mathcal{C})u))\|_{L^2(\Omega)}}_{=:\xi_2}. \end{aligned} \tag{3.141}$$

Using this in (3.140) yields

$$\|\nabla(u - \breve{\mathcal{Q}}^{j,\mathrm{loc}}u)\|_{L^2(\Omega)} \lesssim H^{\kappa+1}C_{\mathrm{data}} + \ell^{\frac{d}{2}} \exp(-C\ell)C_{\mathrm{data}} + \xi_1 + \xi_2. \tag{3.142}$$

Employing Theorem 3.19 we readily have

$$\begin{aligned} \xi_1 &\lesssim \sum_{\nu=1}^{j} \ell^{\frac{d}{2}} \exp(-C\ell)\|\nabla\partial_t^{2\nu}u\|_{L^2(\Omega)} \\ &\lesssim \ell^{\frac{d}{2}} \exp(-C\ell)C_{\mathrm{data}}. \end{aligned} \tag{3.143}$$

Finally, we consider the last term on the right-hand side. We abbreviate

$$w = \sum_{\nu=1}^{j} \mathcal{D}^\nu(\partial_t^{2\nu}(\mathcal{C}^{[\ell]} - \mathcal{C})u) \in W.$$

Then by the coercivity (2.6) and the definition of the enriched correction operator (3.23) we have

$$\left.\begin{aligned} \xi_2^2 &\lesssim a(\sum_{\nu=1}^{j} \mathcal{D}^\nu(\partial_t^{2\nu}(\mathcal{C}^{[\ell]} - \mathcal{C})u), w) \\ &= -(\partial_t^2(\mathcal{C}^{[\ell]} - \mathcal{C})u, w)_{L^2(\Omega)} \\ &\quad -(\partial_t^2 \textstyle\sum_{\nu=2}^{j} \mathcal{D}^{\nu-1}(\partial_t^{2(\nu-1)}(\mathcal{C}^{[\ell]} - \mathcal{C})u), w)_{L^2(\Omega)} \end{aligned}\right\} = (\star). \tag{3.144a}$$

Since $w \in W$ we can subtract the L^2-projection from both sides and use (2.13) to obtain

$$\begin{aligned} (\star) &= -((\mathrm{id} - \Pi_H)\partial_t^2(\mathcal{C}^{[\ell]} - \mathcal{C})u, (\mathrm{id} - \Pi_H)w)_{L^2(\Omega)} \\ &\quad - ((\mathrm{id} - \Pi_H)\partial_t^2 \sum_{\nu=2}^{j} \mathcal{D}^{\nu-1}(\partial_t^{2(\nu-1)}(\mathcal{C}^{[\ell]} - \mathcal{C})u), (\mathrm{id} - \Pi_H)w)_{L^2(\Omega)} \\ &\lesssim H^2 \|\nabla \partial_t^2(\mathcal{C}^{[\ell]} - \mathcal{C})u\|_{L^2(\Omega)} \|\nabla w\|_{L^2(\Omega)} \\ &\quad + H^2 \|\nabla \partial_t^2 \sum_{\nu=2}^{j} \mathcal{D}^{\nu-1}(\partial_t^{2(\nu-1)}(\mathcal{C}^{[\ell]} - \mathcal{C})u)\|_{L^2(\Omega)} \|\nabla w\|_{L^2(\Omega)} \end{aligned} \tag{3.144b}$$

Dividing both sides by $\|\nabla w\|_{L^2(\Omega)}$ yields

$$\xi_2 \lesssim H^2 \|\nabla \partial_t^2(\mathcal{C}^{[\ell]} - \mathcal{C})\|_{L^2(\Omega)} + H^2 \|\nabla \partial_t^2 \sum_{\nu=2}^{j} \mathcal{D}^{\nu-1}(\partial_t^{2(\nu-1)}(\mathcal{C}^{[\ell]} - \mathcal{C})u)\|_{L^2(\Omega)} \tag{3.144c}$$

The last term on the right-hand side has the same form as the term on the left-hand side, and thus can be estimated analogously to (3.144), i.e.,

$$\begin{aligned} &\|\nabla \partial_t^2 \sum_{\nu=2}^{j} \mathcal{D}^{\nu-1}(\partial_t^{2(\nu-1)}(\mathcal{C}^{[\ell]} - \mathcal{C})u)\|_{L^2(\Omega)} \\ &\lesssim H^2 \|\nabla \partial_t^4(\mathcal{C}^{[\ell]} - \mathcal{C})u\|_{L^2(\Omega)} + H^2 \|\nabla \partial_t^4 \sum_{\nu=3}^{j} \mathcal{D}^{\nu-2}(\partial_t^{2(\nu-2)}(\mathcal{C}^{[\ell]} - \mathcal{C})u)\|_{L^2(\Omega)}. \end{aligned} \tag{3.145}$$

This argument can be applied iteratively such that we obtain

$$\xi_2 \lesssim H^2 \sum_{\nu=1}^{j} H^{2(\nu-1)} \|\nabla \partial_t^{2\nu}(\mathcal{C}^{[\ell]} - \mathcal{C})u\|_{L^2(\Omega)}. \tag{3.146}$$

Finally, we apply Lemma 2.5 and the definition of the constant (3.5) to obtain

$$\begin{aligned}\xi_2 &\lesssim H^2\ell^{\frac{d}{2}}\exp(-C\ell)\sum_{\nu=1}^{j}H^{2(\nu-1)}\|\nabla\partial_t^{2\nu}u\|_{L^2(\Omega)}\\ &\lesssim H^2\ell^{\frac{d}{2}}\exp(-C\ell)C_{\mathrm{data}}.\end{aligned}\tag{3.147}$$

Thus, applying (3.143) and (3.147) in (3.142) yields the assertion. □

Example 3.13. This example is concerned with the addition of the enriched correction space $j = 1$. We again consider the coefficient A_1 from Figure 2.5 with oscillations on the scale $\varepsilon = 2^{-8}$. The setup is otherwise the same as in Example 3.5. In Figure 3.6 for $p = 0$ we see again the optimal convergence rate of 2. We also observe that including the enriched correction space yields a smaller error, which is more apparent for lower mesh sizes. This error then approaches the second-order rate from the sp-LOD which is supported by the theory due to the choice of the polynomial degree. Further, the plot shows that if the localization is not chosen appropriately, a plateau can be observed. Here, the error of the eho-LOD with $j = 1$ also seems to approach the same plateau as the sp-LOD which is backed by the localization result in Theorem 3.19.

For $p = 2$, the error of the sp-LOD for $j = 0$ seems to show have smaller errors for low mesh sizes and then approach the second-order convergence. For $j = 1$, we observe a similar phenomenon, where the error is lower for smaller mesh sizes and then eventually approaches the fourth order convergence.

Example 3.14. This example complements the previous Example 3.13. Here, we consider eho-LOD now for $j = 0, 1, 2$ in $d = 1$. We choose the dimension one in this example as we need a much finer resolution for the enriched spaces with $j = 2$. This is briefly outlined in the following. If we have a rather large mesh size, e.g., $H = 2^{-5}$ and polynomial degree $p = 4$, then we have for $j = 2$ already 15 basis function per dimension. For a fine mesh with mesh size $h = 2^{-9}$ we have only 17 degrees of freedom per dimension per coarse element. Thus, in order to have a remainder of sufficient size, the localization parameter needs to be chosen large enough, otherwise the system matrix is badly conditioned.

We turn back to the example at hand. The PDE coefficient is chosen with random values and an oscillation scale $\varepsilon = 2^{-10}$. The fine-scale discretization is $h = 2^{-12}$. For the right-hand side

$$f(x,t) = \cos(\pi x)\sin(t)^8$$

is chosen with zero initial conditions. Figure 3.7 portrays the errors of the eho-LOD method for $j = 0, 1, 2$ and the polynomial degrees $p = 0, 2, 4$. We chose a localization parameter such that the rates can be observed. Similar to Example 3.5, we observe that the error for $j = 0$ are capped at second order. Increasing $j = 1$ already yields fourth-order convergence for $p = 2$ with a much lower size of the error. For $j = 2$

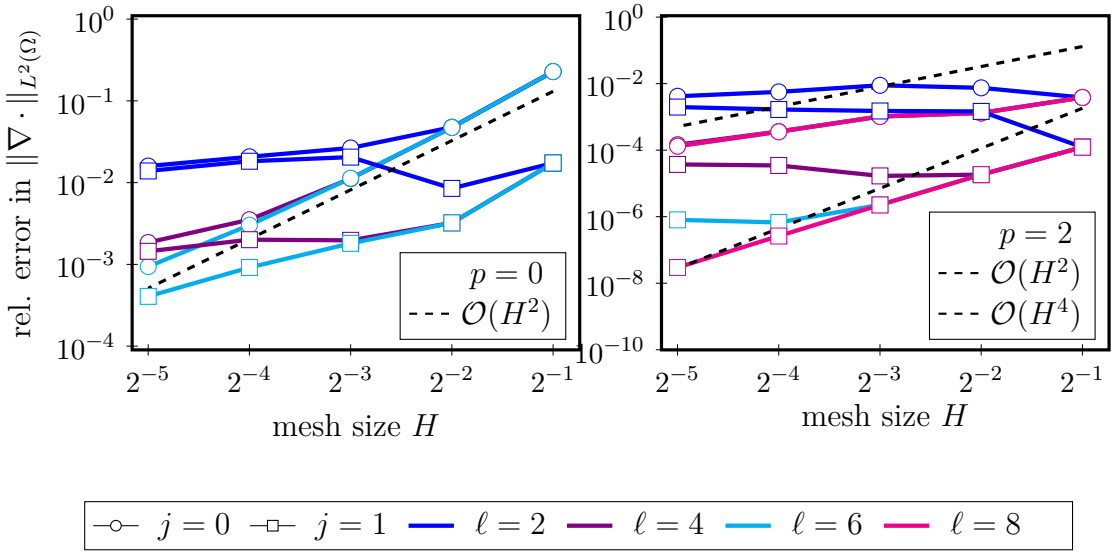

Figure 3.6: Relative errors of the eho-LOD in the norm $\|\nabla \cdot\|_{L^2(\Omega)}$ for the coefficient A_1 from Figure 2.5 that oscillates on the scale $\varepsilon = 2^{-8}$. We show the error for two polynomial degrees and $j = 0, 1$. See Example 3.13.

we observe for $p = 4$ the optimal sixth-order convergence as in the elliptic setting. The last point for $p = 4$ has a reduced error. This is a result on one hand from the localization, as a larger ℓ is able to reduce the error. On the other hand this is also a result from numerical errors. Even if the localization is increased the last plot point does not yield optimal convergence. This motivates further investigation, specifically improving the condition of the system matrix by, e.g., orthogonalizing the enriched corrections such that the matrix can be decoupled and each space can be dealt with separately.

3.5 Time discretization

In the previous sections we considered only the semi-discrete setting. Here, we will finally provide a fully-discrete error analysis. We intend to use the so-called *θ-scheme* as used by Karaa (2011). This time discretization is standard for the wave equation and can be either an explicit or implicit scheme and potentially have fourth-order convergence.

Enriched higher-order LOD-θ. We employ the multiscale space $\check{V}_H^{j,\mathrm{loc}}$ as trial and test space in the variational formulation (3.127) and combine with the θ-scheme as used by Karaa (2011). That is, the *eho-LOD-θ* method seeks for any $\theta \in [0, \frac{1}{2}]$ a

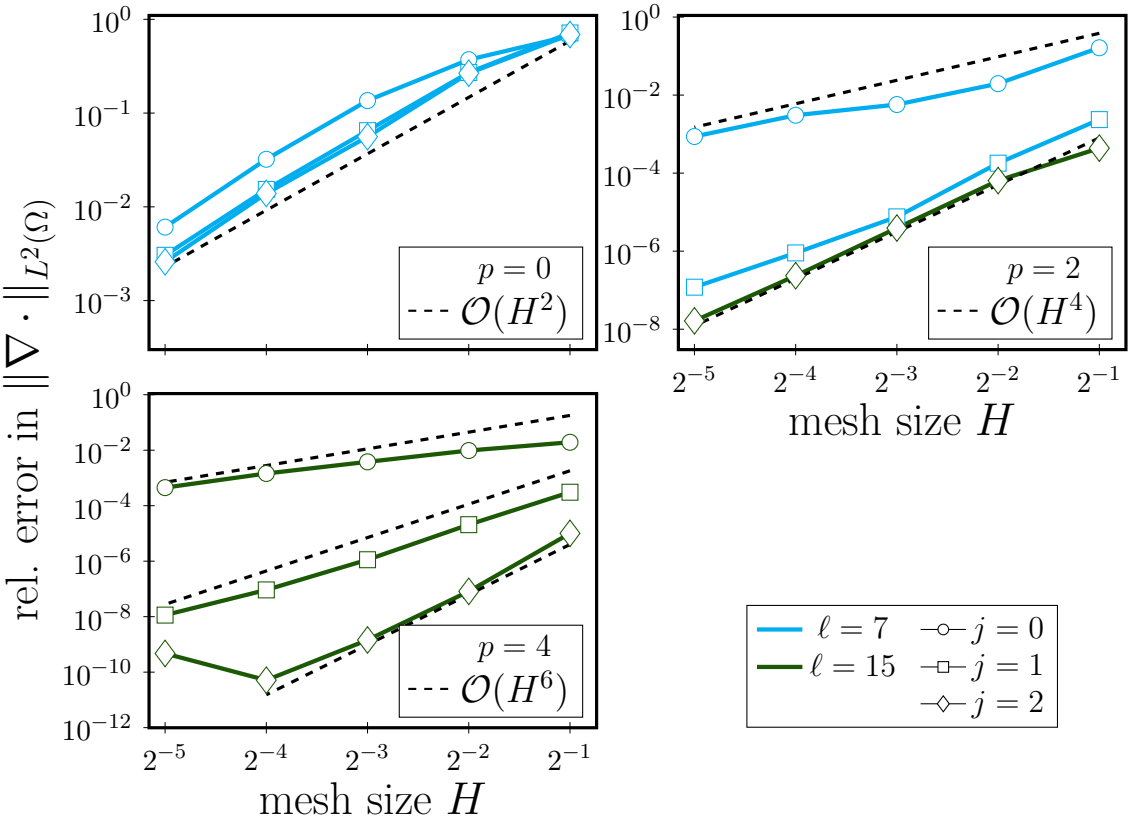

Figure 3.7: Relative errors of the eho-LOD for $d = 1$ in the norm $\|\nabla \cdot\|_{L^2(\Omega)}$ for a random coefficient A oscillating on the scale $\varepsilon = 2^{-10}$. See Example 3.14.

sequence of solutions $\check{\boldsymbol{u}}_{\boldsymbol{H}} = \{\check{u}_H^n\}_{n=0}^N \subset \check{V}_H^{j,\mathrm{loc}}$ such that for $n \geq 1$

$$\tau^{-2}(\check{u}_H^{n+1} - 2\check{u}_H^n + \check{u}_H^{n-1}, \check{v}_H)_{L^2(\Omega)} + a(\check{u}_H^{n;\theta}, \check{v}_H) = (f(t_n^\theta), \check{v}_H)_{L^2(\Omega)} \tag{3.148}$$

for all $\check{v}_H \in \check{V}_H^{j,\mathrm{loc}}$ with appropriately chosen $\check{u}_H^0$, and $\check{u}_H^1$ and the time step size $\tau = \frac{T}{N}$. Here, the θ-weighted difference is given for any sequence $\{v^n\}_{n=0}^N$ by

$$v^{n;\theta} := \theta v^{n+1} + (1 - 2\theta)v^n + \theta v^{n-1}, \tag{3.149}$$

and for a continuous-in-time function $v\colon C([0,T]; L^2(\Omega))$

$$v(t_n^\theta) = \theta v(t_{n+1}) + (1 - 2\theta)v(t_n) + \theta v(t_{n-1}), \tag{3.150}$$

where $t_n = n\tau$.

The error analysis of the eho-LOD-θ method is rather classical, and tries to mimic the semi-discrete error analysis. First, we show that the discrete time discretization conserves a discrete energy, and after we show that the method is stable. The proof of the convergence in time then uses the stability and properly chosen initial conditions.

3.5.1 Energy Conservation

In this section we show that the θ-method conserves a discrete energy. Using this energy conservation we can later show that the eho-LOD-θ method is stable and derive an error recursion.

We define the discrete energy of the θ-method as

$$\mathcal{E}^{n+\frac{1}{2}} \coloneqq \tfrac{1}{2}\Big[\|\mathrm{D}_\tau \check{u}_H^{n+\frac{1}{2}}\|^2_{L^2(\Omega)} + a(\check{u}_H^{n+\frac{1}{2}}, \check{u}_H^{n+\frac{1}{2}}) + \tau^2(\theta - \tfrac{1}{4})a(\mathrm{D}_\tau \check{u}_H^{n+\frac{1}{2}}, \mathrm{D}_\tau \check{u}_H^{n+\frac{1}{2}})\Big]. \quad (3.151)$$

Here, we define the discrete time-derivate for any sequence $\{\check{v}_H^n\}_{n=0}^N$ as

$$\mathrm{D}_\tau \check{v}_H^{n+\frac{1}{2}} \coloneqq \tau^{-1}(\check{v}_H^{n+1} - \check{v}_H^n). \quad (3.152)$$

We note that with this definition we can also define the second discrete time-derivative as

$$\mathrm{D}_\tau^2 \check{v}_H^n \coloneqq \tau^{-2}(\check{v}_H^{n+1} - 2\check{v}_H^n + \check{v}_H^{n-1}). \quad (3.153)$$

Further, the half step of a sequence $\{\check{v}_H^n\}_{n=0}^N$ is defined by

$$\check{v}_H^{n+\frac{1}{2}} \coloneqq \tfrac{1}{2}(\check{v}_H^{n+1} + \check{v}_H^n). \quad (3.154)$$

We will show that this energy is conserved by the eho-LOD-θ method.

Lemma 3.25 (Energy conservation)**.** *The eho-LOD-θ method* (3.148) *conserves the discrete energy* (3.151) *in the sense that*

$$(f(t_n^\theta), \check{u}_H^{n+1} - \check{u}_H^{n-1})_{L^2(\Omega)} = 2(\mathcal{E}^{n+\frac{1}{2}} - \mathcal{E}^{n-\frac{1}{2}}). \quad (3.155)$$

Particularly, if the source term $f \equiv 0$ we obtain energy conservation in the classical sense, i.e.,

$$\mathcal{E}^{n+\frac{1}{2}} = \mathcal{E}^{n-\frac{1}{2}} = \cdots = \mathcal{E}^{\frac{1}{2}}.$$

Proof. We choose

$$\check{v}_H = \check{u}_H^{n+1} - \check{u}_H^{n-1}$$

as a test function in (3.148) and obtain

$$\begin{aligned}(f(t_n^\theta), \check{u}_H^{n+1} - \check{u}_H^{n-1})_{L^2(\Omega)} \\ = \tau^{-2}(\check{u}_H^{n+1} - 2\check{u}_H^n + \check{u}_H^{n-1}, \check{u}_H^{n+1} - \check{u}_H^{n-1})_{L^2(\Omega)} + a(\check{u}_H^{n;\theta}, \check{u}_H^{n+1} - \check{u}_H^{n-1})\end{aligned} \quad (3.156)$$

The first term on the right-hand side can be estimated straight-forward by adding and subtracting the term $\check{u}_H^n$ on the test-side of the scalar product, which yields

$$\begin{aligned}
&\tau^{-2}(\check{u}_H^{n+1} - 2\check{u}_H^n + \check{u}_H^{n-1}, \check{u}_H^{n+1} - \check{u}_H^{n-1})_{L^2(\Omega)} \\
&= \tau^{-2}(\check{u}_H^{n+1} - \check{u}_H^n, \check{u}_H^{n+1} - \check{u}_H^{n-1})_{L^2(\Omega)} - \tau^{-2}(\check{u}_H^n - \check{u}_H^{n-1}, \check{u}_H^{n+1} - \check{u}_H^{n-1})_{L^2(\Omega)} \\
&= \tau^{-2}(\check{u}_H^{n+1} - \check{u}_H^n, \check{u}_H^{n+1} - \check{u}_H^n)_{L^2(\Omega)} - \tau^{-2}(\check{u}_H^n - \check{u}_H^{n-1}, \check{u}_H^{n+1} - \check{u}_H^n)_{L^2(\Omega)} \\
&\quad + \tau^{-2}(\check{u}_H^{n+1} - \check{u}_H^n, \check{u}_H^n - \check{u}_H^{n-1})_{L^2(\Omega)} - \tau^{-2}(\check{u}_H^n - \check{u}_H^{n-1}, \check{u}_H^n - \check{u}_H^{n-1})_{L^2(\Omega)} \qquad (3.157a) \\
&= \|\mathrm{D}_\tau \check{u}_H^{n+\frac{1}{2}}\|^2_{L^2(\Omega)} - \|\mathrm{D}_\tau \check{u}_H^{n-\frac{1}{2}}\|^2_{L^2(\Omega)} \\
&\quad + \tau^{-2}(\check{u}_H^{n+1} - \check{u}_H^n, \check{u}_H^n - \check{u}_H^{n-1})_{L^2(\Omega)} - \tau^{-2}(\check{u}_H^n - \check{u}_H^{n-1}, \check{u}_H^{n+1} - \check{u}_H^n)_{L^2(\Omega)}.
\end{aligned}$$

Due to the symmetry of the L^2-scalar product, the last two terms cancel, and we have

$$\tau^{-2}(\check{u}_H^{n+1} - 2\check{u}_H^n + \check{u}_H^{n-1}, \check{u}_H^{n+1} - \check{u}_H^{n-1})_{L^2(\Omega)} = \|\mathrm{D}_\tau \check{u}_H^{n+\frac{1}{2}}\|^2_{L^2(\Omega)} - \|\mathrm{D}_\tau \check{u}_H^{n-\frac{1}{2}}\|^2_{L^2(\Omega)}. \qquad (3.157b)$$

Next, we turn to the last term on the right-hand side of (3.156). We obtain by adding and subtracting the term $\check{u}_H^n$ on the test-side of the inner product

$$\begin{aligned}
a(\check{u}_H^{n;\theta}, \check{u}_H^{n+1} - \check{u}_H^{n-1}) &= a(\theta\check{u}_H^{n+1} + (1-2\theta)\check{u}_H^n + \theta\check{u}_H^{n-1}, \check{u}_H^{n+1} - \check{u}_H^{n-1}) \\
&= a(\theta\check{u}_H^{n+1} - \theta\check{u}_H^n, \check{u}_H^{n+1} - \check{u}_H^{n-1}) - a(\theta\check{u}_H^n - \theta\check{u}_H^{n-1}, \check{u}_H^{n+1} - \check{u}_H^{n-1}) \\
&\quad + a(\check{u}_H^n, \check{u}_H^{n+1} - \check{u}_H^{n-1}) \\
&= a(\theta\check{u}_H^{n+1} - \theta\check{u}_H^n, \check{u}_H^{n+1} - \check{u}_H^n) - a(\theta\check{u}_H^n - \theta\check{u}_H^{n-1}, \check{u}_H^{n+1} - \check{u}_H^n) \\
&\quad + a(\theta\check{u}_H^{n+1} - \theta\check{u}_H^n, \check{u}_H^n - \check{u}_H^{n-1}) - a(\theta\check{u}_H^n - \theta\check{u}_H^{n-1}, \check{u}_H^n - \check{u}_H^{n-1}) \\
&\quad + a(\check{u}_H^n, \check{u}_H^{n+1} - \check{u}_H^{n-1}) \qquad (3.158a) \\
&= \theta\tau^2 a(\mathrm{D}_\tau \check{u}_H^{n+\frac{1}{2}}, \mathrm{D}_\tau \check{u}_H^{n+\frac{1}{2}}) - \theta\tau^2 a(\mathrm{D}_\tau \check{u}_H^{n-\frac{1}{2}}, \mathrm{D}_\tau \check{u}_H^{n-\frac{1}{2}}) \\
&\quad + a(\theta\check{u}_H^{n+1} - \theta\check{u}_H^n, \check{u}_H^n - \check{u}_H^{n-1}) - a(\theta\check{u}_H^n - \theta\check{u}_H^{n-1}, \check{u}_H^{n+1} - \check{u}_H^n) \\
&\quad + a(\check{u}_H^n, \check{u}_H^{n+1} - \check{u}_H^{n-1}) =: (\star).
\end{aligned}$$

Similar to above by symmetry the second-to-last line vanishes. Consider the last term on the right-hand side. We have by adding and subtracting equal terms

$$\begin{aligned}
(\star) &= \tfrac{1}{4}a(\check{u}_H^n, \check{u}_H^{n+1}) - \tfrac{1}{4}a(\check{u}_H^n, \check{u}_H^{n-1}) + \tfrac{3}{4}a(\check{u}_H^n, \check{u}_H^{n+1} - \check{u}_H^{n-1}) \\
&= \tfrac{1}{4}a(\check{u}_H^n, \check{u}_H^{n+1} + \check{u}_H^n) - \tfrac{1}{4}a(\check{u}_H^n, \check{u}_H^n + \check{u}_H^{n-1}) + \tfrac{3}{4}a(\check{u}_H^n, \check{u}_H^{n+1} - \check{u}_H^{n-1}) \\
&= \tfrac{1}{4}a(\check{u}_H^{n+1} + \check{u}_H^n, \check{u}_H^{n+1} + \check{u}_H^n) - \tfrac{1}{4}a(\check{u}_H^n + \check{u}_H^{n-1}, \check{u}_H^n + \check{u}_H^{n-1}) \\
&\quad - \tfrac{1}{4}a(\check{u}_H^{n+1}, \check{u}_H^{n+1} + \check{u}_H^n) + \tfrac{1}{4}a(\check{u}_H^{n-1}, \check{u}_H^n + \check{u}_H^{n-1}) \\
&\quad + \tfrac{3}{4}a(\check{u}_H^n, \check{u}_H^{n+1} - \check{u}_H^{n-1}) \qquad (3.158b) \\
&= a(\check{u}_H^{n+\frac{1}{2}}, \check{u}_H^{n+\frac{1}{2}}) - a(\check{u}_H^{n-\frac{1}{2}}, \check{u}_H^{n-\frac{1}{2}}) \\
&\quad - \tfrac{1}{4}a(\check{u}_H^{n+1}, \check{u}_H^{n+1} + \check{u}_H^n) + \tfrac{1}{4}a(-\check{u}_H^{n-1}, -\check{u}_H^n - \check{u}_H^{n-1}) \\
&\quad + \tfrac{3}{4}a(\check{u}_H^n, \check{u}_H^{n+1} - \check{u}_H^{n-1}) \\
&=: (\star\star).
\end{aligned}$$

Finally, we estimate the last three terms on the right-hand side to obtain

$$\begin{aligned}(\star\star) &= -\tfrac{1}{4}a(\check{u}_H^{n+1}, \check{u}_H^{n+1} - \check{u}_H^n) + \tfrac{1}{4}a(-\check{u}_H^{n-1}, \check{u}_H^n - \check{u}_H^{n-1}) \\ &\quad - \tfrac{1}{2}a(\check{u}_H^{n+1}, \check{u}_H^n) + \tfrac{1}{2}a(-\check{u}_H^{n-1}, -\check{u}_H^n) + \tfrac{3}{4}a(\check{u}_H^n, \check{u}_H^{n+1} - \check{u}_H^{n-1}) \\ &= -\tfrac{1}{4}a(\check{u}_H^{n+1}, \check{u}_H^{n+1} - \check{u}_H^n) + \tfrac{1}{4}a(\check{u}_H^{n-1}, \check{u}_H^n - \check{u}_H^{n-1}) \\ &\quad - \tfrac{1}{2}a(\check{u}_H^{n+1}, \check{u}_H^n) - \tfrac{1}{2}a(-\check{u}_H^{n-1}, \check{u}_H^n) + \tfrac{3}{4}a(\check{u}_H^n, \check{u}_H^{n+1} - \check{u}_H^{n-1}) \\ &= -\tfrac{1}{4}a(\check{u}_H^{n+1}, \check{u}_H^{n+1} - \check{u}_H^n) + \tfrac{1}{4}a(\check{u}_H^{n-1}, \check{u}_H^n - \check{u}_H^{n-1}) \\ &\quad + \tfrac{1}{4}a(\check{u}_H^n, \check{u}_H^{n+1} - \check{u}_H^n + \check{u}_H^n - \check{u}_H^{n-1}) \\ &= \tau^2 \tfrac{1}{4}a(\mathrm{D}_\tau \check{u}_H^{n+\frac{1}{2}}, \mathrm{D}_\tau \check{u}_H^{n+\frac{1}{2}}) - \tau^2 \tfrac{1}{4}a(\mathrm{D}_\tau \check{u}_H^{n-\frac{1}{2}}, \mathrm{D}_\tau \check{u}_H^{n-\frac{1}{2}}).\end{aligned} \tag{3.158c}$$

Combining both estimates (3.157) and (3.158) in (3.156) yields the energy conservation. □

3.5.2 Stability

In order to show stability of the θ-method we first show that the energy is positive and then use the energy conservation to proof an error recursion such that the energy of the solution can be estimated by the right-hand side and initial data. In order to show the positivity of the energy a CFL condition is necessary for $\theta < \frac{1}{4}$. This is however only possible to show if $j = 0$. Thus, we restrict ourselves to the case that $\theta \geq \frac{1}{4}$.

Lemma 3.26 (Stability)**.** *Let $\frac{1}{4} \leq \theta \leq \frac{1}{2}$. Then the eho-LOD-$\theta$ method* (3.148) *is unconditionally stable. Further,*

$$\begin{aligned}&\|\mathrm{D}_\tau \check{u}_H^{n+\frac{1}{2}}\|_{L^2(\Omega)} + \|\nabla \check{u}_H^{n+\frac{1}{2}}\|_{L^2(\Omega)} \\ &\quad \lesssim \|\mathrm{D}_\tau \check{u}_H^{\frac{1}{2}}\|_{L^2(\Omega)} + \sqrt{\|\nabla \check{u}_H^1\|_{L^2(\Omega)} \|\nabla \check{u}_H^0\|_{L^2(\Omega)}} + \tau\sqrt{\theta}\|\nabla \mathrm{D}_\tau \check{u}_H^{\frac{1}{2}}\|_{L^2(\Omega)} \\ &\qquad + \sum_{i=1}^n \tau \|f(t_i^\theta)\|_{L^2(\Omega)}.\end{aligned} \tag{3.159}$$

Proof. The stability follows directly from $\theta \geq \frac{1}{4}$, since

$$\mathcal{E}^{n+\frac{1}{2}} > 0.$$

Next, we prove the stability estimate (3.159). Employing Young inequality we obtain

$$\|\mathrm{D}_\tau \check{u}_H^{n+\frac{1}{2}}\|_{L^2(\Omega)} + \|\nabla \check{u}_H^{n+\frac{1}{2}}\|_{L^2(\Omega)} \lesssim \sqrt{\mathcal{E}^{n+\frac{1}{2}}}. \tag{3.160}$$

We further bound the term on the right-hand side. Using the energy conservation property (3.155) and Cauchy-Schwarz inequality we get

$$\begin{aligned}\mathcal{E}^{n+\frac{1}{2}} - \mathcal{E}^{n-\frac{1}{2}} &= \tfrac{1}{2}\tau(f(t_n^\theta), \mathrm{D}_\tau \check{u}_H^{n+\frac{1}{2}} + \mathrm{D}_\tau \check{u}_H^{n-\frac{1}{2}})_{L^2(\Omega)} \\ &\lesssim \tau \|f(t_n^\theta)\|_{L^2(\Omega)} (\|\mathrm{D}_\tau \check{u}_H^{n+\frac{1}{2}}\|_{L^2(\Omega)} + \|\mathrm{D}_\tau \check{u}_H^{n-\frac{1}{2}}\|_{L^2(\Omega)}) \\ &\lesssim \tau \|f(t_n^\theta)\|_{L^2(\Omega)} (\sqrt{\mathcal{E}^{n+\frac{1}{2}}} + \sqrt{\mathcal{E}^{n-\frac{1}{2}}}).\end{aligned} \tag{3.161}$$

Using the third binomial formula we obtain directly

$$\sqrt{\mathcal{E}^{n+\frac{1}{2}}} \lesssim \sqrt{\mathcal{E}^{n-\frac{1}{2}}} + \tau \|f(t_n^\theta)\|_{L^2(\Omega)}. \tag{3.162}$$

This iteratively leads to

$$\sqrt{\mathcal{E}^{n+\frac{1}{2}}} \lesssim \sqrt{\mathcal{E}^{\frac{1}{2}}} + \sum_{i=1}^{n} \tau \|f(t_i^\theta)\|_{L^2(\Omega)}. \tag{3.163}$$

Finally, consider the initial energy

$$\mathcal{E}^{\frac{1}{2}} = \tfrac{1}{2}\Big[\|\mathrm{D}_\tau \check{u}_H^{\frac{1}{2}}\|_{L^2(\Omega)}^2 + a(\check{u}_H^{\frac{1}{2}}, \check{u}_H^{\frac{1}{2}}) + \tau^2(\theta - \tfrac{1}{4}) a(\mathrm{D}_\tau \check{u}_H^{\frac{1}{2}}, \mathrm{D}_\tau \check{u}_H^{\frac{1}{2}})\Big].$$

Then, we can use symmetry to obtain

$$\begin{aligned} a(\check{u}_H^{\frac{1}{2}}, \check{u}_H^{\frac{1}{2}}) - \tau^2 \tfrac{1}{4} a(\mathrm{D}_\tau \check{u}_H^{\frac{1}{2}}, \mathrm{D}_\tau \check{u}_H^{\frac{1}{2}}) \\ = \tfrac{1}{4} a(\check{u}_H^1 + \check{u}_H^0, \check{u}_H^1 + \check{u}_H^0) - \tfrac{1}{4} a(\check{u}_H^1 - \check{u}_H^0, \check{u}_H^1 - \check{u}_H^0) \\ = a(\check{u}_H^1, \check{u}_H^0). \end{aligned} \tag{3.164}$$

Thus, the initial energy can be bounded by

$$\mathcal{E}^{\frac{1}{2}} \lesssim \|\mathrm{D}_\tau \check{u}_H^{\frac{1}{2}}\|_{L^2(\Omega)}^2 + \|\nabla \check{u}_H^1\|_{L^2(\Omega)} \|\nabla \check{u}_H^0\|_{L^2(\Omega)} + \tau^2 a(\mathrm{D}_\tau \check{u}_H^{\frac{1}{2}}, \mathrm{D}_\tau \check{u}_H^{\frac{1}{2}}). \tag{3.165}$$

Then, taking the square root and combining the estimates (3.165) with (3.160) in (3.163) we obtain the assertion. □

3.5.3 Error analysis for the fully-discrete enriched higher-order LOD

Assumption 3.15. Let the initial conditions for the eho-LOD-θ method be given as the solution to the equation

$$\check{u}_H^0 = \mathfrak{u}_0, \tag{3.166a}$$

and

$$\begin{aligned} (\check{u}_H^1 - \check{u}_H^0, \check{v}_H)_{L^2(\Omega)} + \tau^2 \theta a(\check{u}_H^1 - \check{u}_H^0, \check{v}_H) \\ = \tau(\mathfrak{v}_0, \check{v}_H)_{L^2(\Omega)} - \tfrac{\tau^2}{2} a(\mathfrak{u}_0, \check{v}_H) + \tfrac{\tau^2}{2} a(f(0,\cdot), \check{v}_H), \end{aligned} \tag{3.166b}$$

where the maps into the enriched multiscale space of the initial conditions are given by

$$\mathfrak{u}_0 = \check{\mathcal{Q}}^{j,\mathrm{loc}} u_0, \qquad \mathfrak{v}_0 = \check{\mathcal{Q}}^{j,\mathrm{loc}} v_0 \tag{3.167}$$

Theorem 3.27. *Let Assumption 3.1 hold for some $k \in \mathbb{N}_0$, and $m \geq 2j+4$, Assumption 3.10 hold for some $\ell, j \in \mathbb{N}$, and Assumption 3.15 hold. Further, let u be the solution to* (3.2)*, and $\check{u}_H$ be the solution to* (3.148)*. Then if $j \geq \lceil \frac{p}{2} \rceil$, $\ell \gtrsim |\log H|$, and $\frac{1}{4} \leq \theta \leq \frac{1}{2}$, the following estimate holds*

$$\|\mathrm{D}_\tau \check{u}_H^{n+\frac{1}{2}} - \tau^{-1}(u(t_{n+1}) - u(t_n))\|_{L^2(\Omega)} + \|\nabla(\check{u}_H^{n+\frac{1}{2}} - u(t_{n+\frac{1}{2}}))\|_{L^2(\Omega)} \lesssim (H^{\kappa+1} + \tau^2) C_{\mathrm{data}}, \quad (3.168)$$

where $\kappa = \min\{k, p+1\}$ and $t_{n+\frac{1}{2}} = \frac{1}{2}(t_{n+1} + t_n)$.

The following lemma provides an estimate for the time discretization error. We make use of the stability estimate (3.159) to derive an error estimate and motivate the choice for the initial conditions. The ideas in the proof follow Karaa (2011) with some technicalities related to the eho-LOD method.

Lemma 3.28 (Temporal error)**.** *Let Assumption 3.1 hold for some $k \in \mathbb{N}_0$, and $m \geq 2j+4$, Assumption 3.10 hold for some $\ell, j \in \mathbb{N}$, and Assumption 3.15 hold. Further, let $\check{u}_H$ be the solution to* (3.127)*, and $\{\check{u}_H^n\}_{n=0}^N$ be the solution to* (3.148)*. With $\zeta^n = \check{u}_H(t_n) - \check{u}_H^n$, and if $\frac{1}{4} \leq \theta \leq \frac{1}{2}$, the following estimate holds*

$$\|\mathrm{D}_\tau \zeta^{n+\frac{1}{2}}\|_{L^2(\Omega)} + \|\nabla \zeta^{n+\frac{1}{2}}\|_{L^2(\Omega)} \lesssim \tau^2 C_{\mathrm{data}}. \quad (3.169)$$

Proof. The sequence $\{\zeta^n\}_{n=0}^N$ solves for all $n = 1, \cdots, N-1$ the variational wave equation

$$\begin{aligned}
&(\mathrm{D}_\tau^2 \zeta^n, \check{v}_H)_{L^2(\Omega)} + a(\zeta^{n;\theta}, \check{v}_H) \\
&\quad = (\mathrm{D}_\tau^2 \check{u}_H^n, \check{v}_H)_{L^2(\Omega)} + a(\check{u}_H^{n;\theta}, \check{v}_H) - (\mathrm{D}_\tau^2 \check{u}_H(t_n), \check{v}_H)_{L^2(\Omega)} - a(\check{u}_H(t_n^\theta), \check{v}_H) \\
&\quad = (f^{n;\theta}, \check{v}_H)_{L^2(\Omega)} - (\mathrm{D}_\tau^2 \check{u}_H(t_n), \check{v}_H)_{L^2(\Omega)} - a(\check{u}_H(t_n^\theta), \check{v}_H) \\
&\quad = (\partial_t^2 \check{u}_H(t_n^\theta), \check{v}_H)_{L^2(\Omega)} + a(\check{u}_H(t_n^\theta), \check{v}_H) - (\mathrm{D}_\tau^2 \check{u}_H(t_n), \check{v}_H)_{L^2(\Omega)} - a(\check{u}_H(t_n^\theta), \check{v}_H) \\
&\quad = (\partial_t^2 \check{u}_H(t_n^\theta), \check{v}_H)_{L^2(\Omega)} - (\mathrm{D}_\tau^2 \check{u}_H(t_n), \check{v}_H)_{L^2(\Omega)}
\end{aligned} \quad (3.170)$$

for all $\check{v}_H \in \check{V}_H^j$. Thus, we can apply the stability estimate (3.159), which yields

$$\begin{aligned}
&\|\mathrm{D}_\tau \zeta^{n+\frac{1}{2}}\|_{L^2(\Omega)} + \|\nabla \zeta^{n+\frac{1}{2}}\|_{L^2(\Omega)} \\
&\qquad \lesssim \|\mathrm{D}_\tau \zeta^{\frac{1}{2}}\|_{L^2(\Omega)} + \sqrt{\|\nabla \zeta^1\|_{L^2(\Omega)} \|\nabla \zeta^0\|_{L^2(\Omega)}} + \tau \|\nabla \mathrm{D}_\tau \zeta^{\frac{1}{2}}\|_{L^2(\Omega)} \\
&\qquad\quad + \sum_{i=1}^n \tau \|\partial_t^2 \check{u}_H(t_i^\theta) - \mathrm{D}_\tau^2 \check{u}_H(t_i)\|_{L^2(\Omega)}.
\end{aligned} \quad (3.171)$$

By construction, we have

$$\zeta^0 = \check{u}_H^0 - \check{u}_H(t_0) = 0, \quad (3.172)$$

and thus the second term under the square root vanishes. Consider the first and third term on the right-hand side together. At the initial time steps we have for the semi-discrete solution

$$\begin{aligned} &a(\check{u}_H(t_1) - \check{u}_H(t_0), \check{v}_H) \\ &\qquad = (f(t_1) - f(t_0), \check{v}_H)_{L^2(\Omega)} - (\partial_t^2(\check{u}_H(t_1) - \check{u}_H(t_0)), \check{v}_H)_{L^2(\Omega)}. \end{aligned} \tag{3.173}$$

Thus, employing the initial condition (3.166), we obtain

$$\begin{aligned} &(\zeta^1 - \zeta^0, \check{v}_H)_{L^2(\Omega)} + \tau^2\theta a(\zeta^1 - \zeta^0, \check{v}_H) \\ &\quad = (\check{u}_H^1 - \check{u}_H^0, \check{v}_H)_{L^2(\Omega)} + \tau^2\theta a(\check{u}_H^1 - \check{u}_H^0, \check{v}_H) \\ &\qquad - (\check{u}_H(t_1) - \check{u}_H(t_0), \check{v}_H)_{L^2(\Omega)} - \tau^2\theta a(\check{u}_H(t_1) - \check{u}_H(t_0), \check{v}_H) \\ &\quad = \tau(\mathfrak{v}_0, \check{v}_H)_{L^2(\Omega)} - \tfrac{\tau^2}{2} a(\mathfrak{u}_0, \check{v}_H) + \tfrac{\tau^2}{2} a(f(0), \check{v}_H) \\ &\qquad - (\check{u}_H(t_1) - \check{u}_H(t_0), \check{v}_H)_{L^2(\Omega)} \\ &\qquad - \tau^2\theta(f(t_1) - f(t_0), \check{v}_H)_{L^2(\Omega)} + \tau^2\theta(\partial_t^2(\check{u}_H(t_1) - \check{u}_H(t_0)), \check{v}_H)_{L^2(\Omega)} \end{aligned} \tag{3.174}$$

Employing Taylor-expansion of the semi-discrete solution around $t_0 = 0$, there exists $\xi_1 \in [t_0, t_1]$ such that

$$\check{u}_H(t_1) = \check{u}_H(t_0) + \tau\partial_t\check{u}_H(t_0) + \tfrac{\tau^2}{2}\partial_t^2\check{u}_H(t_0) + \tfrac{\tau^3}{6}\partial_t^3\check{u}_H(\xi_1).$$

This yields using the definition of the initial conditions (3.166) and (3.128)

$$\mathfrak{u}_0 = \check{u}_H(t_0), \qquad \mathfrak{v}_0 = \partial_t\check{u}_H(t_0)$$

that

$$\begin{aligned} &(\check{u}_H(t_1) - \check{u}_H(t_0), \check{v}_H)_{L^2(\Omega)} + \tfrac{\tau^2}{2} a(\mathfrak{u}_0, \check{v}_H) \\ &\qquad = \tau(\mathfrak{v}_0, \check{v}_H)_{L^2(\Omega)} + \tfrac{\tau^2}{2}(\partial_t^2\check{u}_H(t_0), \check{v}_H)_{L^2(\Omega)} + \tfrac{\tau^2}{2} a(\check{u}_H(t_0), \check{v}_H) \\ &\qquad\quad + \tfrac{\tau^3}{6}(\partial_t^3\check{u}_H(\xi_1), \check{v}_H)_{L^2(\Omega)} \\ &\qquad = \tau(\mathfrak{v}_0, \check{v}_H)_{L^2(\Omega)} + \tfrac{\tau^2}{2}(f(t_0), \check{v}_H)_{L^2(\Omega)} + \tfrac{\tau^3}{6}(\partial_t^3\check{u}_H(\xi_1), \check{v}_H)_{L^2(\Omega)}. \end{aligned} \tag{3.175}$$

Applying this Taylor-expansion in (3.174) shows that the third- and second-to-last lines are equal up to the third order term

$$-\tfrac{\tau^3}{6}(\partial_t^3\check{u}_H(\xi_1), \check{v}_H)_{L^2(\Omega)}.$$

Further, we have with similar Taylor-expansions, that there exist $\xi_2 \in [t_0, t_1]$, and $\xi_3 \in [t_0, t_1]$, such that

$$\begin{aligned} f(t_1) &= f(t_0) + \tau\partial_t f(\xi_2) \\ \partial_t^2\check{u}_H(t_1) &= \partial_t^2\check{u}_H(t_0) + \tau\partial_t^3\check{u}_H(\xi_3). \end{aligned}$$

This implies

$$(f(t_1) - f(t_0), \check{v}_H)_{L^2(\Omega)} = \tau(\partial_t f(\xi_2), \check{v}_H)_{L^2(\Omega)}$$
$$(\partial_t^2(\check{u}_H(t_1) - \check{u}_H(t_0)), \check{v}_H)_{L^2(\Omega)} = \tau(\partial_t^3 \check{u}_H(\xi_3), \check{v}_H)_{L^2(\Omega)}.$$

Finally, using this in (3.174) yields

$$\begin{aligned}(\zeta^1 - \zeta^0, \check{v}_H)_{L^2(\Omega)} + \tau^2\theta a(\zeta^1 - \zeta^0, \check{v}_H) \\ = -\tfrac{\tau^3}{6}(\partial_t^3 \check{u}_H(\xi_1), \check{v}_H)_{L^2(\Omega)} - \tau^3\theta(\partial_t f(\xi_2), \check{v}_H)_{L^2(\Omega)} + \tau^3\theta(\partial_t^3 \check{u}_H(\xi_3), \check{v}_H)_{L^2(\Omega)}.\end{aligned} \tag{3.176}$$

Next, we use $\check{v}_H = \mathrm{D}_\tau \zeta^{\frac{1}{2}}$ as a test function and divide both side by τ. Then we obtain with Cauchy-Schwarz inequality and the definition of the constant C_{data} from (3.5)

$$\begin{aligned}(\mathrm{D}_\tau \zeta^{\frac{1}{2}}, \mathrm{D}_\tau \zeta^{\frac{1}{2}})_{L^2(\Omega)} + \tau^2\theta a(\mathrm{D}_\tau \zeta^{\frac{1}{2}}, \mathrm{D}_\tau \zeta^{\frac{1}{2}}) \\ &= -\tfrac{\tau^2}{6}(\partial_t^3 \check{u}_H(\xi_1), \mathrm{D}_\tau \zeta^{\frac{1}{2}})_{L^2(\Omega)} - \tau^2\theta(\partial_t f(\xi_2), \mathrm{D}_\tau \zeta^{\frac{1}{2}})_{L^2(\Omega)} \\ &\quad + \tau^2\theta(\partial_t^3 \check{u}_H(\xi_3), \mathrm{D}_\tau \zeta^{\frac{1}{2}})_{L^2(\Omega)} \\ &\lesssim \tau^2(\|\partial_t^3 \check{u}_H(\xi_1)\|_{L^2(\Omega)} + \|\partial_t f(\xi_2)\|_{L^2(\Omega)} + \|\partial_t^3 \check{u}_H(\xi_3)\|_{L^2(\Omega)}) \\ &\quad \cdot (\|\mathrm{D}_\tau \zeta^{\frac{1}{2}}\|_{L^2(\Omega)} + \tau\sqrt{\theta}\|\mathrm{D}_\tau \zeta^{\frac{1}{2}}\|_{L^2(\Omega)}) \\ &\lesssim \tau^2 C_{\mathrm{data}}(\|\mathrm{D}_\tau \zeta^{\frac{1}{2}}\|_{L^2(\Omega)} + \tau\sqrt{\theta}\|\mathrm{D}_\tau \zeta^{\frac{1}{2}}\|_{L^2(\Omega)}).\end{aligned} \tag{3.177}$$

Since by Young inequality

$$(\|\mathrm{D}_\tau \zeta^{\frac{1}{2}}\|_{L^2(\Omega)} + \tau\sqrt{\theta}\|\mathrm{D}_\tau \zeta^{\frac{1}{2}}\|_{L^2(\Omega)})^2 \lesssim (\mathrm{D}_\tau \zeta^{\frac{1}{2}}, \mathrm{D}_\tau \zeta^{\frac{1}{2}})_{L^2(\Omega)} + \tau^2\theta a(\mathrm{D}_\tau \zeta^{\frac{1}{2}}, \mathrm{D}_\tau \zeta^{\frac{1}{2}}),$$

dividing by

$$\|\mathrm{D}_\tau \zeta^{\frac{1}{2}}\|_{L^2(\Omega)} + \tau\sqrt{\theta}\|\mathrm{D}_\tau \zeta^{\frac{1}{2}}\|_{L^2(\Omega)}$$

in (3.177) yields

$$\|\mathrm{D}_\tau \zeta^{\frac{1}{2}}\|_{L^2(\Omega)} + \tau\|\mathrm{D}_\tau \zeta^{\frac{1}{2}}\|_{L^2(\Omega)} \lesssim \tau^2 C_{\mathrm{data}}. \tag{3.178}$$

Using both equations (3.172) and (3.178) in (3.171) yields

$$\begin{aligned}\|\mathrm{D}_\tau \zeta^{n+\frac{1}{2}}\|_{L^2(\Omega)} + \|\nabla\zeta^{n+\frac{1}{2}}\|_{L^2(\Omega)} \\ &\lesssim \tau^2 C_{\mathrm{data}} + \sum_{i=1}^{n} \tau\|\partial_t^2 \check{u}_H(t_i^\theta) - \mathrm{D}_\tau^2 \check{u}_H(t_i)\|_{L^2(\Omega)}.\end{aligned} \tag{3.179}$$

Finally, we consider the last term on the right-hand side of (3.179). Fix any $i = 1, \cdots, n$. Then using Taylor-expansion, there exist $\sigma_1 \in [t_i, t_{i+1}]$ and $\sigma_2 \in [t_{i-1}, t_i]$, such that

$$\check{u}_H(t_{i+1}) = \check{u}_H(t_i) + \tau\partial_t \check{u}_H(t_i) + \tfrac{\tau^2}{2}\partial_t^2 \check{u}_H(t_i) + \tfrac{\tau^3}{6}\partial_t^3 \check{u}_H(t_i) + \tfrac{\tau^4}{24}\partial_t^4 \check{u}_H(\sigma_1)$$
$$\check{u}_H(t_{i-1}) = \check{u}_H(t_i) - \tau\partial_t \check{u}_H(t_i) + \tfrac{\tau^2}{2}\partial_t^2 \check{u}_H(t_i) - \tfrac{\tau^3}{6}\partial_t^3 \check{u}_H(t_i) + \tfrac{\tau^4}{24}\partial_t^4 \check{u}_H(\sigma_2).$$

This yields

$$\begin{aligned}\tau^2 \,\mathrm{D}_\tau^2 \,\check{u}_H(t_i) &= \check{u}_H(t_{i+1}) - 2\check{u}_H(t_i) + \check{u}_H(t_{i-1}) \\ &= \tau^2 \partial_t^2 \check{u}_H(t_i) + \tfrac{\tau^4}{24}\partial_t^4 \check{u}_H(\sigma_1) + \tfrac{\tau^4}{24}\partial_t^4 \check{u}_H(\sigma_2).\end{aligned} \tag{3.180}$$

Similarly, using Taylor-expansion, there exist $\sigma_3 \in [t_i, t_{i+1}]$ and $\sigma_4 \in [t_{i-1}, t_i]$, such that

$$\begin{aligned}\partial_t^2 \check{u}_H(t_{i+1}) &= \partial_t^2 \check{u}_H(t_i) + \tau \partial_t^3 \check{u}_H(t_i) + \tfrac{\tau^2}{2}\partial_t^4 \check{u}_H(\sigma_3) \\ \partial_t^2 \check{u}_H(t_{i-1}) &= \partial_t^2 \check{u}_H(t_i) - \tau \partial_t^3 \check{u}_H(t_i) + \tfrac{\tau^2}{2}\partial_t^4 \check{u}_H(\sigma_4).\end{aligned}$$

Thus, we have

$$\begin{aligned}\partial_t^2 \check{u}_H(t_i^\theta) &= \theta \partial_t^2 \check{u}_H(t_{i+1}) + (1-2\theta)\partial_t^2 \check{u}_H(t_i) + \theta \partial_t^2 \check{u}_H(t_{i-1}) \\ &= \partial_t^2 \check{u}_H(t_i) + \tfrac{\theta\tau^2}{2}\partial_t^4 \check{u}_H(\sigma_3) + \tfrac{\theta\tau^2}{2}\partial_t^4 \check{u}_H(\sigma_4).\end{aligned} \tag{3.181}$$

Overall, dividing (3.180) by τ^2 and subtracting from (3.181) we obtain

$$\begin{aligned}&\|\partial_t^2 \check{u}_H(t_\nu^\theta) - \mathrm{D}_\tau^2 \,\check{u}_H(t_\nu)\|_{L^2(\Omega)} \\ &\qquad = \tau^2 \|\partial_t^4 (\tfrac{\theta}{2}\check{u}_H(\sigma_3) + \tfrac{\theta}{2}\check{u}_H(\sigma_4) - \tfrac{1}{24}\check{u}_H(\sigma_1) - \tfrac{1}{24}\check{u}_H(\sigma_2))\|_{L^2(\Omega)} \\ &\qquad \lesssim \tau^2 C_{\mathrm{data}}.\end{aligned} \tag{3.182}$$

Thus, for the sum in (3.171), we have

$$\begin{aligned}\sum_{\nu=1}^{n} \tau \|\partial_t^2 \check{u}_H(t_\nu^\theta) - \mathrm{D}_\tau^2 \,\check{u}_H(t_\nu)\|_{L^2(\Omega)} &\lesssim n\tau^3 C_{\mathrm{data}} \\ &\lesssim_T \tau^2 C_{\mathrm{data}}.\end{aligned} \tag{3.183}$$

Inserting this into (3.179) yields the assertion. □

This lemma completes all ingredients to proof the error of the eho-LOD-θ method. The idea is to split the error into the temporal error and semi-discrete error and previous results provide the estimation.

Proof of Theorem 3.27. We start by inserting the semi-discrete solution and using the triangle inequality to obtain

$$\begin{aligned}&\|\mathrm{D}_\tau \,\check{u}_H^{n+\frac{1}{2}} - \tau^{-1}(u(t_{n+1}) - u(t_n))\|_{L^2(\Omega)} + \|\nabla(\check{u}_H^{n+\frac{1}{2}} - u(t_{n+\frac{1}{2}}))\|_{L^2(\Omega)} \\ &\quad \le \|\mathrm{D}_\tau \,\zeta^{n+\frac{1}{2}}\|_{L^2(\Omega)} + \|\nabla \zeta^{n+\frac{1}{2}}\|_{L^2(\Omega)} + \|\mathrm{D}_\tau \,e^{n+\frac{1}{2}}\|_{L^2(\Omega)} + \|\nabla e^{n+\frac{1}{2}}\|_{L^2(\Omega)},\end{aligned} \tag{3.184}$$

where $e^n = \check{u}_H(t_n) - u(t_n)$. By Taylor-expansion we have

$$\|\mathrm{D}_\tau \,e^{n+\frac{1}{2}}\|_{L^2(\Omega)} \lesssim \|\partial_t e^{n+\frac{1}{2}}\|_{L^2(\Omega)}.$$

Then, we apply Theorem 3.27 to the first two terms on the right-hand side and Theorem 3.21 to the last two terms after the Taylor-expansion to obtain the assertion. □

4 Conclusions and Outlook

4.1 Conclusions

Numerically solving partial differential equations (PDEs) with highly oscillatory material coefficients poses many challenges. Classically, the finite element method (FEM) is used to discretize and then approximate the solution to the PDE. However, in this setting with non-smooth, highly oscillatory coefficients the FEM may perform arbitrarily bad. Choosing a different spatial discretization as, e.g., the higher-order localized orthogonal decomposition (ho-LOD) method generally yields much better results.

In Chapter 2 we have briefly investigated why the FEM is suboptimal when dealing with non-smooth and highly oscillatory PDE coefficients. Furthermore, in this chapter we provided a construction of a ho-LOD method, which provably achieves higher-order convergence independent of the oscillations of the material and independent of the regularity of the solution in space.

Chapter 3 then introduced the acoustic wave equation and in a first step we applied the ho-LOD method to the time-dependent PDE. We found that similar to the FEM (however not as severe) the ho-LOD yields a reduced error convergence for higher polynomial degrees in the time-dependent setting as opposed to the elliptic setting. In this chapter we investigated the reduced order and found out that it stems from the low regularity of the exact solution to wave equation. While the idea of the ho-LOD method is to achieve higher-order convergence independent of the regularity of the solution, this goal is not achieved for the wave equation. An interpretation is that the ho-LOD is well-suited to tackle elliptic problems, however is not adapted to time-dependent differential operators.

Subsequently, we defined a novel *enriched correction operator* in the spirit of the LOD, that can be used in a prototypical setting to correct the shortcomings of the ho-LOD method. The idea is that the enriched correction operator eliminates the residual of the ho-LOD method applied to the wave equation and obtain the higher-order convergence independent of the oscillations of the PDE coefficient and the regularity of the solution. This first achievement, however, was set in a prototypical setting where knowledge of the solution is required. We could in the following construct discrete so-called *enriched correction spaces* that are added to the ho-LOD multiscale space, and together they are able to recover the higher-order convergence without requiring any additional spatial regularity of the solution.

With the construction of these discrete spaces we still require one more ingredient. In order to compute a basis of the enriched correction spaces, we have to solve

global corrector problem for every multiscale basis function, which is computationally unfeasible. Thus, a localization strategy is needed for the additional corrections as well. It can be straight-forward shown, that the enriched corrections obey an exponential decay similarly to the classical corrector from the ho-LOD. However, the localization strategy from the ho-LOD is insufficient for application to the enriched basis functions, since this would result in almost global corrector problems which then becomes unfeasible. In this thesis a novel localization strategy is introduced that adapts the localization parameter dependent on where the enriched correction operator is applied. Employing this strategy we proved that the localization error of the localized enriched correction operator is asymptotically the same as for the classical correction when calculating all enriched basis functions on patches of the same size. This remarkable result ensures that the enriched ho-LOD (eho-LOD) method is computationally feasible in practise.

Finally, we put the method into practice on a few examples, and the theoretical results were confirmed. We have observed that the novel eho-LOD method is able to recover the higher-order convergence rate from the elliptic setting for the acoustic wave equation without requiring any additional spatial regularity of the solution. Further, we have seen that the localization strategy performs similar to the ho-LOD method while all basis functions have support on the same sized patch.

4.2 Outlook

There are two possible improvements in the future. The first has to do with the fact that as of now there has no inverse estimate been shown for the new enriched multiscale spaces. The reason is that this is typically shown employing the bubble operator, however, with this idea information is lost as the enriched corrections lie in the kernel. In practise, proving an inverse estimate can be very beneficial when trying to employ certain time discretization schemes. With this, e.g., the fourth-order θ-method or the leapfrog can be used, as they require inverse estimates to prove stability. In the same breath it is worth mentioning that in general different higher-order can be applied to complement the higher-order spatial convergence, e.g., Runge-Kutta or BDF methods. We note here, that the spatial discretization of the eho-LOD already requires assumptions such that the solution has additional temporal regularity such that higher-order time discretizations also seem natural.

The second improvement is concerned with the condition of the system matrix. In the numerical experiments we found that the system matrix in general has a large condition number which of course comes with slow convergence and inaccurate solves. This makes this improvement very important for an efficient implementation. The large condition number comes on the one hand from the fact that enriching the spaces increases the dimension of the finite spaces on each patch by a large amount. This can lead to instabilities when solving the corrector problems, as a

larger number of degrees of freedom on the coarse mesh have to share the same number of the degrees of freedom on the patch of the fine mesh. This can lead to the basis functions being numerically (almost) linearly dependent which results in indefinite matrices and need to be avoided. Another reason is the size of the norms of the enriched correction, as they scale with the square of the mesh size compared to the multiscale basis, the smallest and largest eigenvalue of the system matrix can differ greatly which also increases the condition number. In practice this can be overcome by, e.g., using a solver based on the Schur complement where solving for the multiscale space with $j = 0$ is decoupled from the spaces for $j > 0$. An idea how to avoid badly conditioned matrices is the idea that each enriched correction space is orthogonalized to each previous space. With this orthogonality it is possible to decouple the system and solve each part separately with better conditioned matrices. This could even be done in parallel to speed up the online computation.

Finally, a smaller improvement could be the following. Since each enriched correction space only increases the convergence by two order, creating the enriched correction spaces with lower polynomial degrees would suffice for the optimal rate. However, in the proofs orthogonality between spaces is necessary which would need to be overcome.

Bibliography

A. Abdulle and P. Henning. Localized orthogonal decomposition method for the wave equation with a continuum of scales. *Math. Comp.*, 86(304):549–587, 2017. ISSN 0025-5718,1088-6842. doi: 10.1090/mcom/3114. URL https://doi.org/10.1090/mcom/3114.

R. Altmann, P. Henning, and D. Peterseim. Numerical homogenization beyond scale separation. *Acta Numer.*, 30:1–86, 2021. ISSN 0962-4929,1474-0508. doi: 10.1017/S0962492921000015. URL https://doi.org/10.1017/S0962492921000015.

R. Araya, C. Harder, D. Paredes, and F. Valentin. Multiscale hybrid-mixed method. *SIAM J. Numer. Anal.*, 51(6):3505–3531, 2013. ISSN 0036-1429,1095-7170. doi: 10.1137/120888223. URL https://doi.org/10.1137/120888223.

I. Babuška. Error-bounds for finite element method. *Numer. Math.*, 16:322–333, 1970/71. ISSN 0029-599X,0945-3245. doi: 10.1007/BF02165003. URL https://doi.org/10.1007/BF02165003.

I. Babuška and M. R. Dorr. Error estimates for the combined h and p versions of the finite element method. *Numer. Math.*, 37(2):257–277, 1981. ISSN 0029-599X,0945-3245. doi: 10.1007/BF01398256. URL https://doi.org/10.1007/BF01398256.

I. Babuška and R. Lipton. Optimal local approximation spaces for generalized finite element methods with application to multiscale problems. *Multiscale Model. Simul.*, 9(1):373–406, 2011. ISSN 1540-3459,1540-3467. doi: 10.1137/100791051. URL https://doi.org/10.1137/100791051.

I. Babuška and J. E. Osborn. Generalized finite element methods: their performance and their relation to mixed methods. *SIAM J. Numer. Anal.*, 20(3):510–536, 1983. ISSN 0036-1429. doi: 10.1137/0720034. URL https://doi.org/10.1137/0720034.

I. Babuška and W. C. Rheinboldt. Error estimates for adaptive finite element computations. *SIAM J. Numer. Anal.*, 15(4):736–754, 1978. ISSN 0036-1429. doi: 10.1137/0715049. URL https://doi.org/10.1137/0715049.

I. Babuška and M. Suri. The h-p version of the finite element method with quasi-uniform meshes. *RAIRO Modél. Math. Anal. Numér.*, 21(2):199–238, 1987. ISSN 0764-583X,1290-3841. doi: 10.1051/m2an/1987210201991. URL https://doi.org/10.1051/m2an/1987210201991.

A. Bensoussan, J.-L. Lions, and G. Papanicolaou. *Asymptotic analysis for periodic structures*, volume 5 of *Studies in Mathematics and its Applications*. North-Holland Publishing Co., Amsterdam-New York, 1978. ISBN 0-444-85172-0.

S. C. Brenner. Poincaré-Friedrichs inequalities for piecewise H^1 functions. *SIAM J. Numer. Anal.*, 41(1):306–324, 2003. ISSN 0036-1429,1095-7170. doi: 10.1137/S0036142902401311. URL https://doi.org/10.1137/S0036142902401311.

P. G. Ciarlet. *The finite element method for elliptic problems*, volume Vol. 4 of *Studies in Mathematics and its Applications*. North-Holland Publishing Co., Amsterdam-New York-Oxford, 1978. ISBN 0-444-85028-7.

M. Cicuttin, A. Ern, and S. Lemaire. A hybrid high-order method for highly oscillatory elliptic problems. *Comput. Methods Appl. Math.*, 19(4):723–748, 2019. ISSN 1609-4840,1609-9389. doi: 10.1515/cmam-2018-0013. URL https://doi.org/10.1515/cmam-2018-0013.

B. Cockburn, J. Gopalakrishnan, and R. Lazarov. Unified hybridization of discontinuous Galerkin, mixed, and continuous Galerkin methods for second order elliptic problems. *SIAM J. Numer. Anal.*, 47(2):1319–1365, 2009. ISSN 0036-1429,1095-7170. doi: 10.1137/070706616. URL https://doi.org/10.1137/070706616.

Z. Dong, M. Hauck, and R. Maier. An improved high-order method for elliptic multiscale problems. *SIAM J. Numer. Anal.*, 61(4):1918–1937, 2023. ISSN 0036-1429,1095-7170. doi: 10.1137/22M153392X. URL https://doi.org/10.1137/22M153392X.

W. Dörfler. A convergent adaptive algorithm for Poisson's equation. *SIAM J. Numer. Anal.*, 33(3):1106–1124, 1996. ISSN 0036-1429. doi: 10.1137/0733054. URL https://doi.org/10.1137/0733054.

W. E and B. Engquist. The heterogeneous multiscale methods. *Commun. Math. Sci.*, 1(1):87–132, 2003. ISSN 1539-6746,1945-0796. doi: 10.4310/cms.2003.v1.n1.a8. URL https://doi.org/10.4310/cms.2003.v1.n1.a8.

Y. Efendiev, J. Galvis, and T. Y. Hou. Generalized multiscale finite element methods (GMsFEM). *J. Comput. Phys.*, 251:116–135, 2013. ISSN 0021-9991,1090-2716. doi: 10.1016/j.jcp.2013.04.045. URL https://doi.org/10.1016/j.jcp.2013.04.045.

L. C. Evans. *Partial differential equations*, volume 19 of *Graduate Studies in Mathematics*. American Mathematical Society, Providence, RI, second edition, 2010. ISBN 978-0-8218-4974-3. doi: 10.1090/gsm/019. URL https://doi.org/10.1090/gsm/019.

S. Geevers and R. Maier. Fast mass lumped multiscale wave propagation modelling. *IMA J. Numer. Anal.*, 43(1):44–72, 2023. ISSN 0272-4979,1464-3642. doi: 10.1093/imanum/drab084. URL https://doi.org/10.1093/imanum/drab084.

B. Q. Guo and H. S. Oh. The *h-p* version of the finite element method for problems with interfaces. *Internat. J. Numer. Methods Engrg.*, 37(10):1741–1762, 1994. ISSN 0029-5981,1097-0207. doi: 10.1002/nme.1620371007. URL https://doi.org/10.1002/nme.1620371007.

C. Harder, D. Paredes, and F. Valentin. A family of multiscale hybrid-mixed finite element methods for the Darcy equation with rough coefficients. *J. Comput. Phys.*, 245:107–130, 2013. ISSN 0021-9991,1090-2716. doi: 10.1016/j.jcp.2013.03.019. URL https://doi.org/10.1016/j.jcp.2013.03.019.

M. Hauck and D. Peterseim. Super-localization of elliptic multiscale problems. *Math. Comp.*, 92(341):981–1003, 2023. ISSN 0025-5718,1088-6842. doi: 10.1090/mcom/3798. URL https://doi.org/10.1090/mcom/3798.

M. Hauck, A. Lozinski, and R. Maier. A generalized framework for higher-order localized orthogonal decomposition methods, 2025. URL https://arxiv.org/abs/2506.19462.

F. Hellman and A. Målqvist. Contrast independent localization of multiscale problems. *Multiscale Model. Simul.*, 15(4):1325–1355, 2017. ISSN 1540-3459,1540-3467. doi: 10.1137/16M1100460. URL https://doi.org/10.1137/16M1100460.

P. Henning and D. Peterseim. Oversampling for the multiscale finite element method. *Multiscale Model. Simul.*, 11(4):1149–1175, 2013. ISSN 1540-3459,1540-3467. doi: 10.1137/120900332. URL https://doi.org/10.1137/120900332.

J. S. Hesthaven and T. Warburton. *Nodal discontinuous Galerkin methods*, volume 54 of *Texts in Applied Mathematics*. Springer, New York, 2008. ISBN 978-0-387-72065-4. doi: 10.1007/978-0-387-72067-8. URL https://doi.org/10.1007/978-0-387-72067-8. Algorithms, analysis, and applications.

T. Y. Hou and X.-H. Wu. A multiscale finite element method for elliptic problems in composite materials and porous media. *J. Comput. Phys.*, 134(1):169–189, 1997. ISSN 0021-9991,1090-2716. doi: 10.1006/jcph.1997.5682. URL https://doi.org/10.1006/jcph.1997.5682.

P. Houston, C. Schwab, and E. Süli. Discontinuous *hp*-finite element methods for advection-diffusion-reaction problems. *SIAM J. Numer. Anal.*, 39(6):2133–2163, 2002. ISSN 0036-1429,1095-7170. doi: 10.1137/S0036142900374111. URL https://doi.org/10.1137/S0036142900374111.

T. J. R. Hughes. Multiscale phenomena: Green's functions, the Dirichlet-to-Neumann formulation, subgrid scale models, bubbles and the origins of stabilized methods. *Comput. Methods Appl. Mech. Engrg.*, 127(1-4):387–401, 1995. ISSN 0045-7825,1879-2138. doi: 10.1016/0045-7825(95)00844-9. URL https://doi.org/10.1016/0045-7825(95)00844-9.

T. J. R. Hughes, G. R. Feijóo, L. Mazzei, and J.-B. Quincy. The variational multiscale method—a paradigm for computational mechanics. *Comput. Methods Appl. Mech. Engrg.*, 166(1-2):3–24, 1998. ISSN 0045-7825,1879-2138. doi: 10.1016/S0045-7825(98)00079-6. URL https://doi.org/10.1016/S0045-7825(98)00079-6.

P. Joly. Variational methods for time-dependent wave propagation problems. In *Topics in computational wave propagation*, volume 31 of *Lect. Notes Comput. Sci. Eng.*, pages 201–264. Springer, Berlin, 2003. ISBN 3-540-00744-X. doi: 10.1007/978-3-642-55483-4_6. URL https://doi.org/10.1007/978-3-642-55483-4_6.

B. Kalyanaraman, F. Krumbiegel, R. Maier, and S. Wang. Optimal higher-order convergence rates for parabolic multiscale problems, 2025. URL https://arxiv.org/abs/2510.09514.

S. Karaa. Finite element θ-schemes for the acoustic wave equation. *Adv. Appl. Math. Mech.*, 3(2):181–203, 2011. ISSN 2070-0733,2075-1354. doi: 10.1007/s12190-012-0558-8. URL https://doi.org/10.1007/s12190-012-0558-8.

F. Krumbiegel and R. Maier. A higher order multiscale method for the wave equation. *IMA J. Numer. Anal.*, 45(4):2248–2273, 2025. ISSN 0272-4979,1464-3642. doi: 10.1093/imanum/drae059. URL https://doi.org/10.1093/imanum/drae059.

J.-L. Lions and E. Magenes. *Non-homogeneous boundary value problems and applications. Vol. I*, volume Band 181 of *Die Grundlehren der mathematischen Wissenschaften*. Springer-Verlag, New York-Heidelberg, 1972. Translated from the French by P. Kenneth.

C. Ma and R. Scheichl. Error estimates for discrete generalized FEMs with locally optimal spectral approximations. *Math. Comp.*, 91(338):2539–2569, 2022. ISSN 0025-5718,1088-6842. doi: 10.1090/mcom/3755. URL https://doi.org/10.1090/mcom/3755.

C. Ma, R. Scheichl, and T. Dodwell. Novel design and analysis of generalized finite element methods based on locally optimal spectral approximations. *SIAM J. Numer. Anal.*, 60(1):244–273, 2022. ISSN 0036-1429,1095-7170. doi: 10.1137/21M1406179. URL https://doi.org/10.1137/21M1406179.

R. Maier. *Computational Multiscale Methods in Unstructured Heterogeneous Media*. PhD thesis, University of Augsburg, 2020.

R. Maier. A high-order approach to elliptic multiscale problems with general unstructured coefficients. *SIAM J. Numer. Anal.*, 59(2):1067–1089, 2021. ISSN 0036-1429,1095-7170. doi: 10.1137/20M1364321. URL https://doi.org/10.1137/20M1364321.

R. Maier and D. Peterseim. Explicit computational wave propagation in micro-heterogeneous media. *BIT*, 59(2):443–462, 2019. ISSN 0006-3835,1572-9125. doi: 10.1007/s10543-018-0735-8. URL https://doi.org/10.1007/s10543-018-0735-8.

A. Målqvist and D. Peterseim. Localization of elliptic multiscale problems. *Math. Comp.*, 83(290):2583–2603, 2014.

A. Målqvist and D. Peterseim. *Numerical homogenization by localized orthogonal decomposition*, volume 5 of *SIAM Spotlights*. Society for Industrial and Applied Mathematics (SIAM), Philadelphia, PA, 2021. ISBN 978-1-611976-44-1.

N. C. Nguyen, J. Peraire, and B. Cockburn. High-order implicit hybridizable discontinuous Galerkin methods for acoustics and elastodynamics. *J. Comput. Phys.*, 230(10):3695–3718, 2011. ISSN 0021-9991,1090-2716. doi: 10.1016/j.jcp.2011.01.035. URL https://doi.org/10.1016/j.jcp.2011.01.035.

H. Owhadi. Multigrid with rough coefficients and multiresolution operator decomposition from hierarchical information games. *SIAM Rev.*, 59(1):99–149, 2017. ISSN 1095-7200,0036-1445. doi: 10.1137/15M1013894. URL https://doi.org/10.1137/15M1013894.

H. Owhadi and C. Scovel. *Operator-adapted wavelets, fast solvers, and numerical homogenization*, volume 35 of *Cambridge Monographs on Applied and Computational Mathematics*. Cambridge University Press, Cambridge, 2019. ISBN 978-1-108-48436-7. From a game theoretic approach to numerical approximation and algorithm design.

H. Owhadi and L. Zhang. Gamblets for opening the complexity-bottleneck of implicit schemes for hyperbolic and parabolic ODEs/PDEs with rough coefficients. *J. Comput. Phys.*, 347:99–128, 2017. ISSN 0021-9991,1090-2716. doi: 10.1016/j.jcp.2017.06.037. URL https://doi.org/10.1016/j.jcp.2017.06.037.

H. Owhadi, L. Zhang, and L. Berlyand. Polyharmonic homogenization, rough polyharmonic splines and sparse super-localization. *ESAIM Math. Model. Numer. Anal.*, 48(2):517–552, 2014. ISSN 2822-7840,2804-7214. doi: 10.1051/m2an/2013118. URL https://doi.org/10.1051/m2an/2013118.

D. Peterseim and M. Schedensack. Relaxing the CFL condition for the wave equation on adaptive meshes. *J. Sci. Comput.*, 72(3):1196–1213, 2017. ISSN 0885-7474,1573-7691. doi: 10.1007/s10915-017-0394-y. URL https://doi.org/10.1007/s10915-017-0394-y.

C. Schwab. *p- and hp-finite element methods*. Numerical Mathematics and Scientific Computation. The Clarendon Press, Oxford University Press, New York, 1998. ISBN 0-19-850390-3. Theory and applications in solid and fluid mechanics.

E. Süli, P. Houston, and C. Schwab. *hp*-finite element methods for hyperbolic problems. In *The mathematics of finite elements and applications, X, MAFELAP 1999 (Uxbridge)*, pages 143–162. Elsevier, Oxford, 2000. ISBN 0-08-043568-8. doi: 10.1016/B978-008043568-8/50008-0. URL https://doi.org/10.1016/B978-008043568-8/50008-0.

R. Verfürth. *A posteriori error estimation techniques for finite element methods*. Numerical Mathematics and Scientific Computation. Oxford University Press, Oxford, 2013. ISBN 978-0-19-967942-3. doi: 10.1093/acprof:oso/9780199679423.001.0001. URL https://doi.org/10.1093/acprof:oso/9780199679423.001.0001.